Chronic Stress Induces Specific Cellular and Morphological Astroglial Changes Associated with Depressive-like Phenotypes

by

Dipashree (Dipa) Chatterjee

A thesis submitted in conformity with the requirements
for the degree of Master of Science

Department of Pharmacology & Toxicology
University of Toronto

Chronic Stress Induces Specific Cellular and Morphological Astroglial Changes Associated with Depressive-like Phenotypes

Dipashree (Dipa) Chatterjee

Master of Science

Department of Pharmacology & Toxicology
University of Toronto

2019

Abstract

In major depressive disorder (MDD), one of the most consistent findings from post-mortem studies is decreased astroglia number and function in limbic brain regions including the prefrontal cortex (PFC). However, the contribution of astroglial pathology in synaptic dysfunction and depressive symptoms associated with MDD remains unclear. Here, using chronic restraint stress (CRS) in mice to model MDD, we demonstrate that CRS induced time-dependant decreases in astrocytic and synaptic protein expression in the PFC, which correlated with both anxiety- and anhedonia-like deficits. We also investigated CRS effects on astroglial cell morphology using Sholl analysis and found CRS decreased distal processes while increasing proximal processes. This structural rearrangement may parallel functional astrocytic and synaptic changes. Furthermore, we validated a custom-designed plasmid, allowing astroglial activity enhancement in vitro. This novel tool will allow us to test if PFC astroglial activation prevents CRS effects. This work substantiates astroglia as targets for antidepressant development.

Acknowledgments

I would like to express my gratitude to my supervisors Dr. Etienne Sibille and Dr. Mounira Banasr for their continued support and guidance. I would also like to thank Dr. Thomas Prevot for guiding me through experiments and procedures. Additionally, I would like to thank Dr. Jerry Warsh and Marty Green for their help with the calcium mobilization assay and access to the confocal microscope.

Lastly, I want to thank my family, friends, and colleagues who have supported me throughout my graduate studies.

Table of Contents

List of Tables

List of Figures

List of Appendices

Abbreviations

5-HT	Serotonin
5HTT/SERT	Serotonin Transporter
AAV	Adeno-associated Virus
ACC	Animal Care Committee
AD	Antidepressants
Akt	Protein Kinase B
ALDH1-L1	Aldehyde Dehydrogenase 1 Family Member L1
AMPA	α-amino-3-hydroxy-5-methyl-4-isoxazolepropionic Acid
AmpR	Ampicillin Resistance Gene
ANOVA	Analysis of Variance
BCA	Bicinchoninic Acid
BDNF	Brain Derived Neurotrophic Factor
BSA	Bovine Serum Albumin
C21	DREADDs Agonist 21
CAMH	Centre for Addiction and Mental Health
cAMP	Cyclic Adenosine Monophosphate
CCAC	Canadian Council on Animal Care
CMHA	Canadian Mental Health Association
CMV	Cytomegalovirus
CNO	Clozapine-N-Oxide
CRS	Chronic Restraint Stress
CUS	Chronic Unpredictable Stress
DAM	Defined Astrocyte Media
dBcAMP	Dibutyryl Cyclic Adenosine Monophosphate
DMEM	Dulbecco`s Modified Eagle Media
DREADDs	Designer Receptor Exclusively Activated by Designer Drugs
DSM-V	Diagnostic and Statistical Manual of Mental Disorders, 5th Edition
EAAT1	Excitatory Amino Acid Transporter 1
EAAT2	Excitatory Amino Acid Transporter 2
EAAT3	Excitatory Amino Acid Transporter 3

(e)GFP	(enhanced) Green Fluorescent Protein
ECL	Enhanced Chemiluminescence
FACS	Fluorescence Activated Cell Sorting
FBS	Fetal Bovine Serum
fMRI	Functional Magnetic Resonance Imaging
GABA	γ-aminobutyric acid
GFAP	Glial Fibrillary Acidic Protein
GFP	Green Fluorescence Protein
GLAST	Glutamate Aspartate Transporter 1
GLT1	Glutamate Transporter 1
GPCR	G Protein Coupled Receptor
GS	Glutamine Synthetase
GWAS	Genome Wide Association Studies
HEK293	Human Embryonic Kidney 293
HEPES	4-(2-hydroxyethyl)-1-piperazineethanesulfonic Acid
hGFAP	Human Glial Fibrillary Acidic Protein Promoter
hM3Dq	Modified human M3 muscarinic receptor
hM4Di	Modified human M4 muscarinic receptor
Iba1	Ionized Calcium Binding Adaptor Molecule 1
iCre	Improved Cre
IHC/ICC	Immunohistochemistry/Immunocytochemistry
ITR	Inverted Terminal Repeat Sequences
LB	Lysogeny Broth
MAOi	Monoamine Oxidase Inhibitors
MAPK	Mitogen-Activated Protein Kinase
MDD	Major Depressive Disorder
mGFAP	Mouse Glial Fibrillary Acidic Protein Promoter
MRI	Magnetic Resonance Imaging
mRNA	Messenger RNA
NDS	Normal Donkey Serum
NE	Norepinephrine
NET	Norepinephrine Transporter

NeuN	Neuronal Nuclei
NMDA	N-methyl-D-aspartate
OBX	Olfactory Bulbectomy
p/t	phospho/total
PAC	Primary Astrocyte Culture
PBS(-T)	Phosphate Buffer Saline (-TritonX)
PFA	Paraformaldehyde
PFC	Prefrontal Cortex
PSD95	Postsynaptic Density Protein 95
RA	Residual Avoidance
RAM	Regular Astrocyte Media
ROI	Region of Interest
RT	Room Temperature
SLC64A	Serotonin Transporter Gene
SNRI	Serotonin and Norepinephrine Reuptake Inhibitors
SSRI	Selective Serotonin Reuptake Inhibitors
SV40pA	SV40 Polyadenylation Signal
Syn1	Synapsin 1
TBS-T	Tris Buffer Saline-Tween 20
TPH2	Tryptophan Hydroxylase 2
UCMS	Unpredictable Chronic Mild Stress
VEH	Vehicle
vGLUT	Vesicular Glutamate Transporter
vGLUT1	Vesicular Glutamate Transporter 1
WHO	World Health Organization
WPRE	Woodchuck Hepatitis Virus Posttranscriptional Regulatory Element
WT	Wild Type

1 Project Overview

Major Depressive Disorder (MDD) is a debilitating mental illness that affects a large portion of the population worldwide. It is estimated that 1 in 4 Canadians are suffering from depression, resulting in significant economic burden. According to the World Health Organization, there are more than 300 million adults living with depression (WHO, 2017). MDD is a multifaceted disease with various contributing risk factors, including genetics, sex, environment, socioeconomic status. The importance of these factors and how they interact to affect aspects of MDD, including its time course and severity, remain unclear. Growing evidence suggest that MDD is a morphological pathology where brain regions, cells, and cell compartments lose integrity, complexity, and function.

Research over the past 20 years has consistently demonstrated structural and cellular changes in the brains of individuals with MDD and other stress-related illnesses (see for review Banasr and Duman, 2007; Duman et al., 2016; Rajkowska and Miguel-Hidalgo, 2007; Sanacora and Banasr, 2013; Sheline et al., 2003). Evidence from post-mortem and preclinical studies implicates synaptic dysfunctions affecting glutamatergic neurons (Duric et al., 2013; Northoff and Sibille, 2014; Sanacora, 2010), but also astroglial anomalies (Nagy et al., 2015; Rajkowska and Stockmeier, 2013; Sanacora and Banasr, 2013), as underlying substrates of MDD. Replicable findings show marked changes in the number and function of astroglial cells (Nagy et al., 2015; Rajkowska and Stockmeier, 2013; Sanacora and Banasr, 2013) as well as neuronal atrophy and synaptic loss found in MDD (Duric et al., 2013; Kang et al., 2012), and further characterized in rodent models (Duman and Duman, 2015; Duman et al., 2016; Li et al., 2011; Qiao et al., 2016; Radley et al., 2006; Son et al., 2012). In support of a role for astroglial dysfunction in MDD, it was demonstrated that: 1) similar synaptic and astrocyte changes occur in rodent chronic stress models (Banasr et al., 2010; Lin and Sibille, 2015; Son et al., 2012; Voleti et al., 2013); 2) induction of astroglial dysfunctions produce depressive-like behaviours within 3 days (Banasr and Duman, 2008); and 3) enhancing synaptic or astroglial function has antidepressant-like potential (Banasr et al., 2010; Li et al., 2010; Lin and Sibille, 2015). Together, these findings provide conceptual evidence that both synaptic and astroglial dysfunctions occur in MDD, and suggest that depression is partly “a glial–based synaptic dysfunction” (Rial et al., 2015)

Here I propose to investigate a potential link between the astroglial dysfunctions and glutamatergic synapse dysfunctions associated with chronic stress in mice (Aim 1) and characterize the astroglial morphological changes induced by chronic stress (Aim 2) in the prefrontal cortex (PFC). Lastly, I will adapt a new tool based on the Designer Receptor Exclusively Activated by Designer Drugs (DREADDs) method and validate its ability to alter the activity of astroglia (Aim 3).

1.1 Three Experimental Aims

1.1.1 Aim 1: Identify chronic stress-induced astroglial and synaptic alterations and determine their contribution to specific depressive-like behaviours.

Rationale: Chronic stress induces depressive-like behaviours and decreases in astroglial and synaptic markers. However, the trajectory or clear links between these changes, and the development of behavioural deficits, remains to be determined.

Hypothesis: Chronic stress induces astroglial alterations similar to depression that contribute to the synaptic and depressive-like behavioural deficits.

Approach: To test this hypothesis, mice were subjected to 1, 2, 3, 4, or 5 weeks of stress and underwent a battery of tests measuring anxiety- and anhedonia-like behaviour. I then characterized the changes in expression level of specific astroglial and synaptic proteins using western blot analysis. Finally, I performed correlation analysis to assess potential contributions of these molecular changes to each other and to the behavioural deficits observed.

Predictions: Chronic stress would altered the animal's regular behaviour and this effect would progressively worsened over the stress exposure. At the cellular level, I anticipated that astroglial-specific protein expression changes would precede or be concomitant to the synapse-specific protein expression changes, and both would correlate with each other and behavioural performances.

1.1.2 Aim 2: Identify astroglial morphological changes induced by chronic stress.

Rationale: Chronic stress and depression are associated with decreased astroglial marker expression and astroglial density. However, the question remains whether chronic stress alters the morphology and complexity of astrocytes.

Hypothesis: Chronic stress alters astrocyte morphology and complexity in a time dependent manner.

Approach: Mice were subjected to 1, 3, or 5 weeks of stress and underwent a battery of tests measuring anxiety- and anhedonia-like behaviour. I then adapted a technique classically used to measure neuronal morphology to astrocytes (Sholl analysis) and determined whether stress induced changes in the astrocyte morphology and complexity.

Predictions: I anticipated that chronic exposure to stress would induce a progressive atrophy and reduction of astrocyte complexity in the PFC. This would be associated with a decrease in the number of processes and branching.

1.1.3 Aim 3: Validate the action of hM3Dq receptors in astrocytes and comparing ligand exposure.

Rationale: Since depression- & chronic stress-induced astroglial pathology in the PFC is thought to contribute to expression of depressive behaviour, enhancing astroglial function may oppositely have antidepressant and resiliency effects.

Hypothesis: Enhancing cortical astroglial activity prevents stress-induced cellular alterations that contribute to depressive-like deficits.

Approach: I aimed to adapt and validate the Designer Receptor Exclusively Activated by Designer Drugs (DREADD) method to activate the function of astrocytes. I used HEK293 cell and astrocyte culture to validate the effectiveness of a custom-designed plasmid, expressing the hM3Dq (modified human M3 muscarinic receptor) receptor, and confirmed activation of the transfected cells upon application of the DREADD ligand.

Predictions: I will have successfully adapted this technique to increase astroglial activity. Cells would conditionally express the hM3Dq receptor and show cell activation upon application of the DREADD ligand.

At completion, these studies will provide a deeper understanding of the nature and role of astroglial dysfunction in MDD and stress-related illnesses. This work will provide critical insight into the underlying mechanisms involved in the synaptic and astroglial changes associated with MDD as well as shed light onto the potential role of impaired neuron-astroglia cross talk in the context of stress-related disorders. Finally, this study will also set the stage toward a new avenue of investigation for the development of novel antidepressant treatment targeting astroglia.

2 Background

2.1 Major Depressive Disorder

2.1.1 Major Depressive Disorder Symptomology

MDD is a debilitating disorder affecting a large portion of the population worldwide. Affected individuals experience a host of symptoms including core symptoms of low mood and diminished interest/anhedonia (Fried et al., 2016; Kendler, 2016; Kessler et al., 2005; Zimmerman et al., 2018). According to DSM-V, MDD can also be accompanied by significant weight/appetite changes, psychomotor agitation/retardation, fatigue, excessive feelings of worthlessness/inappropriate guilt, diminished ability to concentrate, and recurrent thoughts/ideations of suicide or suicide attempts (DSM-V, 2013). For an individual to be diagnosed with MDD, they must be experiencing five or more symptoms (mentioned above) for a minimum of 2 weeks, and one of the symptoms must be either depressed mood or anhedonia. Often these symptoms continue for months and affect an individual's daily life, productivity, and coping abilities (Deussing, 2006; Dunkley et al., 2017; WHO, 2018). Additionally, mental awareness shifts from external to internal, leading to detrimental rumination (Northoff and Sibille, 2014). MDD is often accompanied by other physiological and systemic disorders such as diabetes or cardiovascular disease (Baghai et al., 2018; Deschenes et al., 2015; Fugger et al., 2019; Goldstein et al., 2015; Rosedale et al., 2015). MDD is a chronic recurrent disorder which is often comorbid with other psychiatric illnesses such as anxiety disorders, addiction, substance

abuse, cognitive impairment/dementia, etc. (Read et al., 2017; Thaipisuttikul et al., 2014). Various subtypes of depression have been described and classified depending on either the etiology (e.g. post-partum, atypical, etc.) or associated comorbidities (e.g. anxious depression) (Nagayama et al., 1991; Payne et al., 2009; Rantala et al., 2018; Ten Have et al., 2016). MDD is a highly complex heterogeneous disorder, which may partially explain why antidepressants are only effective in 50% of patients (Al-Harbi, 2012; Fava, 2003; Ward and Irazoqui, 2010). Indeed, MDD patients often require a combination of multiple therapeutic interventions (drug treatment, cognitive therapy, etc.). Nevertheless, 4-13% of the MDD population do not respond to multiple treatment attempts and are characterized as treatment-resistant (Holtzheimer and Mayberg, 2011; Narasimhan and Lohoff, 2012; Rush et al., 2006).

2.1.2 Epidemiology of Major Depression

Societal impact: According to the World Health Organization (WHO), depression is the leading cause of ill health and disability worldwide. In 2017, WHO reported that there are more than 300 million people living with depression worldwide, showing an increase of more than 18% between 2005 and 2015. At the most extreme depression can lead to suicide, which is the leading cause of death in 15-29 year-olds (WHO, 2017). In general, patients with MDD account for almost 60% of all suicides completed per year (Mann, 2003). MDD affects 1 in 8 Canadians at some point of their lives and is a source of great economic burden (Statistics Canada, 2013). According to the Canadian Mental Health Association each year 6.5% of youth between 15-24 experience MDD, 7% of seniors experience some form of depression, a third of people with chronic physical illnesses experience depression, and 12-16% of Aboriginal Canadians are affected (CMHA, 2013).

Sex: Sex differences are associated with MDD, with women being twice more likely to be diagnosed with MDD than men (Albert, 2015; Kessler, 2003; Kessler et al., 2005; Piccinelli and Wilkinson, 2000; Rai et al., 2013; Whiteford et al., 2013). Women often report greater number and severity of symptoms including changes in weight, appetite, anxiety, loss of interest, and psychosomatic symptoms (Frank et al., 1988; Kessler et al., 1993; Labaka et al., 2018; Silverstein, 2002; Smith et al., 2008; Young et al., 1990). These differences may be associated with gonadal hormonal changes, thus increasing the risk of MDD especially during the post-partum and post-menopausal periods in women (Cohen et al., 2006; Hammarstrom et al., 2009).

Genetics: MDD incidence has been shown to be linked to genetic factors, as there is a greater chance of an individual to be diagnosed with MDD if they have a first degree relative with the disorder (Sullivan et al., 2000). Twin studies have shown an additive 37% genetic contribution of MDD with an overall heritability of 31-42%, and that women had higher heritability rates compared to men (42 vs 29%) (Kendler et al., 2006; Sullivan et al., 2000). Specific genes have been linked to depression and/or response to antidepressant including genes that encode the serotonin transporter 5HTT (or SLC6A4 or SERT) (Camp et al., 2005; Caspi et al., 2003; Middeldorp et al., 2009; Serretti et al., 2007), brain derived neurotrophic factor (BDNF) (Homberg et al., 2014; Hosang et al., 2014; Peng et al., 2018), or the tryptophan hydroxylase-2 (TPH2) gene (Gao et al., 2012; Lopez de Lara et al., 2007; Ping et al., 2019). Genome wide association studies and meta analyses have found common genetic variants between individuals but with limited success in elucidating universal genetic markers for MDD (Bosker et al., 2011; Major Depressive Disorder Working Group of the Psychiatric GWAS Consortium et al., 2013; McMahon et al., 2010; Witt et al., 2017; Wray et al., 2012).

Comorbidity: Major depression is often comorbid with many disorders. One major comorbid disorder is anxiety, which is usually seen in 21-57% of patients with MDD (Hirschfeld, 2001; Melartin et al., 2002; Thaipisuttikul et al., 2014). Studies have also found significant comorbidities with substance abuse including alcohol use disorders and drug dependence (Boden and Fergusson, 2011; Currie et al., 2005; Melartin et al., 2002). Thaipisuttikul et al. (2014) described comorbidities with dysthymia, psychotic disorders, personality disorder, past panic disorder, obsessive-compulsive disorder, and suicidal risk. Other than mental disorders, MDD is also comorbid with physical disorders including a 1.5 to 2-fold increase in cardiovascular disease as well as strong association with chronic pain (Bair et al., 2003; Swardfager et al., 2011).

Age: With increasing life expectancy comes higher risk for the development of neurological illnesses including neuropsychiatric disorders and depression (Fiske et al., 2009). While MDD is less prevalent (~1%) in elderly (> 65 years of age) than in young individuals (Weissman et al., 1988), 15-25% of elders experience depressive symptoms without meeting MDD criteria but show significant distress and disability (Koenig and Blazer, 1992). Elderly people with MDD suffer from a greater risk of medical comorbidities and cognitive impairments, although it is unclear if depression is a result of these comorbidities or vice versa (Alexopoulos, 2005;

Mitchell and Subramaniam, 2005; Schaakxs et al., 2018). There are many psychosocial factors that can cause late-onset depression including disability, isolation, caregiving, loss of family and friends, and cognitive issues (Alexopoulos, 2005; Steffens and Potter, 2008; Wilson et al., 2015). Elderly people also have increased levels of corticosterone, which has been associated with increased chances of developing mood disorders (Savas et al., 2019).

2.1.3 Antidepressant Medications

Traditional antidepressants (ADs) enhance monoaminergic transmission to counteract the monoaminergic neurochemical imbalance extensively reported as the primary issue in MDD (Kohler et al., 2016; Meyer et al., 2006; Mulinari, 2012). Two major classes of monoaminergic ADs are the selective serotonin (5HT) reuptake inhibitors (SSRIs) and serotonin & norepinephrine (NE) reuptake inhibitors (SNRIs) (Machado and Einarson, 2010; Thase, 2008). SSRIs work by blocking the presynaptic 5HT reuptake transporter SERT, allowing greater 5HT levels to remain in the extra-synaptic cleft for a longer duration (Nutt et al., 1999; Stahl, 1998). SNRIs work by blocking both SERT and the NE reuptake transporter (NET), leading to an increased 5HT and NE in the synaptic cleft (Lambert and Bourin, 2002). Other classes of ADs include atypical antidepressants, tricyclic antidepressants, and monoamine oxidase inhibitors (MAOis); all increasing monoaminergic levels or pathway which, along with the documented decreased in monoamine in MDD, gave rise to the "monoamine hypothesis of depression" (Hillhouse and Porter, 2015; Kohler et al., 2016; Mulinari, 2012). More recently, the field moved beyond this hypothesis linking other processes and dysregulations affected in MDD, which are reversed by antidepressants. For example, the 'neurotrophic hypothesis of depression' is based on studies describing reduced neurotrophic support including brain derived neurotrophic factor (BDNF) expression in the blood and brain of MDD patients, while treatment with ADs for at least four weeks restored BDNF levels (Guilloux et al., 2012; Lee and Kim, 2010; Sen et al., 2008). Similar parallel findings regarding other factors have been described and led to multiple new hypotheses including the γ-aminobutyric acid (GABA)-ergic (Chang et al., 2014; Lin and Sibille, 2013; Luscher et al., 2011) or glutamatergic hypothesis of depression (Popoli et al., 2011; Sanacora et al., 2012). It is important to mention that these hypotheses are not exclusive. For example, scopolamine (a newly identified rapid acting antidepressant) exerts its antidepressant effect through blockade of the muscarinic receptors present on the GABAergic neurons (Anacker, 2018; Drevets et al., 2013; Wohleb et al., 2017) and increases BDNF release

(Ghosal et al., 2018; Wohleb et al., 2017). Ketamine, the first identified rapid acting antidepressant (Andrade, 2017; Wohleb et al., 2017), a selective antagonist of the N-methyl-D-aspartate (NMDA) receptor (Abdallah et al., 2016; Strasburger et al., 2017; Wohleb et al., 2017), was found to exert its antidepressant effect through increased BDNF release (Cavalleri et al., 2018; Choi et al., 2017; Wohleb et al., 2017), increased 5HT levels (Pham and Gardier, 2019), and was shown to induce synaptogenesis within 24 hours (Li et al., 2010) in animals subjected to chronic stress (Li et al., 2011). The synaptogenic effect of ketamine (and scopolamine, Voleti et al., 2013) may counteract the reduced spine density and neuronal atrophy seen in MDD (Kang et al., 2012, see section 2.3 for details).

2.2 Chronic Stress Based Rodent Models

One of the common approaches to model aspects of human MDD pathology, either behavioural or cellular, in rodents employs the use of chronic stress-based paradigms (Nollet et al., 2013; Willner and Belzung, 2015). Current models use environmental, physical, or endocrinological approaches to study depressive-like symptomology in animals. These models include chronic stress exposure such as the chronic unpredictable stress (Willner, 2005), chronic restraint stress (Wood et al., 2008), or chronic exposure to social defeat (Takahashi et al., 2017). Other models may be more physical, such as foot shock or learned helplessness, but are critically closer to models of post-traumatic stress disorder than depression (Cryan and Mombereau, 2004). Additionally, models may use transgenic approaches such as knockout of receptors or transporters (e.g. glucocorticoid receptor or glutamatergic transporter) (Perona et al., 2008; Soderlund and Lindskog, 2018), or are specific to rodent physiology such as olfactory bulbectomy (OBX) (Morales-Medina et al., 2017; Rajkumar and Dawe, 2018). Since rodents strongly rely on their sense of smell, OBX was shown to induce depressive-like behaviours (Morales-Medina et al., 2017; Rajkumar and Dawe, 2018; Song and Leonard, 2005). Pharmacological approaches, including chronic corticosterone administration (Bai et al., 2018; Guarnieri et al., 2012; Ma et al., 2018), have also been used to induce depressive-like deficits. These models are traditionally employed in adult animals but it is important to mention the existence of specific stress models that measure the impact of early-life stress in adulthood, such as prenatal stress (Fatima et al., 2017; Sickmann et al., 2018) or maternal separation (Olivier et al., 2013; Vetulani, 2013). In this section I will focus on the chronic restraint stress (CRS) and the unpredictable chronic mild stress (UCMS) paradigms since they are the 2 models primarily

used to study neuronal/synaptic morphology (see Qiao et al., 2016) and astroglial function in the context of depression (Banasr et al., 2010; Banasr et al., 2007; Miguel-Hidalgo et al., 2018; Simard et al., 2018).

Chronic Variable Stress: Chronic variable stress is a generic term that encompasses various models including unpredictable chronic mild stress (UCMS) or chronic unpredictable stress (CUS). These procedures involve subjecting animals to mild or variable stressors on a randomized schedule over an extended period of time (usually for a minimum of 3 weeks) (Bambico et al., 2019; Castanheira et al., 2018; Cryan and Sweeney, 2011; Ferreira et al., 2018; Mahar et al., 2014; Willner, 2017a, b). The UCMS and CUS are extensively used to study depressive-like behaviour and cellular changes associated with chronic stress exposure that potentially parallel human MDD behavioural or cellular pathology (Banasr et al., 2017; Hamani et al., 2012; Li et al., 2011; Prevot et al., 2019b). Exposure to UCMS or CUS induces behavioural deficits that include helplessness- (Strekalova and Steinbusch, 2010; Valentine et al., 2008), anhedonia- (Banasr and Duman, 2008; Hamani et al., 2012; Mahar et al., 2014; Papp et al., 2017), and anxiety-like deficits (Belzung and Lemoine, 2011; Soumier and Sibille, 2014). The main issue with this paradigm is the variability in response at the behavioural and cellular levels, in particular as the individual stressors are, by definition, 'mild'. A recent survey of UCMS paradigm users reports that one-fifth of experimenters have difficulties replicating their results (Willner, 2017b). Because of mild nature of the stressors and small magnitude changes in neuronal morphology classically documented (see below section synaptic section), we decided that the CRS model might be better-suited and more practical for trajectory analysis, such as in the present study.

Chronic Restraint Stress: The CRS paradigm requires restricting the animal's movement during 15 minutes to 6 hours, and for 7 days to 5 weeks, depending on the studies (see Qiao et al., 2016). The CRS model can be criticized for its weaker face validity compared to the UCMS or CUS models regarding MDD, and for the potential risk of habituation when the same stressor is applied. However, many studies report physical deterioration, anxiety- and anhedonia-like (Ampuero et al., 2015; Strekalova et al., 2004) behavioural deficits in animals subjected to CRS similar to UCMS or CUS. Indeed, CRS studies have shown increased anxiety-like behaviour in the elevated plus maze and open field tests (Gameiro et al., 2006; Manchanda et al., 2011), in the novelty suppressed feeding and the phenotyper tests (Prevot et al., 2019b). One element of high

relevance in the context of my study is that CRS model is widely used to assess morphological and synaptic changes induced by chronic stress in the PFC and in the hippocampus (Donohue et al., 2006; Imbe et al., 2012; Lowery-Gionta et al., 2018; Qiao et al., 2016; Zhang et al., 2019).

2.3 Importance of Morphological Changes in Depression

Macromorphological changes: Imaging studies have shown that volumetric changes within specific brain regions of the corticolimbic circuit occur in brains of MDD patients (Arnone et al., 2012; Konarski et al., 2008; Maller et al., 2018). These changes, usually identified using structural MRI (magnetic resonance imaging), were related to changes in activity or connectivity of these brain regions, which were determined using fMRI (functional magnetic resonance imaging) (Hariri and Holmes, 2015). More precisely, brain imaging studies reported that patients with MDD showed volumetric changes in the prefrontal cortex (Drevets et al., 2008; Nakano et al., 2014; Scheinost et al., 2018), hippocampus (Bremner et al., 2000; Hamilton and Gotlib, 2008; MacQueen et al., 2003; Sheline et al., 2019), and the amygdala (Bremner et al., 2000; Frodl et al., 2008; Hamilton and Gotlib, 2008). Other studies have shown reduced grey matter in various cortical regions such as the anterior cingulate cortex and medial orbitofrontal cortex, as well as the thalamus and nucleus accumbens (Ancelin et al., 2018; Disabato et al., 2014; Hastings et al., 2004). Some of these volumetric changes were shown to be directed correlated with the duration of the illness (MacQueen et al., 2003), and were reversed/normalised in remission or in patients taking antidepressant medications (Arnone, 2019; Chen et al., 2007; Dusi et al., 2015; Frodl et al., 2008).

Neuronal changes: These macromorphological changes have been attributed to neuronal and glial alterations (Banasr et al., 2011; Cobb et al., 2013). Growing evidence from post-mortem studies report increased microglial and decreased oligodendrocytes density, morphology, and function in MDD brains (Miyata et al., 2015; Pepper et al., 2018; Singhal and Baune, 2017; Yirmiya et al., 2015). However, in this thesis we will limit our focus to the glutamatergic neuron/synaptic (see in this section) and astroglial changes (see section 2.4) associated with MDD (in humans) and chronic stress (in rodents), with particular attention to changes found in the PFC.

Historically, post-mortem studies have reported neuronal atrophy as well as reduced size of neurons, but there were inconsistent findings regarding reduced neuronal density in the PFC and

hippocampus (Boku et al., 2018; Cotter et al., 2002; Qiao et al., 2016). Parallel rodent studies using chronic stress models described similar neuronal atrophy in these brain regions (Qiao et al., 2016). Few key studies suggest that chronic stress may not induce neuronal loss since these neuronal atrophy can be reversed after a stress-free period (Qiao et al., 2016) or antidepressant treatment (McEwen et al., 1997). Other studies have shown decreased neuronal marker expression in the PFC but not actual numbers of cells in MDD post-mortem brains (Rajkowska et al., 2007; Seney et al., 2015). The dendritic shrinkage of the pyramidal neurons of the PFC and altered dendritic complexity (Kang et al., 2012) may be associated with reduced synaptic proteins as well as physical number of synapses (Kang et al., 2012). The same changes were initially identified in rodents subjected to CRS in the PFC and the hippocampus (Cook and Wellman, 2004; Radley et al., 2006; Radley et al., 2004), and shown to translate into reduced synaptic protein expression (Kang et al., 2012; Li et al., 2011; Voleti et al., 2013). Post-mortem and preclinical studies report that neuronal atrophy or impaired function affects both glutamatergic and GABAergic neurons (see review by Duman et al., 2019). In short, there are decreases within both the glutamate and GABA neurotransmitter systems leading to decreased cellular markers (mRNA and protein), signal to noise ratio, and synapse-associated receptors (Duman et al., 2019). These findings suggest that atrophy is occurring but not necessarily apoptosis, thus shifting focus towards a more synapse-centered hypothesis of depression.

Synaptic protein changes: Decreased both pre- and post-synaptic proteins were reported in post-mortem and preclinical studies. For example, Kang et al. (2012) found a decrease in synaptic-function–related genes (including the vesicle release protein synapsin 1 (Syn1)) in the dorsolateral PFC of subjects with MDD, a finding replicated by Li et al (2011) and Mitra et al. (2018) using stress-based rodent models. In glutamatergic neurons, the vesicular glutamate transporter (vGLUT1) is important for packaging glutamate inside the vesicles, and it was found reduced in post-mortem MDD brains and rodents subject to stress (Uezato et al., 2009; Zink et al., 2010). Additional rodent studies have shown vGLUT1 knockout mice displayed higher levels of anhedonia-like behaviour compared to wild type controls (Garcia-Garcia et al., 2009; Munoz-Cobo et al., 2017; Yu et al., 2018). Similarly the post-synaptic scaffolding protein post-synaptic density 95 (PSD95) was shown to be decreased in the PFC in MDD brains (Doucet et al., 2012; Feyissa et al., 2009; Karolewicz et al., 2009), and in CUS and CRS models (Li et al., 2011; Qiao et al., 2016; Voleti et al., 2013).

Glial changes: Astroglial changes in MDD and chronic stress models will be addressed at length in the next section, but it is important to mention that microglia and oligodendrocytes also are affected in MDD.

Microglia are resident immune cells of the nervous system and are involved in regular maintenance and inflammation responses, in healthy and pathological conditions (Wolf et al., 2017). In MDD, most studies describe increases in activated microglia in size and number (Mechawar and Savitz, 2016; Reus et al., 2018; Wohleb et al., 2016) as well as increased inflammatory cytokines such as interleukin-1β and tumor necrosis factor-α (Reus et al., 2015). The consistency in changes demonstrating activated microglia in MDD gave rise to the "inflammatory hypothesis of depression" (Steiner et al., 2011). Chronic stress-based studies reported similar findings in rodents, and administration of drugs that inhibit microglial activation reverses behavioural deficits induced by chronic stress (Wang et al., 2018).

Oligodendrocytes are responsible for myelination of axons and creating white matter tracts in the normal brain (Bradl and Lassmann, 2010). Studies have described decreased oligodendrocyte function, genes, density, and ultrastructure in post-mortem brains of MDD patients (Edgar and Sibille, 2012; Pantazatos et al., 2017; Rajkowska et al., 2015; Rajkowska and Miguel-Hidalgo, 2007) reflected in compromised white matter integrity (Miguel-Hidalgo et al., 2017; Miyata et al., 2016; Sacchet and Gotlib, 2017). These changes were also observed in chronic stress rodent models, with detrimental changes occurring as early as one week following stress (Edgar and Sibille, 2012; Liu et al., 2018).

2.4 Astrocytes in Depression

2.4.1 General Aspects Concerning Astrocytes

In the brain, astrocytes are responsible for many functions including ion homeostasis, providing nutrients to neurons, neurotransmitter and hormone recycling, structural and trophic support, and maintaining the extracellular space to name a few (Singh and Abraham, 2017; Vasile et al., 2017; Verkhratsky et al., 2017). Astroglia represent ~40% of all brain cells, have a 1:1 ratio of abundance compared to neurons, and are highly heterogeneous between species and brain areas (Verkhratsky et al., 2017). During development, astrocytes have region-specific differences that aides in the formation of the correct type of synapse in the forming brain (Testen et al., 2019). Sex-specific astroglial differences in formation and response are also found due to regulation by

gonadal hormones (Bollinger et al., 2019; Chowen et al., 2018; McCarthy et al., 2003). Although there are almost as many types of astrocytes as there are neurons, they are usually separated into protoplasmic (located in grey matter) or fibrous (located in white matter) astrocytes, and are important in the fabrication, organization and maintenance of extracellular matrix as well as maintenance of neurons (Wiese et al., 2012). Over the past years, astrocytes have emerged as important regulators/maintainers of synaptic function and synaptogenesis, in addition to clearing glutamate from synapses to avoid excitotoxicity (see Elsayed and Magistretti, 2015) . Astrocytes are involved in regulating the formation, size, maturation and elimination of synapses (Kucukdereli et al., 2011; Risher et al., 2014). Additionally, each astrocyte is involved in the regulation of 100 000 synapses (Allen and Eroglu, 2017). Altogether, substantial evidence demonstrate that astrocytes are crucial for neuronal function and plasticity (Bolton and Eroglu, 2009; Eroglu and Barres, 2010). Although this will not be addressed in this thesis, it is important to mention that astrocytes are also involved in regulating the function of all the cells in the brain including microglia, oligodendrocytes, or endothelial cells (Domingues et al., 2016; Jha et al., 2019; Kiray et al., 2016) . In this section, we will focus on markers specifically expressed by astrocytes in the cortex and known to be affected in MDD and chronic stress models.

2.4.2 The Glutamatergic Tripartite Synapses

One of the primary roles of astrocytes in regulating neuronal functions is the tight modulation of the neurotransmitter function of GABA and/or glutamate tripartite synapses (Elsayed and Magistretti, 2015; Haydon, 2001; Martin and Rimvall, 1993; Risher et al., 2014; Schousboe and Waagepetersen, 2006; Serrano et al., 2006; Yoon et al., 2012). Neurons rely on astrocytic participation to synthesize and metabolize GABA and glutamate *de novo* (Martin and Rimvall, 1993). In the glutamatergic tripartite synapse (Figure 1), glutamate is released by neurons and binds to its receptors including post-synaptic α-amino-3-hydroxy-5-methyl-4-isoxazolepropionic acid (AMPA) or NMDA receptors, which are maintained at the membrane surface via a scaffolding protein called post-synaptic density 95 (PSD95) (Chen et al., 2011; Sun and Turrigiano, 2011). Excess glutamate is up taken by astrocytes via the high affinity glial glutamate transporters (GLT1 and GLAST) or the neuronal transport EAAT3 (Figure 1). In the astrocytes, glutamate is then converted to glutamine via glutamine synthetase (GS) (Suarez et al., 2002). Glutamine re-enters the pre-synaptic neuron where it is converted back to glutamate via glutaminase (Hertz et al., 1999; Schousboe and Waagepetersen, 2006), which is then transported

back into vesicles via vesicular glutamate transporter including vGLUT1. This process is called the astroglial glutamate-glutamine shuttle and the aforementioned proteins will be the focus of this thesis (Figure 1).

2.4.3 Astrocytes in Post-Mortem MDD Brains

Considering the tight relationship between astrocytes and synapses, and the fact that MDD/ chronic stress alters synapse morphology and function (Duman and Duman, 2015; Duman et al., 2016; Qiao et al., 2016), it is not surprising that astroglial dysfunction are found in MDD. Indeed, post-mortem studies of brain tissue from adult MDD patients consistently report reduced number, density, and size of glial cells (Cotter et al., 2002; Cotter et al., 2001; Ongur et al., 1998; Rajkowska, 2000; Rajkowska and Miguel-Hidalgo, 2007; Rajkowska et al., 1998). Rajkowska et al. (1998) found a reduction in both density and size of neurons and glial cells in the supragranular and infragranular layers of the dorsolateral PFC. Many studies have described significantly lower protein and mRNA levels of the microtubule associated protein glial fibrillary associated protein (GFAP) in limbic regions including dorsolateral PFC, orbitofrontal cortex, anterior cingulate cortex, and hippocampus (Meyer, 2017; Miguel-Hidalgo et al., 2010; Si et al., 2004). Similarly, post-mortem studies have found decreases in GS densities in the cortical regions, and reduced methylation levels in the genes encoding for GS (Bernstein et al., 2015; Nagy et al., 2015). GLT1 levels were also seen reduced in the PFC and striatum of depressed patients (Rappeneau et al., 2016; Takahashi et al., 2015; Zhao et al., 2016). Other studies have reported reductions in specific markers of astroglial cell function (Miguel-Hidalgo et al., 2010; Nagy et al., 2015), including aldehyde dehydrogenase 1 family member L1 (ALDH1-L1) and connexion-43, clearly suggesting reductions in astroglia number and function in MDD (Choudary et al., 2005; Miguel-Hidalgo et al.; Nagy et al., 2015). For details see review by Sanacora and Banasr (2013).

2.4.4 Astrocytes in Stress-Based Rodent Models

Parallel reports have described decreased number of GFAP+ cells in the hippocampus following chronic stress exposure (Czeh et al., 2006). Importantly, these findings are numerous and highly consistent in the PFC. Specifically, reduced levels of GFAP mRNA expression, number of GFAP+ cells and reduced glutamate/glutamine cycling were found in rodent subjected to CUS (Banasr et al., 2010; Banasr and Duman, 2008; Gosselin et al., 2009). Additionally, loss of

GFAP+ cells (via ablation or gliotoxin) in the PFC induces anxiety- and anhedonia-like behavioural deficits similar to those seen following chronic stress (Banasr and Duman, 2008; Banasr et al., 2014). Altering astroglial function in the amygdala also produces anxiety-like (via blockade and activation) and anhedonia-like (via blockade) behaviours in rodents (Martin-Fernandez et al., 2017). In addition, UCMS mice displayed decreased GS expression levels, and GS inhibition induces anhedonia-like behaviour, which is reversible by intracerebral infusion of L-glutamine (Lee et al., 2013; Rao et al., 2016). This suggests that impairing glutamate-glutamine conversion may alter depressive-like state of the animals. In parallel, the GLT1 expression levels were also found decreased in animals subjected to stress; similarly, glutamine supplementation rescues GLT1 expression and behavioural effects (Baek et al., 2019; Zink et al., 2010). Importantly GLT1 knockout or blockade induces anhedonia-like behaviour in rodent (Cui et al., 2014; John et al., 2012; John et al., 2015). Other key markers expressed by astrocytes including aquaporin-4 and connexin-43 were shown to be reduced in chronic stress animals (Bernard et al., 2011; Ernst et al., 2011; Rajkowska et al., 2013; Rajkowska and Stockmeier, 2013; Sun et al., 2012). It is important to note that while not all astrocytes express detectable amount of GFAP in healthy tissues, and may express other astroglial markers such as S100β, chronic stress-induced effects on astrocytes appear selective to GFAP+ astroglial while cortical S100β+ cell density remains unaffected by chronic stress (Cobb et al., 2013; Gosselin et al., 2009; Miguel-Hidalgo et al., 2000; Miguel-Hidalgo et al., 2002; Nagy et al., 2015; Rajkowska and Stockmeier, 2013; Torres-Platas et al., 2016). For these reasons, we opted to use the GFAP promoter for transgenic studies for targeting this astrocyte population in our experiments. Finally, most rodent studies focused either on the synaptic changes or on astroglial changes independently and no correlations or links were made between the two compartments nor to behaviour, a primary aim of the present work.

3 Materials & Methods

3.1 Animals

In this study, we used three mouse lines to conduct the designed experiments and achieve our aims. The first experiment was performed on adult male and female C57BL/6 mice (wild-type mice purchased from Jackson Laboratories, Bar Harbor, Maine, USA), the second required transgenic mice expressing GFP (green fluorescent protein) under an astrocyte specific promoter

(GFAP-GFP mice on a C57BL/6 background generated in our colony), while the third necessitated mice expressing Cre under the GFAP promoter (GFAP-Cre mice on the same background purchased from Jackson Laboratories and bred in our facility). All animals were housed under normal conditions, an artificial 12h light/dark cycle (light from 7:00-19:00) with *ad libitum* access to food and water, except when deprived for testing. To allow for individual monitoring of sucrose or water intake and weekly behavioural assessment, all animals (including control groups) were single-housed the week before the beginning of the stress experiments. All procedures and experiments followed guidelines set by the Canadian Council on Animal Care (CCAC) and approved by Centre for Addiction and Mental Health (CAMH) animal care committee (ACC).

Experiment 1: Eight-week-old male and female C57BL/6 (Jackson Laboratories) were allowed 2 weeks of habituation to the animal facility conditions before the start of the experiment. This experiment required 6 animal groups subjected to different durations of CRS exposure mice (n=16/group, 50% female), entailing 96 animals in total. Because of the workload associated with such large sample size, this experiment was split in two identical cohorts of 38 each (6 groups, n=8/group, 50% female). As the first cohort was antecedent to my arrival in the lab, I was only responsible for conducting the behavioural and cellular analysis of the second cohort, and data pooling and analysis of both studies. Results from the pooled analysis are presented in this thesis.

Experiment 2: The FVB/N-Tg(GFAPGFP)14Mes/J transgenic mice (Jackson Laboratories, stock #003257) were backcrossed with wild type (WT) C57BL/6 mice for five generations to generate the GFAP-GFP mouse line on C57BL/6 background used in this study. Then, GFAP-GFP mice were harem bred (one wild type C57BL/6 male with two heterozygous GFAP-GFP females) to generate the 32 GFAP-GFP+ mice required for the second experiment. The GFAP-GFP negative animals were euthanized.

Experiment 3: C57BL/6.Cg-Tg(Gfap-cre)77.6Mvs/2J transgenic mice (Jackson Laboratories, stock #024098) were harem bred (one heterozygous GFAP-Cre+ male with two wildtype females from Jackson Laboratories) to generate the animals required for the 3rd experiment. This entailed the validation of the plasmid before we could infuse the virus in the PFC of animals. For this set of experiments, primary astrocytes cultures were generated from P0 pups (*N*=12 GFAP-Cre+,

N=41 wild type littermates) and used for the in vitro studies (western blot analysis and immunocytochemistry).

At P21, the CAMH animal facility staff conducted the weaning, ear tagging, and genotyping of the animals, using the following primers: GFAP-Cre mouse line (Forward: TCCATAAAGGCCCTGACATC, Reverse: TGCGAACCTCATCACTCGT); GFAP-GFP mouse line (Forward: AAGTTCATCTGCACCACCG, Reverse: TCCTTGAAGAAGATGGTGCG). For the in vitro experiments, I collected tails from the P0 pups and the animal facility staff conducted the genotyping.

3.2 Chronic Restraint Stress

In this thesis, we used the CRS paradigm to induce depressive-like behaviours in mice. The restraint stress procedure consisted of placing each mouse in a custom-made Falcon® Tube (with a hole at the bottom and on the cap to allow air to flow), twice a day, every day for various durations (see experimental design Figure 2). The tube containing the animal was placed back horizontally inside the home-cage and the animal was released after 1h. Animals belonging to the CRS groups were housed without environmental enrichment to prevent blunting the effects of CRS. In addition, CRS animals were housed in a different room from the control group to prevent smell and noise disturbances from the CRS procedure to affect the controls. Throughout the experiment, control animals were handled daily.

As illustrated in Figure 2A, animals from Experiment 1 were divided in 6 groups subjected to CRS of either 0, 1, 2, 3, 4, or 5 weeks (16 animals per group, 50% females) to examine the trajectory of the behavioural effects of chronic stress on behaviour and their potential link to astroglial and synaptic protein expression changes in the PFC. Animals from Experiment 2 were subjected to either 0, 1, 3, or 5 weeks of CRS (8 animals per group, 50% females) to determine the effects of chronic stress on astroglial morphology in GFAP-GFP mice (Figure 2B).

3.3 Behavioural Assessments

All animals from Experiment 1 were behaviourally assessed in each test, once, on the last week of experimentation (see Figure 2A). All animals from Experiment 2 were tested at baseline (one week before the start of the CRS procedure) and on a weekly basis during the experiment (see Figure 2B). For each study, the experimenters were blinded to the mouse treatment history.

3.3.1 Coat State Assessment

Coat state was evaluated following the method described by Yalcin et al. (2005): seven body parts were assessed (head, neck, dorsal coat, ventral coat, tail, forepaws, and hind paws) and a score of 0, 0.5, or 1 was given to each body part. A score of 0 was attributed to a good coat state and a score of 1 to a dirty, deteriorated fur. Intermediary score of 0.5 could be assigned if the area is just starting to look deteriorated. Scores from each area were summed to present the overall deterioration score of the animal's coat state.

3.3.2 Sucrose Preference

The sucrose consumption test was used to assess anhedonia-like behaviour. Animals were habituated to a 1% sucrose solution for 48h. Mice were then fluid deprived overnight from 6pm to 10am. At 10am, the animals were given access to a bottle filled with 1% sucrose solution and the consumption (ml) was measured for a 1h period. The same design of water habituation, deprivation and 1h consumption test was used to measure water consumption.

For repeated sucrose consumption testing, animals were re-habituated to sucrose every week for only 24h prior to the fluid deprivation and tested for 1h as above. Sucrose and water tests were performed in the same environmental conditions for the same duration.

Sucrose preference was calculated as:

$$Sucrose\ Preference\ (\%) = \frac{\text{Sucrose consumption}}{(\text{Sucrose consumption} + \text{water consumption})}\ x\ 100$$

Two animals from Experiment 2 had to be removed from the analysis as they did not drink during the test.

3.3.3 Phenotyper Test

The phenotyper test is a recently designed assay developed in the lab that measures conflict anxiety-like behaviour in mice (Maluach et al., 2017; Nikolova et al., 2018; Prevot et al., 2019b). Each animal was placed in a PhenoTyper® (Noldus: Leesburg, VA, USA) apparatus, which consist of a home cage-like 30cm square arena with delineated food and shelter zones. A spotlight is located over the food zone that can be controlled by a computer, and an infrared camera in the box's ceiling records the animal's behaviour during the dark cycle. After 1h for habituation (6pm-7pm), the animals were monitored for a 12h period (7pm-7am). This test

allows for observation of the animal's normal behaviour (4h baseline) as well as their response during and after an aversive stimulus applied for 1h (spotlight challenge from 11pm-12am). Hourly time spent in either the food or the shelter zone before, during and after the challenge was quantified using the Ethovision® software.

Residual Avoidance calculation: Based on previous finding from our group, the common indicator of anxiety-like behaviours in this test across stress models (UCMS, CRS) is the continued reluctance of the stress-exposed animals to leave the shelter zone, even after termination of the light challenge. This indicator is calculated for the 5 hours duration following the light challenged and is called "Residual Avoidance in the Shelter Zone (RA)" (see details in Prevot et al., 2019b). In this case, greater time spent in the shelter zone after the light challenge indicates higher anxiety-like behaviour. The RA was calculated as follows ("Time" is the time spent in the shelter zone):

$$\left(\frac{\sum Time_{(12am-5am)} - Time_{(11pm-12am)}}{Average\ Control\ Group\ [\sum Time_{(12am-5am)} - Time_{(11pm-12am)}]} - 1\right) \times 100$$

The RA calculation provides a quantitative measure of how stress-exposed animals react after the light challenge compared to controls. Control animals have a RA of zero while positive RA means the animal favours the shelter zone.

3.4 Sample Preparation and Western Blot Analysis

Animals from Experiment 1 were euthanized via live decapitation the day after the last behavioural testing and 24h after the last CRS session. The brains were removed from the skull and placed on an ice-cold glass platform where the PFC of one hemisphere was dissected and collected for RNA/protein extraction. The other hemisphere was kept intact and frozen on dry ice for downstream experiments outside the scope of this thesis. RNA and proteins were extracted from the PFC samples using the Allprep RNA/protein Kit (Qiagen, Toronto, Ontario, Canada). PFC samples then were lysed with 300 µL lysis buffer (0.1% SDS (sodium dodecyl sulphate), phosphatase inhibitor (Roche, Mississauga, Ontario, Canada), protease inhibitor (Roche)), homogenized, sonicated and vortexed before following the kit instructions and running the homogenates through the protein cleanup column and RNAeasy spin column (Qiagen). After

protein and RNA extractions, samples were kept at -80C until further investigation. This thesis focuses on the data collected from the protein sample analysis.

Protein concentration from PFC or primary culture homogenates (see below section 3.9) was measured using the Pierce BCA (Bicinchoninic Acid) Protein Assay Kit (Thermofisher, Massachusetts, USA). 20µg of protein were separated onto pre-cast gels (BioRad Criterion TGX Stain-Free Precast Gels, 4-20%; Mississauga, Ontario, Canada). Total protein was imaged using a molecular imager (ChemiDoc XRS, BioRad) and quantified with ImageLab™ software prior to transferring the gel onto a nitrocellulose membrane (Trans-Blot Turbo Transfer System, BioRad). Membranes were washed in 1X TBS-T (Tris buffer saline-tween 20), blocked in 3% bovine serum albumin (BSA) or 5% skim milk in 1X TBS-T for 1h, washed 3 times with 1X TBS-T and incubated overnight at 4°C with 1° antibody in 3% BSA. We used primary antibodies against the 3 main astroglial markers (GFAP, GS, GLT1) and 3 synaptic markers associated primarily with glutamatergic neurotransmission (vGLUT1, Syn1, PSD95) for Experiment 1. Refer to Table 1 for antibody lists and buffers combination used for western blot analysis. Membranes were then washed and incubated with 2° antibody in 5% milk for 1h at room temperature (see Table 1). Enhanced chemiluminescence (ECL) substrate (Clarity Western ECL Substrate BioRad) was used to detect protein bands which were analyzed with ImageLab™ software. For further western blotting, membranes were stripped with stripping buffer (62.5 mM Tris-HCl, 2% SDS, 0.7% β-mercaptoethanol), washed, blocked and re-incubated with primary antibody. Membrane was discarded after a maximum of 2 strippings.

3.5 Sample Preparation and Immunostaining

For experiment 2, animals were anesthetised with avertin (125mg/kg, i.p.) and intracardially perfused with 4% paraformaldehyde (PFA, pH 7.4), at a speed of 250mL/h using a Pharmacia pump (Cole-Parmer Model 07554-90, Montreal, Quebec, Canada). The brains were post-fixed in 4% PFA overnight at 4°C, cryoprotected in a 30% sucrose solution (48h at 4°C) and frozen on dry ice before being stored at -80°C until sectioning. Using a cryostat (Leica CM1950, Buffalo Grove, Illinois, USA), 40µm-thick sections containing the PFC regions were cut, placed in 12-well plates containing cryoprotectant (30% sucrose, 1% PVP-40, 30% ethylene glycol) and stored at -20°C until immunohistochemistry.

Free-floating sections were washed thrice for 10 mins in 0.3% PBS (phosphate buffer saline)-TritonX (PBS-T), then incubated with 3% H_2O_2 in PBS for 20 mins at room temperature. After 2 PBS-T washes (10 min) washes, sections were blocked for 1h at room temperature in 10% normal donkey serum (NDS) in PBS-T, then incubated with 1° antibody (diluted in 3% NDS PBS-T) for 48h at 4°C. Sections were then washed with PBS and incubated in the 2° antibody (in 1X PBS) for 2h at room temperature. Following multiple PBS washes, sections were mounted onto glass slides with a brush, and cover-slipped with mounting media with or without DAPI (4',6-diamidino-2-phenylindole) (Vector Laboratories H-1500 or H-1400, respectively; Burlington, Ontario, Canada). Slides were labelled, coded for blinding, and kept horizontally in 4°C until imaging. For Experiment 2, a subset of sections was used to first validate the transgenic GFAP-GFP line, using double labelled for GFP and antibodies against either GFAP (astroglial marker), Iba1 (ionised calcium binding adaptor molecule 1, microglial marker), or NeuN (neuron nuclei protein, neuronal marker). Refer to Table 2 for 1° and 2° antibodies used. Then, on a separate set of sections that included all animals, we performed immunohistochemistry against GFAP and GFP for the Sholl analysis necessary for Experiment 2. For Experiment 3, immunocytochemistry was conducted on HEK293 cells and astrocytes from primary cultures using similar antibodies and procedures as detailed here, except cells were fixed on coverslips prior to immunostaining (see section 3.9).

3.6 Confocal Microscopy and Sholl Analysis

A total of 6 GFAP+ and 6 GFP+ cells from the PFC of each animal were imaged using the Olympus Confocal microscope (Olympus, Center Valley, Pennsylvania, USA) with oil-based 100X objective. Non-overlapping immunopositive cells were selected for most accurate Sholl analysis measurements. For each cell, the Z-axis diameter was determined by identifying the upper and lower Z-plane, and the average was defined as middle of the astrocyte or Z0 (Figure 3C,J). Five (GFAP+ cells) or 3 (GFP+ cells) z-stacks equally spanning Z0 (z-step = 5µm or 10 µm, respectively) were imaged using the FluoView FV10-ASW 4.0b software. The chosen z-steps for each cell type was determined based on pilot acquisition and quantification trials optimised for process visualization despite considerable astrocyte complexity (Figure 3O-P). The images were saved as .TIFF and opened in ImageJ's plug-in FIJI (Maryland, USA) (Schindelin et al., 2012). Each cell's stack was z-projected using max intensity. Resulting images were converted to 8-bit, optimized for brightness-contrast before thresholding with minimal

background noise. Maximum surface (AREA) of each GFAP+ and GFP+ cell was determined using a circle of a radius, set by a straight line drawn from the middle of the soma to the end of the most distal process. For the Sholl analysis, we used the aforementioned radius and radius step size, set as one-tenth of the total radius length for each GFAP+ and GFP+ cells. Fixed radius steps allowed for comparing number of intersections across cells and groups, independently from potential bias due to cell length or size. Number of intersections per radius step, defined as number of times processes cross each delineated circle (see Figure 3), as well as the total number of intersections (sum of intersections for all 10 radius steps) were measured automatically. To normalize the number of intersections to the cell-size, total number of intersections was divided by AREA for each cell.

3.7 HEK293 Cell Cultures

HEK293 cells were maintained in DMEM (Dulbecco's Modified Eagle's medium with high glucose, L-glutamine and sodium pyruvate; Gibco, California, USA) containing 5% fetal bovine serum (FBS) and 1% penicillin-streptomycin (Gibco) in 10cm culture dish (Costar, Austin, Texas, USA) in an incubator at constant temperature and CO_2 concentration (37°C, 5% respectively). Media were changed every 2-3 days until cells reached confluence. Cells were then detached by adding 0.25% trypsin (Gibco, 37°C for 2 mins), and re-plated onto 6-wells plates containing sterilized circular glass coverslips at the bottom for immunocytochemistry. Cells were maintained under these conditions for a minimum of 48h prior to transfection.

3.8 Primary Astrocyte Cultures

GFAP-Cre heterozygous and WT littermate pups were collected within 24h of birth (P0) and kept in a warm (30°C) box with ventilated holes until dissection. Each pup was rapidly decapitated and tail clipped for *a posteriori* genotyping. Under a binocular microscope, cortices of each brain were dissected in sterile PBS and meninges were removed. Cortices were then mechanically dissociated in 2 mL regular astrocyte media (RAM: 1X DMEM, 10% inactivated FBS, 5% inactivated horse serum (Sigma, Oakville, Ontario, Canada), 1% penicillin-streptomycin (Gibco). Cell suspension was then diluted into a total of 12ml RAM and plated onto 6-well plates (2 mL per well). Cells were maintained in RAM for 12 days (media changed every 3-4 days) at 37°C with 5% CO_2. This medium allowed for astrocyte proliferation, and cells reached confluence within 2 weeks. On Day 12, RAM was switched to defined astrocyte media

(DAM) containing 1X DMEM, 0.5mg/mL BSA, 5µg/mL human insulin, 1% penicillin-streptomycin and 250µM dBcAMP (dibutyryl cyclic adenosine monophosphate, Sigma). Cells were maintained under these conditions for a minimum of 7 days (media changed every 3-4 days). This medium allowed astrocyte differentiation and astroglial processes were visible within 24-48 h following the switch to DAM. Primary astrocyte cultures were coded and maintained as 'one plate **:** one brain' and then recoded once genotype was identified. Each 6-well plate was divided such that 3 wells were used for immunocytochemistry and contained sterile circular coverslips (Fisherbrand 12-546, Massachusetts, USA) placed at the bottom of the wells, while the wells without coverslips were used for western blot analysis.

3.9 Plasmid Transfection

Plasmids used for transfection included the cytomegalovirus (CMV)-hM3Dq-GFP (purchased from Virovek, Hayward, California, USA), CMV-codon improved Cre (iCre, purchased from Vector Biolabs, Malvern, Pennsylvania, USA), CMV-enhanced GFP (eGFP, purchased from Virovek), and CMV-mCherry (purchased from Virovek). See Figure 4 for details. Importantly, the hM3Dq-GFP plasmid contains 2 sets of *lox* sequences strategically placed around the inverted hM3Dq and GFP coding sequences (separated by a T2A sequence, Figure 4). In the presence of either endogenous (GFAP-Cre cells) or exogenous (cells co-transfected with the CMV-iCre plasmid) Cre, DNA recombination and cleavage occurs and the CMV promoter is expected to drive the expression of hM3Dq and GFP. This is known as the "FLEX-switch" system (for details see Urban & Roth, 2015). For plasmid amplification, competent *E. coli* (Invitrogen, Massachusetts, USA) in lysogeny broth (LB) were transformed with each plasmid. Plasmid containing bacteria were selected using LB-agar plates with ampicillin (100µg/mL; Bioshop, Burlington, Ontario, Canada). Picked colonies were amplified in 75ml LB-ampicillin media. Circular plasmids were purified using a midiprep kit (Qiagen, #12243). DNA from plasmid elution was quantified using a Nanophotometer (IMPLEN P360, Westlake Village, CA, USA). One mL of a standard transfection solution containing 10µL of lipofectamine 2000 (Invitrogen 11668027) and 2.5µg of each plasmid diluted in OptiMem® (Gibco) was applied dropwise to each well of HEK293 cells and cultured astrocytes, and incubated for 6 h (37°C). Note that since HEK293 cells do not express the Cre protein, conditions included co-transfection with Cre expressing plasmid (CMV-iCre). After transfection, HEK293 cells were maintained for 48 h with a low serum concentration media (2% FBS) to limit cells proliferation and subsequent

plasmid dilution. For astrocytes, since dBcAMP is a cell permeable analogue of cAMP and can activate the cells (or increase cFos expression), cells were placed dBcAMP-free DAM the day before ligand exposure.

Forty-eight hours after transfection cells were treated with the ligands, i.e. clozapine-N-oxide (CNO, Tocris 4936; Burlington, Ontario, Canada) or DREADDs agonist 21 (compound 21 or C21, Tocris 5548), diluted at a concentration of 10 µM in vehicle (0.01%DMSO-PBS). Cells were washed with PBS and collected in 100uL lysis buffer (as in section 3.4), 15 minutes after the ligand or vehicle exposure. Cells were sonicated and homogenized, then stored at -80°C until BCA and western blot analysis, which were performed as described in section 3.4. hM3Dq-GFP construct functional validation was conducted on primary astrocyte cultures following ligand exposure. Here, we used the level of phosphorylation of 2 keys kinases of this pathway as an index of activation: MAPK (mitogen-activated protein kinase) and Akt (protein kinase B). Refer to Table 1 for antibodies used.

Additional validation of hM3Dq plasmid cell activation was performed in both HEK293 and astrocyte cultures using cFos immunocytochemistry. In this case, CNO, C21 and vehicle (10 µM) were applied for 1.5h after which the cells were fixed on the coverslips using 4% PFA. Following 1h fixation, and several PBS washes, plates were stored at 4°C until immunocytochemistry. Immunolabelling was conducted using similar procedures and antibodies as described in section 3.5, with the addition of cFos and mCherry antibody (see Table 2).

Time differences in ligand exposure between the 2 assays was strategically chosen for peak detection of phosphorylated MAPK and Akt proteins (Blaukat et al., 2000; Eishingdrelo and Kongsamut, 2013; Law et al., 2016; Murga et al., 1998) or of increased cFos genomic expression (Cullinan et al., 1995; Kazi et al., 2004).

3.10 Calcium Mobilization Assay

The calcium mobilization assay was carried out on HEK293 live cells following the procedure adapted from Uemura et al. (2016). We did not perform this assay in primary astrocyte culture because mouse astrocytes have slight auto-fluorescence in vitro that interfere with the fluorescence of the dye used for calcium mobilization detection. Briefly, the assay was performed with the BD pathway 855 High Cell Content Imaging system (BD Biosciences, San

Jose, CA, USA) at 37°C, 5% CO_2 under subdued ambient light. One day before the assay, cells were transferred from their culture dishes and seeded (2-2.5 $X10^4$) in 96 well imaging plates (BD Bioscience) that had been pre-coated with poly-D-lysine (0.1 mg/mL, Sigma). The day of the assay, cells were gently washed twice with Fura-2 assay buffer (HBS: 20mM HEPES, 140mM NaCl, 5mM KCl, 1.2mM $MgCl_2$, 2mM $CaCl_2$, 10mN glucose, pH 7.4) with 2.5 mM probenecid (Thermofisher) and incubated with Fura-2 dye solution (assay buffer with 5µM Fura-2/AM, Thermofisher) for 30 minutes at 37°C. After incubation, cells were gently washed 3 times with the Fura-2 assay buffer. Cells were left in the third wash and put back in the incubator for an additional 30 minutes at 37°C, prior to acquisition. Images of 5-75 cell bodies or regions of interest (ROI) were captured with a 10X objective. After measurement of the baseline Fura-2 fluorescence ($F_{340/380}$ ratio) for 10 sec, effects of 10 µM CNO, 10 µM C21 or vehicle control (0.01%DMSO-PBS) were assessed. Images were captured every 2 seconds for 80 seconds. Following assay completion, a single image was captured to measure GFP fluorescence (excitation 488nm, emission 510nm) and monitor transfection efficacy for the experiment.

3.11 Statistical Analysis

For Experiment 1, statistical differences between groups were determined by analysis of variance (ANOVA) with sex as factor, followed by Fisher's *post hoc* analysis, on StatView 5 (SAS Institute Inc., Cary, NC, USA). Relationship between behaviour assessment vs. cellular markers and between markers were tested using Pearson's correlation analysis. Pearson's correlation analysis between coat state and protein levels were not conducted since such analysis requires multiple discrete variables to correlate with continuous variables. However, the coat state analysis used here only had 5 measurement points, which was not enough to properly correlate with the protein levels (continuous variable). For behavioural assays performed in Experiment 2, repeated measure ANOVA was used to determine the effects of stress and potential interactions with time and sex. Similarly, repeated measure ANOVA was used to determine the effects of stress on the number of intersections per the radius step. Statistical differences between groups in total intersections/AREA was determined using ANOVA with sex as factor, followed by Fisher's *post hoc* analysis. Relationships between number of intersections and size of the astrocytes (AREA) were determined using Pearson's correlation analysis. For experiment 3, repeated measure ANOVA was used to determine the effects of ligand exposure to different conditions of plasmid (co)transfections for the calcium mobilization assay, while an ANOVA

was used to determine differences in total area under the curve (from time 0 onwards) in the calcium mobilization assay and western blots of phosphorylated/total Akt and MAPK. Fisher's *post hoc* analysis was conducted to determine significance between conditions. All data are expressed as mean ± standard error of the mean (SEM). The level of statistical significance was set at $p<0.05$. Note that we mention some potential trends in the result section, where trend level was set at $0.05<p<0.1$.

4 Results

Experiments were carried out using animal groups consisting of 50% females and analyses were performed using sex as a cofactor. All sex effects will be mentioned in the results section but only the results with significant main effect of sex will be shown as an insert in the corresponding figures.

4.1 Experiment 1 – Effects of CRS on Astroglial and Synaptic protein levels

4.1.1 Behavioural Changes

Coat state, sucrose preference and residual avoidance were performed in animals subjected to 7, 4, 21, 28, 35 days of CRS and compared to controls (Figure 2A).

Coat state: ANOVA of coat state degradation scores, with sex as a factor, revealed a significant main effect of stress ($F_{5,82}=14.98$; $p<0.0001$), a strong trend for an effect of sex ($F_{1,82}=3.78$; $p=0.055$) and no stress*sex interaction (Figure 5A). *Post hoc* analysis identified an increase in coat state deterioration induced by CRS exposure significant for the CRS7 group ($p<0.05$) as well as all the animal groups subjected to at least 14 days of CRS (CRS14-35: $p<0.01$), compared to controls (Figure 5A). On this measure, males showed an overall greater coat state degradation than females (Figure 5A').

Sucrose preference: Similar analysis performed on sucrose preference data showed a significant main effect of stress ($F_{5,79}=2.73$; $p<0.05$) but no significant effect of sex or stress*sex interaction (Figure 5B). Exposure to CRS induced a significant decrease in sucrose preference when animals are subjected to 21, 28 and 35 days of CRS (CRS21 $p<0.05$; CRS28 $p<0.05$; CRS35 $p=0.01$), compared to controls (Figure 5B).

Residual avoidance: Animals were then tested in the phenotyper test and residual avoidance calculated for the shelter zone time after the light challenge. Statistical analysis revealed a significant effect of stress ($F_{5;82}$=10.23; p<0.0001) and sex ($F_{1,82}$= 14.55; p<0.001) with no stress*sex interaction (Figure 6B). *Post hoc* analysis identified that animals subjected to CRS displayed greater time in the shelter zone following the light challenge compared to controls; this increased residual avoidance was significant for all CRS animal groups (CRS7, 14, 21, 28, 35, all p<0.001) (Figure 6B) with the CRS males showing an overall greater residual avoidance than females across groups (Figure 6B').

4.1.2 Western Blotting Results for Astroglial and Synaptic proteins

Western blot analysis of PFC astroglial (GFAP, GS, GLT1) and synaptic (vGLUT1, Syn1, PSD95) markers was performed in animals subjected to 7, 4, 21, 28, 35 days of CRS and compared to controls. These markers were correlated to sucrose consumption and residual avoidance, as well as between each other.

GFAP: ANOVA of GFAP protein expression levels, with sex as a factor, revealed a trend in main effect of stress ($F_{5;82}$=1.96; p=0.092), a significant main effect for sex ($F_{1;82}$=7.59; p<0.01) and no stress*sex interaction (Figure 7B). *Post hoc* analysis identified a significant decrease in GFAP levels induced by CRS exposure at 7, 14, and 28 days (CRS7 p<0.05; CRS14 p<0.05; CRS28 p<0.01), plus trends toward decreased GFAP protein levels at 21 and 35 days of CRS (CRS21 p=0.067; CRS35 p=0.051) when compared to controls (Figure 7B). On this measure, males showed overall higher levels of GFAP than females (Figure 7B').

Correlation analysis showed no significant link overall between GFAP protein levels and residual avoidance (R^2=0.004, p=0.544). However, similar analysis performed separately in males and females showed that GFAP protein levels and residual avoidance negatively correlated in males (R^2=0.16, p<0.01) and not in the females (R^2=0.005, p=0.635) (Figure 7C). Indeed, males with lower levels of GFAP protein expression spent more time in the shelter zone after the light challenge, i.e. displayed greater anxiety-like deficits. In addition, we found a significant positive correlation between GFAP protein levels and sucrose preference (R^2=0.15, p<0.05). Although significant overall (both sexes), this correlation was not significant in the females (R^2=0.003, p=0.698) and was driven by the males (R^2=0.094, p<0.05) (Figure 7D); males with

lower levels of GFAP protein expression displayed lower sucrose preference, i.e. greater anhedonia-like deficits.

GS: ANOVA of GS protein levels, with sex as a factor, revealed no main effect of stress ($F_{5:82}$=1.20; p=0.315), sex, or stress*sex interaction (Figure 8A). Nevertheless, exploratory comparisons between groups identified a significant decrease in GS protein levels in the CRS28 animal group (p<0.05) and a trend towards a decrease for the CRS35 group (p=0.086) when compared to controls (Figure 8A).

We then investigated potential links between GS protein levels and behavioural performances, and found that while the GS protein levels in males significantly correlated with both sucrose preference (positively, R^2=0.16, p<0.01) and residual avoidance (negatively, R^2=0.12, p<0.05), no correlation was found in females (sucrose preference: R^2=0.009, p=0.524; residual avoidance: R^2=0.002, p=0.755). Males with lower levels of GS protein expression displayed lower sucrose preference and greater residual avoidance, i.e. greater anhedonia- and anxiety-like deficits respectively (Figure 8B-C). Note that this effect in males translated into an overall (both sexes) trend towards correlations between GS protein levels and sucrose preference (R^2=0.03, p=0.059) or residual avoidance (R^2=0.03, p=0.070) (Figure 8B-C).

GLT1: ANOVA of GLT1 protein levels, with sex as a factor, revealed no main effect of stress ($F_{5:68}$=0.69; p=0.626), sex, stress*sex interaction (Figure 9A). Nevertheless, exploratory comparisons between groups identified a trend towards a decrease in GLT1 protein levels after 35 days of CRS exposure (p=0.075) when compared to controls (Figure 9A).

A significant negative correlation was identified between GLT1 protein levels and residual avoidance (R^2=0.06, p<0.05). As with GFAP and GS protein levels, low GLT1 protein levels was associated with greater time in the shelter following the light challenge, i.e. greater anxiety-like deficits in males (R^2=0.27, p<0.001) and not in females (R^2=5.94e-5, p=0.964) (Figure 9B). In addition, we found a significant positive correlation between GS protein expression and sucrose preference, overall (R^2=0.16, p<0.001) and in both males (R^2=0.21, p<0.01) and females (R^2=0.17, p<0.05) when analysed separately. Animals with lower levels of GS protein expression displayed lower sucrose preference, i.e. greater anhedonia-like deficits (Figure 9C).

Syn1: Analysis of Syn1 protein levels showed a significant main effect of stress ($F_{5:82}$=2.43; p<0.05) and sex ($F_{1:82}$=12.33; p<0.001) but no stress*sex interaction. We identified an overall significant decrease in Syn1 protein levels in the CRS35 group (p<0.05) when compared to controls (Figure 10A). *Post hoc* analysis revealed a trend toward decreased Syn1 protein levels in the CRS28 group (p=0.059) and a significant decrease in the CRS35 group (p<0.001) in males (Figure 10A'), while the females showed no significant effects between groups (Figure 10A') when compared to controls.

There was a significant negative correlation between Syn1 protein levels and residual avoidance (R^2=0.05, p<0.05) which was driven by data collected in males (R^2=0.09, p<0.05) but not in females (R^2=0.003, p=0.698) (Figure 10B). Similarly, we found the significant positive correlation between Syn1 protein expression and sucrose preference (R^2=0.07, p<0.05) which was driven data obtained in the males (R^2=0.11, p<0.05) but not the females (R^2=0.01, p=0.384) (Figure 10C). These results indicate that animals with lower levels of Syn1 protein expression displayed lower sucrose preference and greater residual avoidance, i.e. greater anhedonia- and anxiety-like deficits respectively; although this association was observed when animals of both sexes were combined, it was highly significant in males (Figure 10B-C).

vGLUT1: ANOVA of vGLUT1 protein levels, with sex as a factor, revealed a significant main effect of stress ($F_{5:68}$=2.76; p<0.05), but no main effect of sex or stress*sex interaction (Figure 11A). *Post hoc* analysis identified significant decreases in vGLUT1 levels in all groups subjected to CRS (CRS7, CRS21, CRS35: p<0.01; CRS14, CRS28: p<0.05) when compared to controls (Figure 11A).

There was no correlation between vGLUT1 protein levels and residual avoidance (R^2=4.57e-4, p=0.850) or sucrose preference (R^2=0.001, p=0.837) overall (both sexes), in males (residual avoidance: R^2=0.004, p=0.696; sucrose preference: R^2=0.01, p=0.473) or females (residual avoidance: R^2=0.008, p=0.620; sucrose preference: R^2=0.06, p=0.149) when analysed separately (Figure 11B-C).

PSD95: Statistical analysis of PSD95 protein levels indicated a significant main effect of stress ($F_{5:82}$=3.12; p<0.05) but no main effect of sex or stress*sex interaction (Figure 12A). *Post hoc* analysis revealed a significant decrease in PSD95 levels in the CRS28 group (p<0.01) and a

trend towards a decrease in the CRS21 and CRS35 groups (p=0.054 and p=0.095 respectively) when compared to controls (Figure 12A).

There was no correlation between PSD95 protein levels and residual avoidance (R^2=0.01, p=0.237), across sexes, or in males and females when analysed separately (males: R^2=0.01, p=0.377; females: R^2=0.02, p=0.320) (Figure 12B). No correlation was found between sucrose preference and PSD95 protein levels (R^2=0.02, p=0.115) across sexes, however when analysed separately males with lower PSD95 protein levels displayed lower sucrose preference (R^2=0.10, p<0.05). No correlation between the two variables was found in females (R^2=1.55e-4, p=0.934) (Figure 12C).

Marker x marker correlation: We found strong correlations between the three astrocytic markers (GFAP, GS, GLT1) (Figure 13A-B). The two functional astroglial markers (GS and GLT1) correlated with each other and strongly co-varied with the structural astroglial marker GFAP (Figure 13A-B). Regarding the synaptic markers (PSD95, Syn1, vGLUT1), they did not significantly correlate with each other, but there was a trend toward a positive correlation between PSD95 and Syn1 levels (Figure 13C). Interestingly, none of the pre-synaptic markers correlated with the astroglial markers, but the levels of the postsynaptic protein PSD95 strongly co-varied with GS levels (P<0.05) and GFAP levels (p=0.055) (Figure 13C). For all marker correlations and sex differences, see Appendix 1.

4.2 Experiment 2 – Effects of CRS on Astrocyte Morphology

4.2.1 Behavioural Changes

Coat state, sucrose preference and residual avoidance were measured at each week in GFAP-GFP mice subjected to 7, 21, 35 days of CRS (Figure 2B).

Coat State: Repeated measures ANOVA of coat state degradation scores, with sex as a factor, revealed a significant main effect of stress ($F_{5,31}$=14.36, p<0.0001), sex ($F_{2,31}$=16.22, p<0.0001), and a trend toward an stress*sex interaction ($F_{5,31}$=1.90, p=0.095) (Figure 14A). *Post hoc* analysis showed that the CRS35 animal group displayed significant deteriorated coat state scores from the second week of CRS (day 14 to 35) (p<0.01). Similarly, the CRS21 animals also showed significant deteriorated coat state scores from second week of CRS (day 28 to 35) (p<0.05). CRS7 animals were not statistically different from controls (Figure 14A). Results

obtained at the end of CRS exposure (day 35) are similar to the results obtained in Experiment 1 (Figure 5A). As in Experiment 1, males showed greater coat state deterioration scores compared to females (data not shown).

Sucrose Preference: Similar analysis performed on weekly sucrose preference data showed a trend towards a main effect of stress ($F_{5,29}$=2.13, p=0.063), no main effect of sex or stress*sex interaction (Figure 14B). Exploratory analysis revealed only the CRS35 animal group on day 35 showed a statistically significant decrease in sucrose preference ($p<0.05$) (Figure 14B).

Residual Avoidance: Animals were also tested in the phenotyper test weekly. Analysis of the residual avoidance calculated for the shelter zone time after the light challenge revealed a significant effect of stress ($F_{5,31}$=5.70, $p<0.0001$) and sex ($F_{2,31}$=22.09, $p<0.0001$) with no stress*sex interaction (Figure 15). *Post hoc* analysis showed that the CRS35 group displayed significantly increased residual avoidance on day 35 ($p<0.05$) with trends on days 7 (p=0.079) and 28 (p=0.064) (Figure 15A,D). CRS21 group showed significantly increased residual avoidance after 2 weeks (day 28) ($p<0.05$) and a trend after 3 weeks of CRS exposure (day 35) (p=0.061) (Figure 15B,D). CRS7 showed a significant increase in residual avoidance after one week of CRS (day 35) ($p<0.05$) (Figure 15C,D). As in Experiment 1, the main effect of sex was due to males showing an overall greater residual avoidance compared to females (data not shown).

4.2.2 Verification of the GFAP-GFP Transgenic mouse line

Immunohistofluoresence and confocal analysis was performed on PFC sections from GFAP-GFP heterozygous mice to determine if GFP+ cells of this mouse line were co-labelled with either NeuN, Iba1 or GFAP staining. We found no overlap between GFP+ and NeuN+ cell populations (Figure 16A-D). Similarly, GFP+ and Iba1+ cells represented two distinct cell types with no overlapping immunostaining (Figure 16E-H). However, we qualitatively found that a vast majority of the GFP+ cells were also GFAP co-labelled (Figure 16I-L). Note that half of GFP+ cells were not co-labelled with GFAP and that half of the GFAP+ cells were not GFP+; these findings will be addressed in the discussion. Wild-type littermates did not express any GFP+ immunofluorescence (Appendix 2).

4.2.3 Sholl Analysis of Astrocytes

Sholl analysis was performed on 6 astrocytes per animal, with 8 animals in each group (4 females and 4 males); because of the small sample size if sex was considered, sex was not included as cofactor in the following analyses.

AREA: Analysis of the AREA of GFAP+ cells revealed a trend towards an effect of stress exposure (ANOVA, $F_{3,188}$=2.14, p=0.097). Comparison between groups showed that the CRS21 animal group display GFAP+ cells with greater AREA than the control group ($p<0.05$) (Figure 17A). Regarding the AREA of the GFP+ cells, there was no difference between groups ($F_{3,164}$=2.08, p=0.104) (Figure 17B).

Total intersections: Similar analysis conducted for the total intersection counts revealed no effect of stress exposure for GFAP+ cells ($F_{3,188}$=1.26, p=0.289) nor for the GFP+ cells ($F_{3,164}$=0.80, p=0.494) (Figure 17C-D).

Total intersections/AREA: ANOVA of total intersections/AREA of GFAP+ cells identified a trend toward an effect of stress exposure ($F_{3,188}$=2.12, p=0.098). Comparison between groups identified a significant decrease in total intersections/AREA of GFAP+ cells of animals subjected to 21 days of CRS compared to controls (Figure 17E). Similarly, analysis of total intersections/AREA of GFP+ cells identified a trend toward an effect of stress exposure ($F_{3,164}$=2.26, p=0.082). Comparison between groups determined that total intersections/AREA of GFP+ cells was significantly decreased of animals subjected to 7, 21 or 35 days of CRS (all $p<0.05$) compared to controls (Figure 17F).

Frequency of intersections: Number of intersections was analysed for each radius-step. Note that the number of radius-steps relative to the soma was fixed to account for potential bias due to cell size. For the GFAP+ cells, ANOVA of the intersection frequency (or number of intersection per radius) showed no main effect of stress exposure ($F_{3,188}$=1.01, p=0.386), but a significant main effect of radius-step ($F_{10,1880}$=401.28 $p<0.0001$) and a stress*radius-step interaction ($F_{30,1880}$=2.23, p=0.0001) (Figure 18A). *Post hoc* analysis revealed that GFAP+ cells from the CRS35 animal group displayed significant increases in number of intersections at the proximal radius-steps (R4,R5 $p<0.05$) and decreases at more distal steps (R10 $p<0.05$) compared to controls (Figure 18A). For the GFP+ cells, intersection frequency analysis also revealed no main

effect of stress exposure ($F_{3,164}$=0.74, p=0.526), but a significant main effect of radius-step ($F_{10,1640}$=534.36, p<0.0001) and a stress*radius-step interaction ($F_{30,1640}$=4.05, p<0.0001) (Figure 18B). Compared to the control group, CRS7, CRS21 and CRS35 animals showed significant decreases in the frequency of intersections at the distal radius-steps (CRS7: R9,R10 p<0.05; CRS21: R9,R10 p<0.05; CRS35: R8,R9,R10 p<0.05) compared to controls (Figure 18B). Interestingly the CRS21 and CRS35 groups showed concomitant increase in the number of intersections at proximal areas (CRS21: R3 p<0.05; CRS35: R2,R3 p<0.05) (Figure 18B).

Relationships between GFAP+ or GFP+ cell morphological changes (AREA, total intersection, total intersections/AREA or frequency of intersections for proximal and distal radius-steps) and final behaviour performances (residual avoidance and sucrose preference) measured was tested using correlation analysis. No significant correlation was found between any of these variables (data not shown).

4.3 Experiment 3 – In Vitro Validation of DREADDs Construct

4.3.1 hM3Dq-GFP Plasmid Validation in HEK293

Immunocytochemistry: Using plasmids expressing GFP or mCherry only, we first tested in vitro co-transfection efficacy of 2 plasmids in HEK293 cells. Qualitatively, using our protocol we achieve a ~65% transfection rate (DAPI+ vs. DAPI+/GFP+ or DAPI+/mCherry+, Figure 19), where >99% of the HEK293 cells were co-transfected (GFP+/mCherry) and <1% expressed one of either fluorescent protein (Figure 19). We then verified that cells transfected with the designed hM3Dq-GFP plasmid required to be co-transfected with Cre to express GFP (Figure 20G); no GFP was detected in conditions without Cre plasmid (Figure 20D-F). We also had to validate activation of the hM3Dq receptor upon CNO or C21 exposure. Cells transfected with the plasmid expressing GFP only showed GFP+ immunostaining and low levels of cFos expression per cell when VEH, CNO or C21 was applied (Figure20A-C). Similar levels of cFos expression were detected in HEK293 cells transfected only with the hM3Dq-GFP plasmid and treated with either VEH, CNO or C21 (Figure 20D-F). However, following co-transfection with hM3Dq-GFP and Cre plasmids, GFP+ cells qualitatively showed greater cFos immunofluorescence when treated with CNO and C21 compared to VEH (Figure 20G-I). This increased cFos immunofluorescence was observed only in hM3Dq-GFP+ cells (Figure 20 G-I, I'-I'''').

Ca^{2+} Assay: We then further validated the efficacy of the hM3Dq-GFP construct using Ca^{2+} mobilization assay in HEK293 cells (hM3Dq [CNO] *N*=4; hM3Dq+Cre [VEH] *N*=6; hM3Dq+Cre [CNO] *N*=7; hM3Dq+Cre [C21] *N*=5). Repeated measures ANOVA of Ca^{2+} mobilization data revealed a significant main effect of plasmid ($F_{3,660}$=18.97, p<0.0001), time ($F_{44,660}$=72.52, p<0.0001) and plasmid*time interaction ($F_{132,660}$=15.98, p<0.0001) (Figure 21A). *Post hoc* analysis revealed that HEK293 cells co-transfected with hM3DqGFP and Cre plasmids showed a 22-42% increase in Fura2 $F_{(340/380)}$ ratio, significant from 4 to 80sec after CNO or C21 application compared to VEH (Figure 21A) or compared to HEK293 cells transfected with hM3DqGFP only treated with CNO (Figure 21A). Note that surprisingly we found a small (~7% $F_{(340/380)}$ ratio) but significant difference between these two "control groups" starting 40sec after the ligand application (Figure 21A). Area under curve (AUC) after ligand application was then calculated for each condition. ANOVA of Ca^{2+} mobilisation AUC ($F_{3,17}$=23.56, p<0.0001) revealed that HEK293 cells transfected with both hM3Dq and Cre plasmids treated with CNO or C21 show significant increases in $F_{(340/380)}$ ratio Ca^{2+} mobilization (both p<0.0001) compared to VEH or cells transfected with only the hM3Dq plasmid treated with CNO (Figure 21B).

4.3.2 hM3Dq-GFP Plasmid Validation in Primary Astrocyte Cultures

Immunocytochemistry: After establishing this method in the lab, I had to verify that the primary astrocyte cultures originated from GFAP-Cre pups were pure astrocyte cultures using immunocytofluorescence and confocal analysis. We found that all cells were GFAP+ (Appendix 3A) and found no NeuN+ or Iba1+ cells (Appendix 3B-C). Then, using a similar protocol as with the HEK293 cells, we tested the constructs in astrocytes from GFAP-Cre or WT littermates; this approach also tested that endogenous expression of Cre was sufficient to achieve expression of the hM3Dq receptor. Qualitatively, we estimated that a ~90% transfection rate in primary astrocyte cultures from either genotype was attained (Figure 22 & 23). We then verified that cells transfected with the designed hM3Dq-GFP plasmid expressed GFP only in the presence of Cre i.e. either when astrocytes are generated from GFAP-Cre pups (Figure 23A,D), or in WT astrocytes co-transfected with a Cre expressing plasmid (Figure 22B); no GFP was detected in conditions without Cre plasmid (Figure 23A). We also had to validate activation of the hM3Dq receptor upon CNO or C21 exposure. WT cells transfected with the hM3Dq-GFP plasmid only (Figure 23A-C) or GFAP-Cre cells transfected with the GFP plasmid only (Figure 22A) displayed low levels of cFos immunoreactivity. Qualitatively higher levels of cFos

immunofluorescence were found in cells transfected with the designed hM3Dq-GFP plasmid in the presence of Cre (i.e. GFAP-Cre astrocytes (Figure 23D-F), or in WT astrocytes co-transfected with a Cre plasmid (Figure 22B-D)) treated with CNO and C21 compared to VEH. This increased cFos immunofluorescence was observed only in hM3Dq-GFP+ cells (Figure 22C-D, 23E-F). In the CNO and C21 conditions, increased cFos immunofluorescence was observed only in hM3Dq transfected and GFP+ cells (Figure 22-23).

Western blot analysis: After multiple attempts, we were not able to optimize the Ca^{2+} mobilization assay in primary astrocyte cultures. This was due to 2 experimental limitations: astrocytes display auto-fluorescence that interferes with Fura2 signal and low survival rate after transfection at cell densities optimal for Ca^{2+} mobilization assay. Thus, we decided to confirm hM3Dq-GFP construct efficacy in the GFAP-Cre transgenic line by demonstrating activation of the G-protein coupled receptor (GPCR) pathway. ANOVA of phospho/total (p/t) Akt levels ($F_{8,12}$=4.79, $p<0.01$) revealed a significant increase in p/t Akt protein levels upon C21 and CNO exposure compared to VEH in GFAP-Cre astrocyte cultures transfected with the hM3Dq plasmid (both $p<0.01$, Figure 24). GFAP-Cre astrocytes transfected with GFP plasmid or WT astrocytes transfected the hM3Dq plasmid did not show increased p/t Akt protein levels upon C21 and CNO exposure compared to VEH (Figure 24). Similar analysis was performed on p/t MAPK protein levels. We found no changes in p/t MAPK protein levels ($F_{8,12}$=1.61, $p=0.218$) following CNO or C21 in WT or GFAP-Cre astrocyte cultures transfected with hM3Dq plasmid (data not shown).

5 Discussion

5.1 Summary of findings

Our findings demonstrate that CRS induces coat state deterioration, anxiety- and anhedonia-like behaviour. CRS also induced time-dependant decreases in astrocytic (GFAP, GS, and to a smaller extent GLT1) and synaptic protein (vGLUT1, PSD95, Syn1) expression levels in the PFC. The protein changes in GLT1, GS, GFAP, and Syn1 correlated with both anxiety- and anhedonia-like deficits, in both sexes. However, most of these effects were driven by strong correlations in males. Indeed, in males GLT1, GS, GFAP, Syn1 protein levels correlated with residual avoidance performances while all these markers and PSD95 correlated with sucrose consumption. Interestingly, vGLUT1 protein levels did not correlate with any of the behaviours.

Females only showed correlation between sucrose preference and GLT1 protein expression levels. We also analysed using the same approach the effects of various duration of CRS exposure on astrocyte morphology labelled with GFAP or GFP in GFAP-GFAP mice and found that astrocyte maximal AREA and total number of intersections did not differ between the groups. However, CRS induced a decrease total number of intersections/AREA of GFP+ cells as early as 7 days of CRS exposure and a rearrangement of GFP+ cells where decreased distal processes were accompanied by increased proximal processes. GFAP+ cells showed similar rearrangement following CRS, however of a lesser magnitude. Furthermore, as part of the preliminary steps aiming to develop a virus that would allow enhancing astroglial activity to prevent the effects of CRS, we validated (in-vitro) a custom-designed plasmid (hM3Dq-GFP) and validated its effectiveness in culture (HEK293 and primary cortical astrocyte culture from GFAP-Cre mice). We demonstrated conditional expression of the hM3Dq receptor and activation of cFos in both HEK293 and astrocyte culture in the presence of (exogenous or endogenous) Cre expression. Activity of the receptor in these conditions was demonstrated by increased calcium mobilisation and phosphorylation of Akt upon CNO or C21 in HEK293 and astroglial cells respectively.

5.2 Chronic stress exposure induced increases in anxiety-like and anhedonia-like behaviours

Previous work using the CRS model have reported coat state deterioration, anxiety- behavioural deficits, including previous studies from our group (Banasr et al., 2017; Nikolova et al., 2018; Prevot et al., 2019a; Prevot et al., 2019b). Here we confirm these changes and found that CRS induced anhedonia-like as indexed by decreased sucrose preference. These results parallel a plethora of data of the literature demonstrating that chronic exposure to stress induces physical changes, as well as anxiety- and anhedonia-like deficits (Ampuero et al., 2015; Strekalova et al., 2004). In addition, while studying the trajectory of the effects of chronic stress exposure, we determine that CRS induces anxiety- (from 7 days, Prevot et al., 2019b) and anhedonia-like (from 21 days) behaviour in a time dependent manner. Here, we confirm that at least 3 weeks of chronic stress exposure are generally required to induce depressive-like behaviour in mice (Willner, 2017a). Interestingly, in our study, females displayed lower levels of coat deterioration and anxiety-like behaviour but followed the same trajectory of change (just at a smaller magnitude). In addition, previous studies have found differences in anxiety-like behavioural

deficits between males and females where the females usually show a lower extent of deficits than males (An et al., 2011; Franceschelli et al., 2014; Seney and Sibille, 2014). While in experiment 1 coat state degradation and sucrose preference deficits were significant at time points earlier than those in experiment 2 i.e. first and third week of CRS (experiment 1) and second and fifth week of CRS (experiment 2), these behavioural findings from Experiment 1 were overall similar to those of Experiment 2. This apparent discrepancy may be due to the fact that Experiment 1 had 16 animals per group (while Experiment 2 had 8 per group) and was powered to detected smaller changes. Similarly, residual avoidance was generally increased in all 3 groups of stressed animals (Experiment 2) from the first week of stress, similar to what was seen in Experiment 1 and to our previous published work (Prevot et al., 2019b).

5.3 Chronic stress exposure resulted in altered astroglial and synaptic protein expression levels

Previous studies have shown that chronic stress exposure reduces astroglial and synaptic markers. Indeed, separate studies have shown that chronic stress to induce decreases in PSD95, Syn1 (Li et al., 2011; Mitra et al., 2018), vGLUT1 (Yu et al., 2018; Zink et al., 2010), as well as decreases GFAP (Banasr et al., 2010; Banasr and Duman, 2008), GLT1 (Baek et al., 2019; John et al., 2012; John et al., 2015; Zink et al., 2010), and GS (Lee et al., 2013; Rao et al., 2016) in the PFC. Here, we showed that all these markers are reduced in the PFC of CRS animals of the same study, and these changes are linked to behavioural deficits. Specifically, our results showed that the astroglial structural protein GFAP decreased from the first week of CRS while the functional proteins (GLT1 and GS) decreased from the fourth week onwards. This suggests that CRS may alter astroglial morphology, and with chronicity affects their function. Note that this hypothesis is supported by the results obtained for the GFAP-GFP+ cells from Experiment 2 where the morphological rearrangements found paralleled, in time, the findings of reduced GFAP protein expression. Regarding the synaptic markers, the functional protein vGLUT1 was decreased from the first week of stress but the synaptic proteins involved in the synapse structure and strength (Syn1 and PSD95) required four weeks of CRS or more to be affected. Altogether, from these results we could speculate that at early state of stress exposure glutamatergic neurons of PFC compensate by trying to package less glutamate (reduced vGLUT1) into vesicles while the astrocytes may atrophy (reduced distal reach, Experiment 2) but retain functionality related to the glutamate-glutamine shuttle (no change in GS or GLT1 at the early stage of CRS exposure).

Extended stress exposure alters integrity of the shuttle as indexed by decreased GLT1 and GS expression, which may then reduce synaptic structure and strength as supported by GS/PSD95 and PSD95/Syn1 correlations.

5.4 Astroglial marker levels correlated with behavioural changes and each other, while synaptic marker levels did not systematically correlate with each other or with behavioural changes

In our study, although the three astroglial markers had individual trajectory of response to CRS, they tightly positively correlated with each other. A recent study supports this close link between the three astroglial proteins since knockdown of GLT1 results in reduced numbers of GFAP+ and GS+ astrocytes (Fullana et al., 2019). This suggests that GLT1 function can regulate structural integrity and number of the astrocytes, while our results of GFAP reduction prior to GS and GLT1 changes suggests that altered morphology may affect function. Considering the strong correlations between the markers found in the present study, it is not surprising that a link between structure and function would be bidirectional for astrocytes, as it is well known for neurons. It is interesting to note that we did not find correlations between astroglial markers and the pre-synaptic proteins i.e. Syn1 and vGLUT1 (only correlations between astroglial markers and PSD95). This could be potentially explained by the fact that PSD95 from the analysed samples originates exclusively from the resident PFC neurons, while Syn1 and vGLUT1 are markers of all neuronal processes, including processes from PFC inputs from other brain regions (Collins et al., 2018; McGarry and Carter, 2017). Indeed, our approach i.e. western blot analysis of PFC homogenates do not allow us to discriminate between local cortico-cortical synapses or synapses resulting from different inputs of the PFC. This could dilute potential correlations with markers from resident astrocytes and pre-synaptic markers.

In addition, we correlated the protein expression levels with behavioural performances and found all three astroglial markers positively correlated with anhedonia-like behaviour while the two functional astroglial markers (GS and GLT1) correlated with anxiety-like behaviour. The only synaptic marker that correlated with anhedonia- or anxiety-like behaviour was Syn1. This suggests that astroglial structural deficits are associated with the initial anxiety-like behaviour while the functional deficits are more related to the later-onset anhedonia-like behaviour and/or maintenance of anxiety-like behaviour. The lack of correlations between changes in synaptic

markers and behavioural outcomes may be due to the cell populations represented by these markers (multiple cell populations from multiple brain regions) or due to complementary contribution of synaptic alterations from other limbic regions involved in emotion regulation such as the hippocampus or the amygdala. Indeed, our lab recently demonstrated that changes in PSD95 expression in the amygdala correlated with performances in the phenotyper test (Nikolova et al., 2018). Interestingly, data analysis revealed that males drove the overall correlations between behaviour and marker expression levels. One potential explanation could be that additional variability due to gonadal hormone cycling in females may interfere with potential correlations with behaviours or cellular readouts. Indeed, estrus cycle affects the function of astrocytes (Acaz-Fonseca et al., 2016; Nelson and Lenz, 2017) and synapse numbers (Alexander et al., 2018; Chen et al., 2009) in the PFC. Since we did not perform vaginal swabs to track the estrus cycle during behavioural assessment or at euthanasia, we could not include this factor/bias in our analysis.

5.5 Chronic stress results in reorganisation of cortical astrocyte (proximal and distal) processes

Since the GFAP-GFP transgenic line was backcrossed in-house, we had to validate the line. We found no overlap with the most commonly used neuronal or microglial markers but only half of GFP+ cells co-labelled with GFAP and that half of the GFAP+ cells were GFP+. Ideally, we expected a 100% overlap of GFP+ cells with GFAP+. There are a few potential reasons for this differential pattern of expression between GFAP and GFP. Since the GFAP-GFP transgenic line expresses GFP under a human GFAP (hGFAP) promoter randomly inserted into the genome, nearby regulatory promoters may alter the expression profile of GFP in comparison to endogenous mouse GFAP (mGFAP) expression. Previous groups have encountered similar issues when using the hGFAP promoter to express GFP in vivo (Bai et al., 2013; Nolte et al., 2001). Additionally, Moon et al. (2011) found the hGFAP promoter-derived GFP expression differs depending on the subtype of astrocyte. Another explanation for this different expression profile between GFAP and GFP may be due to a competition between the mGFAP and hGFAP promotors for the cell's transcriptional resources. Finally, we found that the GFP signal needed to be amplified for the type of analysis we wanted to perform. It is possible that the IHC antibodies and dilutions used, although optimal for the morphology analysis, might not have been optimal for correctly estimating of the number of GFAP+ cells or GFAP+ signal intensity,

or its overlap with the GFP+ signal. We addressed this potential limitation by analyzing the morphology of both the GFAP+ and GFP+ cell populations, and believe that we are observing the same cell population since GFP+ and GFAP+ cells showed similar rearrangement following CRS, albeit in a lesser extent for the GFAP+ cells.

In this study, we identified reductions in total number of intersections/AREA of GFP+ cells that appeared as early as the first week of CRS exposure. However, we did not find similar changes for the GFAP+ cells except in the CRS21 animals group. The discrepancy between findings obtained with the two markers could be due to the differences in localisation of the GFP and GFAP proteins. Indeed, GFAP as a structural microtubule protein and its immunolabelling only allowed for the detection of major processes/branching while GFP labeling was located throughout the cytoplasm of the cell and in all branching including in the fine astrocyte processes. This would explain why lesser magnitude of the CRS-induced changes were found with GFAP immunostaining as compared to the GFP immunostaining when Sholl analysis was performed. Morphology of the GFAP+ and GFP+ cells at distinct distances from the soma (number of intersections at radii farther from the soma) were decreased by chronic stress exposure. Specifically, CRS exposure for 35 days induced a loss in distal processes observable with both markers, however this 'astrocytic atrophy' was probably ongoing and affected the fine processes of the astrocytes since we found reduced GFP+ cells' distal processes in animals subjected to stress for 7 and 21 days. Interestingly, with both markers we found concomitant increase in proximal processes (number of intersections at radii closer to the soma) in animals subjected to 35 days of stress. The distal processes atrophy accompanied by increases in proximal processes suggests that it may not be solely atrophy but more likely a rearrangement of the morphology of the astrocytes. In addition, this proximal reorganisation may be a compensatory mechanism associated with chronic (35 days) stress but was not observed with 7 days of stress. In other words, it is possible that initially repeated stress may cause the astrocytes to lose distal processes and that when the stress becomes chronic, a rearrangement occurs where proximal processes branch out to compensate for the process loss at the distal ends. This astroglial atrophy could be due to excitotoxicity from poor synaptic glutamate regulation (Haas and Erdo, 1991; Matute et al., 2007), increased corticosterone (Zhang et al., 2015; Zhao et al., 2018), or oxidative stress (Bhatia et al., 2019; Palmer and Ousman, 2018). It is important to mention that we observed reductions in GFAP+ protein expression levels from 7 days of CRS

exposure but did not find parallel differences in GFAP+ cell morphology at early time points. There are three possible reasons for this apparent discrepancy: (1) the astrocyte AREA measurement was an overestimated measure (maximal potential surface area covered by the astrocyte) based on the longest process, and not the actual surface area of the cell. It is possible that longer exposure to stress is required to alter the morphology of major processes; (2) the approaches used for two experiments were radically different i.e. measuring GFAP protein expression in total PFC homogenates vs. analysis of 6 individual GFAP+ astrocytes per animal; (3) chronic stress may reduce GFAP cells density (Banasr and Duman, 2008; Simard et al., 2018) by decreasing the total number of astrocytes as reported in human MDD brains (Cobb et al., 2016; Rajkowska et al., 2018) and the present study highlighted an additional effect of chronic stress, i.e. rearrangement of astrocytes morphology. Needlessness, if we were establishing a parallel between the cellular outcomes obtained in Experiment 1 and 2, we could speculate that initially repeated stress may cause atrophy of distal processes and decreased GFAP protein, but at this stage astroglial function is maintained since GS and GLT1 protein level are unchanged. When the stress becomes chronic, the morphological rearrangement and decreased GLT1 and GS expression may have additive actions on the glutamatergic synapse function. Indeed, reduced glutamate uptake and lower rate of glutamate-to-glutamine conversion associated with chronic stress exposure would impair synaptic function and structure. This is supported by our findings of reduced PSD95 or Syn1 expression and data of the literature showing reduced spine numbers and density in animals subjected to chronic stress (Qiao et al., 2016). It would be interesting to investigate in the same animals whether the synaptic morphological changes parallel the astroglial morphological rearrangement.

5.6 Limitations

Our study is not without limitations. First, we focused on the PFC as sole brain region of interest for the analyses performed in both experiments. However, it is highly important to mention that many other limbic areas associated with MDD and chronic stress show altered astrocytic and synaptic function or morphology including the amygdala and hippocampus. We focussed first on the PFC since chronic stress experiments and post-mortem studies on MDD brains have shown greater consistency regarding the astroglial changes in this brain region compared to others. However, at sacrifice we collected other brain regions (hippocampus and amygdala) and sectioned the entire brain for further analysis targeting key brains regions involved in depression

and stress-related illnesses. Second, our study focussed on characterising the cellular changes focussing on only six proteins or markers of synaptic and astrocyte function (3 for each compartment), in addition to only investigating GFAP+ or GFP+ cell morphology. Future studies analysing other markers may yield complementary or additional insight into the trajectory of the effects of chronic stress on astroglial and synaptic function. Third, although the first experiment was powered to assess potential sex differences, this could not be done for the morphological analysis of the second experiment; a second cohort replicating experiment 2 would address this limitation. Finally, we focused on glutamatergic synapses but other synaptic changes were associated with chronic stress and depression including impaired GABAergic neurotransmission. Limitations notwithstanding, we provide evidence for time dependent synaptic and astroglial alterations associated with chronic stress in mice and found morphology reorganization supporting that astrocyte processes (like synaptic processes) are susceptible to chronic stress exposure.

5.7 Validated the DREADDs technique in astrocytes using the hM3Dq receptor (in vitro)

In this thesis we also hypothesised that enhancing astrocyte function may be a valid approach for the development of new MDD pharmacological treatment. Using drugs that enhance glial glutamate transport expression or activity, it has been shown that targeting GLT1 induces antidepressant effects in rodent stress models (Banasr et al., 2010; Gourley et al., 2012) and in human (Zarate and Manji, 2008). Oppositely, drugs that impair GLT1 function or ablate astrocytes were found to induce anxiety- and anhedonia-like deficits (Gasull-Camos et al., 2017; John et al., 2015). These results, in addition to the findings of this thesis, suggest that impaired astroglial function (not necessarily astroglial loss) may be involved in the expression of depressive-like behavioural deficits. Thus, we set out to demonstrate that silencing astrocytes in the PFC would directly induce anxiety- and/or anhedonia-like behaviours. To test this hypothesis, we planned on using the DREADDs hM4Di (modified human M4 muscarinic receptor) method to hyperpolarize astrocytes, thereby silencing their action. In the meantime, a recent study by Durkee et al. (2019) was published (originally presented as a Society for Neuroscience poster in 2018) showing the hM4Di receptor hyperpolarizes neuronal cells but surprisingly activates astroglial cells, invalidating the use of the hM4Di receptor to test our working hypothesis. For this reason, we adapted our experimental design to demonstrate that

enhancing PFC astrocyte function prevent the development of depressive-like behaviour and render the animals resilient to stress. Due the unexpected effect of the hM4Di receptor in astrocytes, it was imperative to test the efficacy of the hM3Dq receptor at activating this cell type. Therefore we tested the hM3Dq-GFP plasmid in vivo using both HEK293 cells and primary cortical astrocyte cultures and used 2 assays for each cell type to demonstrate cell activation. Additionally, there had been several controversy surrounding the use of CNO: 1) clozapine, reverse-metabolized from CNO is a potent psychoactive drug that may affect emotion-related behaviour independently of the presence of the hM3Dq receptor (Gomez et al., 2017; Raper et al., 2017); 2) clozapine may be the ligand of the hM3Dq receptor and CNO may not cross the blood-brain barrier (MacLaren et al., 2016; Manvich et al., 2018), however this last statement is to be taken with caution as it is still controversial. To circumvent this caveat, a modified ligand, compound 21 (C21), was designed and shown to activate the DREADD hM4Di receptor and silence the cells (Jendryka et al., 2019; Thompson et al., 2018). Additional evidence was required regarding cell activation following C21 binding onto hM3Dq receptor. In this aim, I needed not only to validate the efficacy of hM3Dq-GFP plasmid to express the hM3Dq receptor in the presence of Cre but also the use of the approach in astrocytes and activation upon ligand application. In this study, we found that only cre-transfected HEK293 cells and astrocyte cultures from GFAP-Cre+ mice showed GFP expression when transfected with the hM3Dq-GFP plasmid. Additionally, only GFP+ cells showed increased cFos levels i.e. greater cell activation (Adamsky et al., 2018; Groves et al., 2018) upon exposure to CNO or C21. Furthermore, cell activation was confirmed by demonstrating greater Ca^{2+} mobilization and phosphorylation of Akt, protein of the G-protein coupled receptor (GPCR) pathway (Law et al., 2016; Nakano et al., 2017) in the presence of CNO or C21. Interestingly, we also demonstrated that the two ligands (CNO and C21) show similar efficacy at activating hM3Dq receptor in vitro. The question remains whether these ligands have similar efficiency in vivo. Now, the plasmids can be packaged into an adeno-associated virus (AAV5) and infused into the PFC of GFAP-Cre+ mice. In vivo validation of infection and activation of the astrocytes following CNO or C21 i.p. administration will be conducted using cFos immunohistochemistry.

6 Conclusions & Future Directions

Robust morphological changes in the brain are associated with MDD and stress-related disorders. Post-mortem and preclinical research including our own has focused on the in-depth

characterization of the underlying mechanisms of MDD pathophysiology. The work presented here is based on an innovative concept, focusing on the contribution of non-neuronal cells in MDD. Specifically, we are fuelling the hypothesis that astrocytes and astrocyte-synapse cross talk may be vulnerable nodes underlying the neuronal/synaptic dysfunction associated with stress- and depression-related behaviour. We used multi-disciplinary approaches that combined behaviour, genetics, molecular biology, and microscopy to investigate cell-specific molecular mechanisms relevant to chronic stress and MDD. In addition, in this thesis we adapted and established in the lab many tools, classically used for neuronal cell analysis, including Sholl analysis and hM3Dq receptor approach to astrocytes. Altogether this work, although employing rodent models, is translational since it builds on well-replicated human post-mortem evidence of synaptic and astroglial dysfunctions in MDD, as well as establishing a link between chronic stress and astrocyte/synaptic impairment. Finally, my work set the stage for future experiments aiming to demonstrate that astroglia could be targeted to prevent the effects of chronic stress. Indeed, the overarching goals of this work is to better understand the role of astroglia in MDD and stress-related illnesses and identify new targets for the development of novel and more effective therapeutic approaches.

Since our work primarily focussed on a small set of proteins expressed by astroglia and the glutamatergic synapse in the PFC, the immediate future directions would be to extend this study to other astroglial and glutamatergic synapse proteins, as well as markers of the GABAergic tripartite synapses. In addition, we could perform similar analyses in the collected samples from other brain regions involved the mood regulation such as the hippocampus and amygdala. Correlating astrocytic, glutamatergic and GABAergic changes to the behavioural and cellular changes associated with CRS would provide a more complete picture of how the tripartite synapses of these brains are affected by chronic stress exposure. Regarding the work conducted on the effects of chronic stress exposure on astrocyte morphology, we could try to link the rearrangement of the astroglial processes to the synaptic atrophy known to be associated with stress. For this we could, for example, perform a double staining for GFP and PSD95 and conduct a PUNCTA density analysis of PSD95 immunofluorescence overlapping GFP+ astrocytes. This may allow us to determine if the stress-induced reduction of GFP+ distal processes maps onto a reduction of PSD95 puncta density, and oppositely if the increased GFP+ proximal processes maps onto maintenance of PSD95 puncta density. This analysis would

address a possible effect of chronic stress exposure on synapse-astrocyte coupling. Furthermore, although our work characterized a stress-induced astroglia dysfunction and altered morphology, the mechanisms underlying these effects remain unknown. Future studies aiming at identifying these mechanisms can be performed in the GFAP-GFP mouse line I validated. Indeed, we could isolate GFP+ cells from GFAP-GFP mice subjected to CRS, using fluorescence activated cell sorting (FACS), and perform RNAseq analysis. This would permit identifying astroglial-specific gene expression changes induced by chronic stress. Some of these identified genes or pathways could be targeted using viral or genetic approaches to determine if manipulations of these genes either mimics or prevents the effects of chronic stress. In this context, the methods I helped establish in the lab regarding the in vitro validation of the hM3Dq-GFP plasmid could be instrumental to test/validate new plasmids and viruses.

Overall, the work I performed during my Master's provides critical insight into the role of astroglia dysfunction in the cellular and behavioural effects of stress, and fuels to the rising hypothesis that depression can be an astroglial-based synaptic disorder (Rial et al., 2015). I believe that a better understanding of the underlying mechanisms involved in the stress-induced astroglial dysfunctions could lead to novel targets for antidepressant development, translating these findings towards clinical applications.

Tables & Figures

Table 1: ***List of antibodies for western blot analysis*****.**

List of primary (1°) antibodies, blocking solutions, and the concentrations used for the western blot analysis for both 1° and secondary (2°) antibodies.

	Antibody	***Blocking***	***Dilution***	***Reference***
1°	Rabbit α-GLT1 (EAAT2)	5% Milk	1:2000	Santa Cruz Biotechnology sc-15317 (Mississauga, Ontario, Canada)
	Rabbit α-GFAP	5% Milk	1:5000	Cell Signaling Technology 12389 (Danvers, MA, USA)
	Rabbit α-GS	5% Milk	1:5000	Abcam ab176562 (Toronto, Ontario, Canada)
	Rabbit α-Syn1	5% Milk	1:100 000	Millipore AB1543 (Etobicoke, Ontario, Canada)
	GuineaPig α-vGLUT1	5% Milk	1:5000	SYSY* 135304 (Rudolf-Wissell-Str. 28, Goettingen, Germany)
	Rabbit α-PSD95	5% Milk	1:5000	Cell Signaling Technology 2507S (Danvers, MA, USA)
	Rabbit α-tAkt	3% BSA	1:1000	Cell Signaling Technology 4691S (Danvers, MA, USA)
	Rabbit α-pAkt	3% BSA	1:1000	Cell Signaling Technology 4060S (Danvers, MA, USA)
	Rabbit α-tMAPK (Erk1/2)	3% BSA	1:1000	Cell Signaling Technology 4695S (Danvers, MA, USA)
	Rabbit α-pMAPK (Erk1/2)	3% BSA	1:1000	Cell Signaling Technology 4370S (Danvers, MA, USA)
2°	Goat α-Rabbit HRP	-	1:10 000	Vector Labs PI-1000 (Burlingame, CA, USA)
	Goat α-GuineaPig HRP	-	1:10 000	Invitrogen A18769 (Massachusetts, USA)

*SYSY = Synaptic Systems

Table 2. ***List of antibodies for immunohisto-(and cyto-)chemistry*****.**

List of primary (1°) antibodies and the corresponding secondary (2°) antibody. Concentrations of use for both 1° and 2° antibodies are included, for both immunohistochemistry (IHC) and immunocytochemistry (ICC).

	Antibody	***Dilution***	***Reference***	***2° Antibody***
1°	Rabbit α-GFAP	1:200 ***(IHC & ICC)***	Dako Z0334 (Santa Clara, CA, USA)	α-Rabbit DyLight405 α-Rabbit AF488
	Rabbit α-Iba1	1:1000 ***(IHC & ICC)***	Wako 019-19741 (Richmond, VA, USA)	α-Rabbit DyLight405
	Rabbit α-cFos	1:250 ***(ICC)***	SYSY* 226 003 (Rudolf-Wissell-Str. 28, Goettingen, Germany)	α-Rabbit AF555
	Chicken α-GFP	1:500 ***(IHC & ICC)***	Aves GFP-1020 (Davis, CA, USA)	α-Chicken AF488
	GuineaPig α-NeuN	1:500 ***(IHC & ICC)***	EMD Millipore ABN90 (Etobicoke, ON, Canada)	α-GuineaPig CF405M
2°	Donkey α-Rabbit DyLight405	1:200 ***(IHC)*** 1:1000 ***(ICC)***	Jackson ImmunoResearch 711-475-152 (West Grove, PA, USA)	-
	Donkey α-Rabbit AF488	1:1000 ***(ICC)***	Invitrogen A21206 (Massachusetts, USA)	-
	Donkey α-Rabbit AF555	1:1000 ***(ICC)***	Invitrogen A31572 (Massachusetts, USA)	-
	Donkey α-Chicken AF488	1:200 ***(IHC)*** 1:1000 ***(ICC)***	Jackson ImmunoResearch 703-545-155 (West Grove, PA, USA)	-
	Donkey α-GuineaPig CF405M	1:200 ***(IHC)*** 1:1000 ***(ICC)***	Biotium 20376-500uL (Fremont, CA, USA)	-

*SYSY = Synaptic Systems

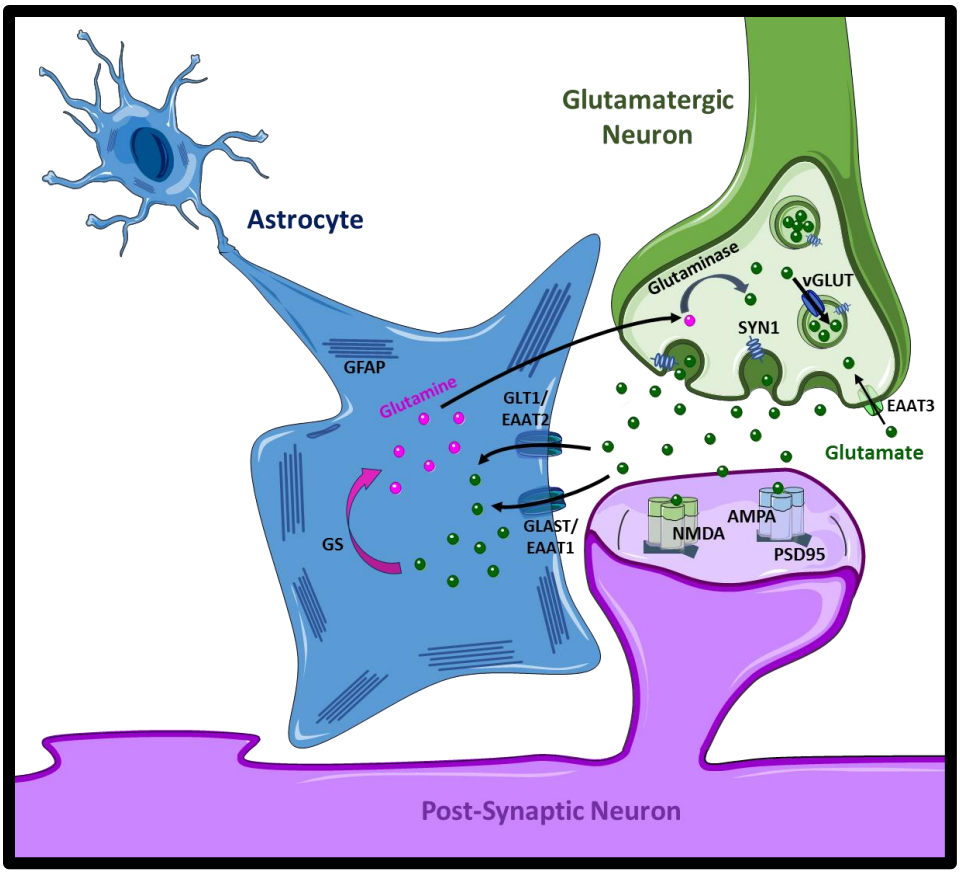

Figure 1: ***Schematic representation of the glutamatergic tripartite synapse*****.**

Presynaptic glutamatergic neuron synapsing onto a post-synaptic neuron with astrocyte processes modulating the synapse. Presynaptic glutamatergic components: vesicular glutamate transporter (vGLUT, transports glutamate into vesicles), synapsin I (SYN1, vesicle release protein), excitatory amino acid transporter 3 (EAAT3, presynaptic glutamate reuptake transporter), and glutaminase (converts glutamine to glutamate). Postsynaptic components: N-methyl-D-aspartate (NMDA) receptor (ionotropic glutamate receptor), α-amino-3-hydroxy-5-methyl-4-isoxazolepropionic acid (AMPA) receptor (ionotropic glutamate receptor), and postsynaptic density protein 95 (PSD95, postsynaptic scaffolding protein for NMDA and AMPA receptors). Astrocytic components: excitatory amino acid transporter 1/glutamate aspartate transporter 1 (EAAT1/GLAST, transports glutamate into the astrocyte), excitatory amino acid transporter 2/glial glutamate transporter 1 (EAAT2/GLT1, transports glutamate into the astrocyte), glutamine synthetase (GS, converts glutamate to glutamine), and glial fibrillary acidic protein (GFAP, microtubule associated protein important for structural integrity).

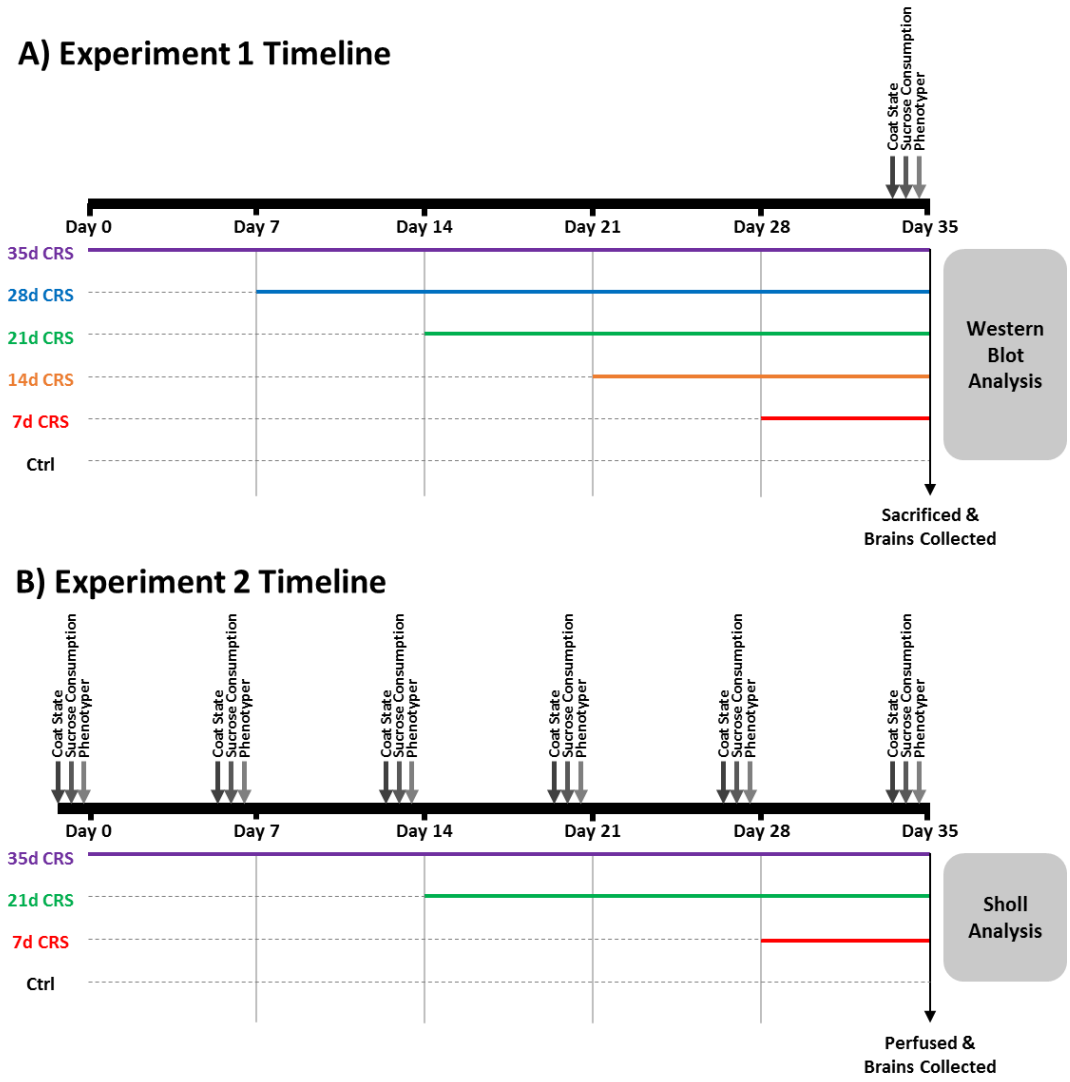

Figure 2. ***Experimental design for the two experiments performed.***

(A) Experiment 1 timeline: mice were exposed to chronic restraint stress (CRS) for either 0 (control, a.k.a. ctrl), 7, 14, 21, 28, or 35 days. Behavioural testing (coat state, sucrose consumption, phenotyper) was conducted on the last week of experimentation. Solid line indicates weeks where mice undergoing CRS, while dotted lines indicate weeks with no CRS. Western blot analysis on dissected PFC homogenate collected at sacrifice.

(B) Experiment 2 timeline: mice were exposed to chronic restraint stress (CRS) for either 0 (ctrl), 7, 21, or 35 days. Behavioural testing (coat state, sucrose consumption and phenotyper test) was conducted at each week of experimentation. Solid line indicates weeks where mice undergoing CRS, while dotted lines indicate weeks with no CRS. Sholl analysis was performed after perfusion.

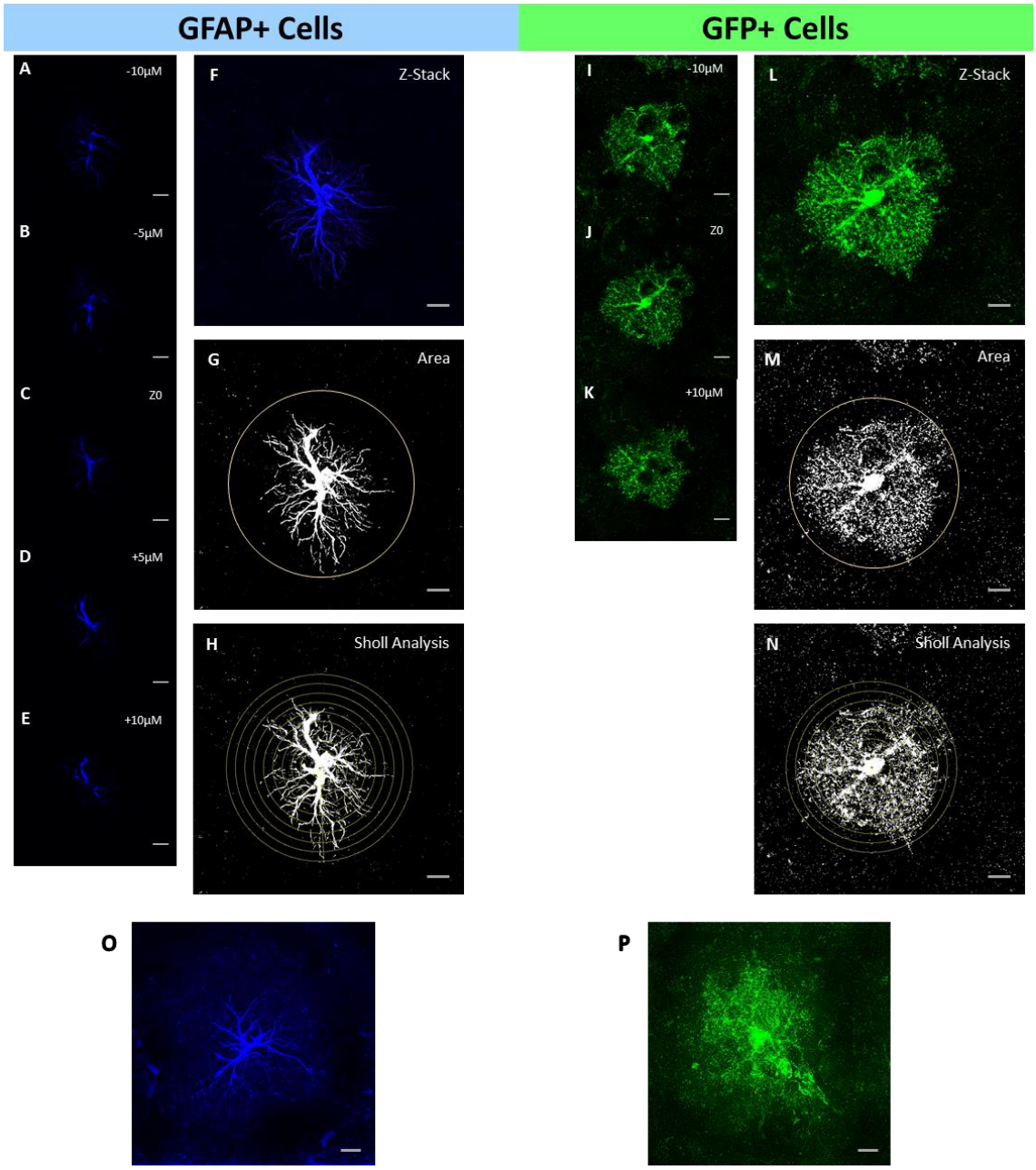
GFAP+ Cells
GFP+ Cells
A
-10µM
B
-5µM
C
Z0
D
+5µM
E
+10µM
F
Z-Stack
G
Area
H
Sholl Analysis
I
-10µM
J
Z0
K
+10µM
L
Z-Stack
M
Area
N
Sholl Analysis
O
P

Figure 3. ***Confocal imaging and Sholl analysis methods for individual astrocytes.***

(**A**-**E**) Tissue were immunostained for GFAP (glial fibrillary acidic protein) and cells imaged over a span of 20µm (images taken every 5µm, spanning Z0 equally, see Methods). (**F**-**H**) Image was z-stacked, thresholded, area calculated, and Sholl analysis was performed. (**I**-**K**) Tissue was immunostained for GFP (glial fibrillary acidic protein) and cells were imaged over a span of 20µm (images taken every 10µm, spanning Z0 equally, see Methods). (**L**-**N**) Image was z-stacked, thresholded, area calculated, and Sholl analysis was performed. (**O**) Image of a GFAP+ cell with images taken every 1µm, to illustrate the necessity of using a z-step of 5µm for analysis. (**P**) Image of GFP+ cell with images taken every 1µm, to illustrate the necessity of using a z-step of 10µm for analysis. Scale bar = 10µm.

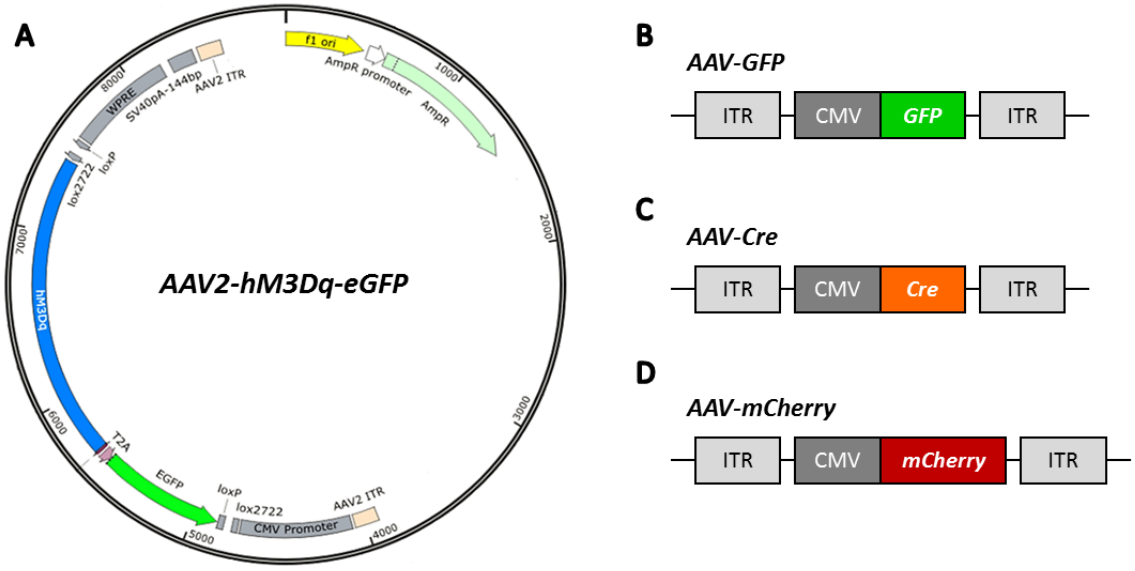

Figure 4. ***Plasmid constructs employed for in-vitro (HEK293 and primary astrocyte culture) validation*****.**

(**A**) Custom designed adeno-associated virus 2 allowing for conditional expression of the modified human M3 muscarinic receptor-enhanced green fluorescent protein (AAV2-hM3Dq-eGFP) plasmid. The inverted hM3Dq sequence and eGFP are linked via a T2A sequence coding for the T2A self-cleaving peptide, and all are flanked by a pair of loxP and lox2722 sites. f1 ori = origin of replication from an f1 phage. AmpR = ampicillin resistance gene. ITR = inverted terminal repeat sequences. WPRE = woodchuck hepatitis virus posttranscriptional regulatory element, used to increase expression of genes. SV40pA = SV40 polyadenylation signal. CMV promoter = cytomegalovirus promoter. (**B**) AAV-GFP plasmid: CMV promoter followed by a GFP sequence, flanked by two ITR sequences. (**C**) AAV-Cre plasmid: CMV promoter followed by the sequence coding for the Cre protein, flanked by two ITR sequences. (**D**) AAV-mCherry plasmid: CMV promoter followed by a monomeric red fluorescent protein (mCherry) sequence, flanked by two ITR sequences.

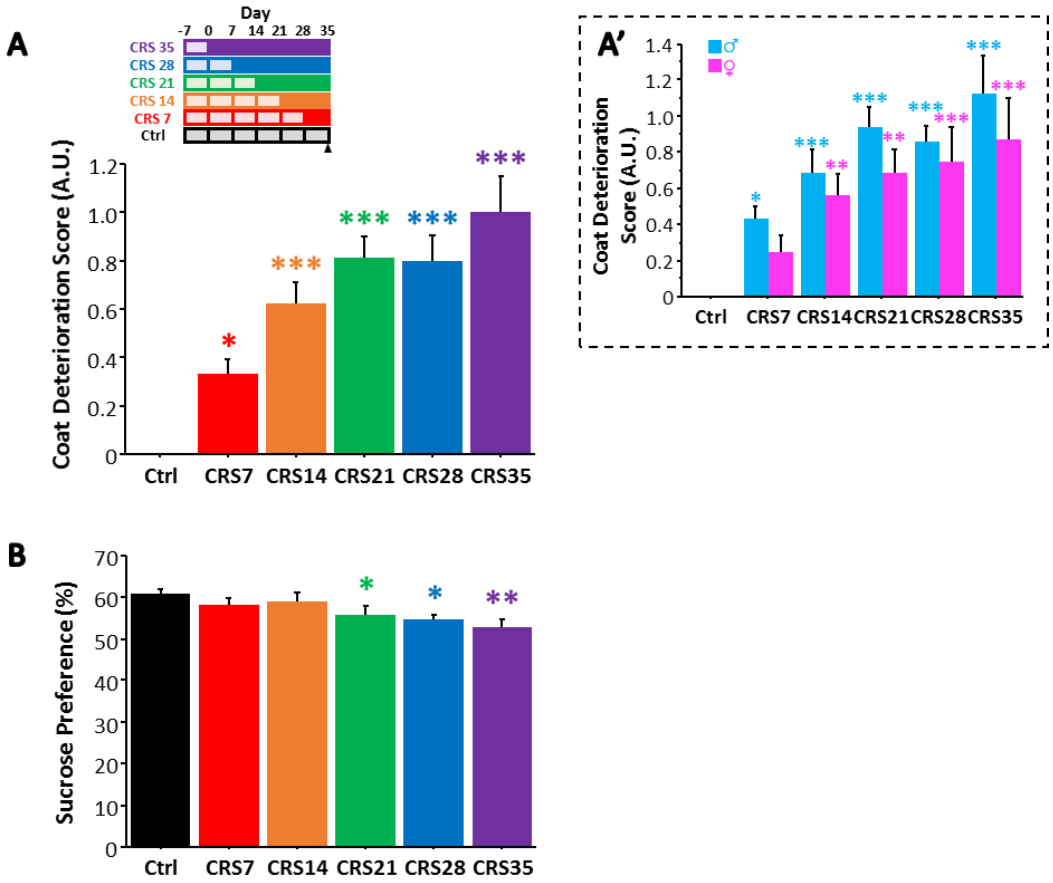

Figure 5. ***Effects of chronic restraint stress (CRS) on coat state quality and sucrose preference (Experiment 1).***

(**A**) A schematic of the experimental paradigm over 35 days. Empty squares indicate weeks with no CRS, filled squares indicate weeks when animals were subjected CRS, with behaviour assessed on last week of experimentation (black arrow). Groups: Ctrl (control; black), CRS7 (red), CRS14 (orange), CRS21 (green), CRS28 (blue), and CRS35 (purple). Coat state was assessed on 7 areas of the animal's body attributing a score of 0, 0.5, or 1 (n=16/group). CRS-exposure exhibited higher scores demonstrating poor coat state, compared to controls. Coat state deterioration was increased over the CRS exposure. (**A'**) Sex differences in coat state quality. Males (light blue) overall showed greater coat state deterioration than females (pink). (**B**) Sucrose preference was decreased from 21 days of CRS onwards, compared to controls. *p<0.05, **p<0.01, ***p<0.001. Error bars ± SEM.

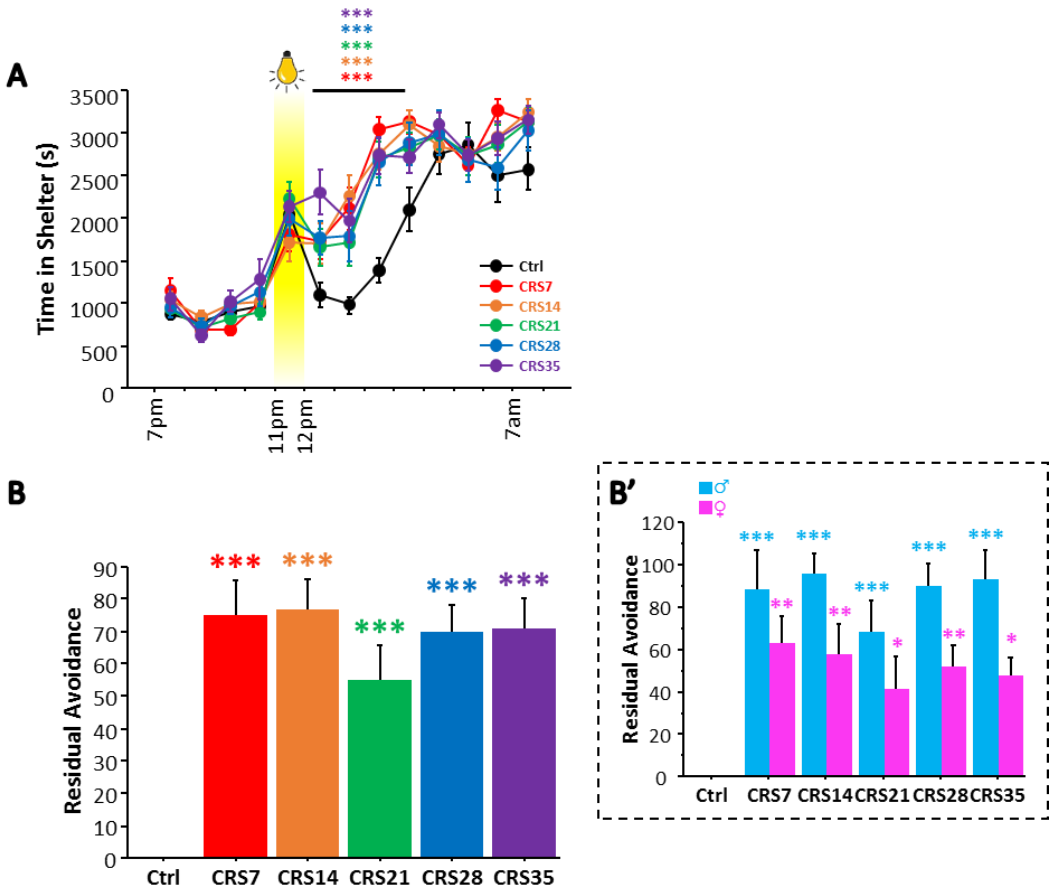

Figure 6. ***CRS induces greater residual avoidance (Experiment 1)*.**

(**A**) Chronic restraint stress (CRS) resulted in increased time spent in the shelter zone for the 4 hours following the light challenge (indicated by lightbulb), as compared to controls (n=16/group). (**B**) Residual avoidance was increased from 7 days of CRS onwards, when compared to controls. (**B'**) Sex differences in residual avoidance. Males (light blue) overall showed greater residual avoidance than females (pink). Groups: Ctrl (control; black), CRS7 (red), CRS14 (orange), CRS21 (green), CRS28 (blue), and CRS35 (purple). *p<0.05, **p<0.01, ***p<0.001. Error bars ± SEM.

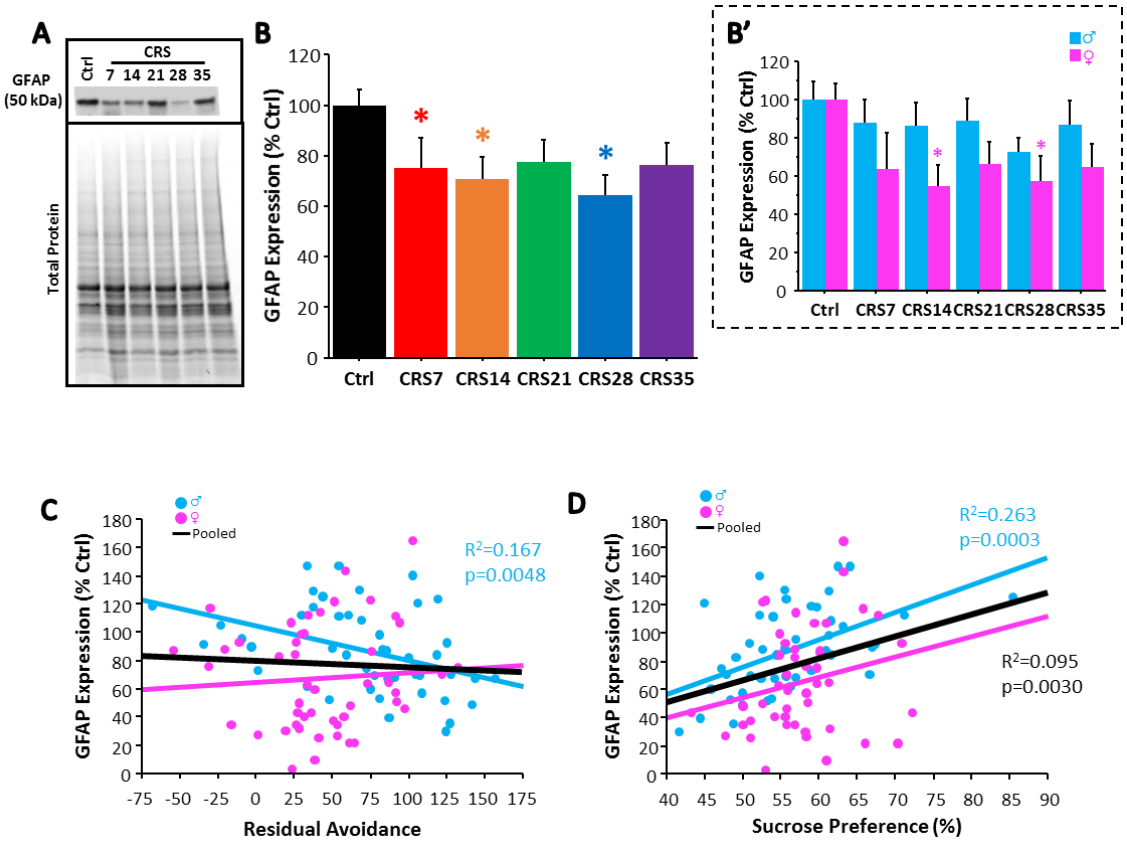

Figure 7. ***CRS results in decreased GFAP protein expression levels, which correlated with sucrose preference.***

(**A**) Nitrocellulose membrane labelled for glial fibrillary acidic protein (GFAP at 50 kDa), and picture of the gel showing total protein (below). (**B**) Chronic restraint stress (CRS) reduces GFAP protein expression levels from 7 days of stress onwards, compared to controls. Groups (n=16/group): Ctrl (control; black), CRS7 (red), CRS14 (orange), CRS21 (green), CRS28 (blue), and CRS35 (purple). (**B'**) Sex differences in GFAP protein levels. Females (pink) overall showed greater reduction in GFAP expression levels than males (light blue). (**C**) GFAP protein expression levels negatively correlated with residual avoidance only in the males (light blue). (**D**) GFAP protein expression levels positively correlated with sucrose preference overall (black), and in males (light blue), but not in females (pink). **p*<0.05. Error bars ± SEM.

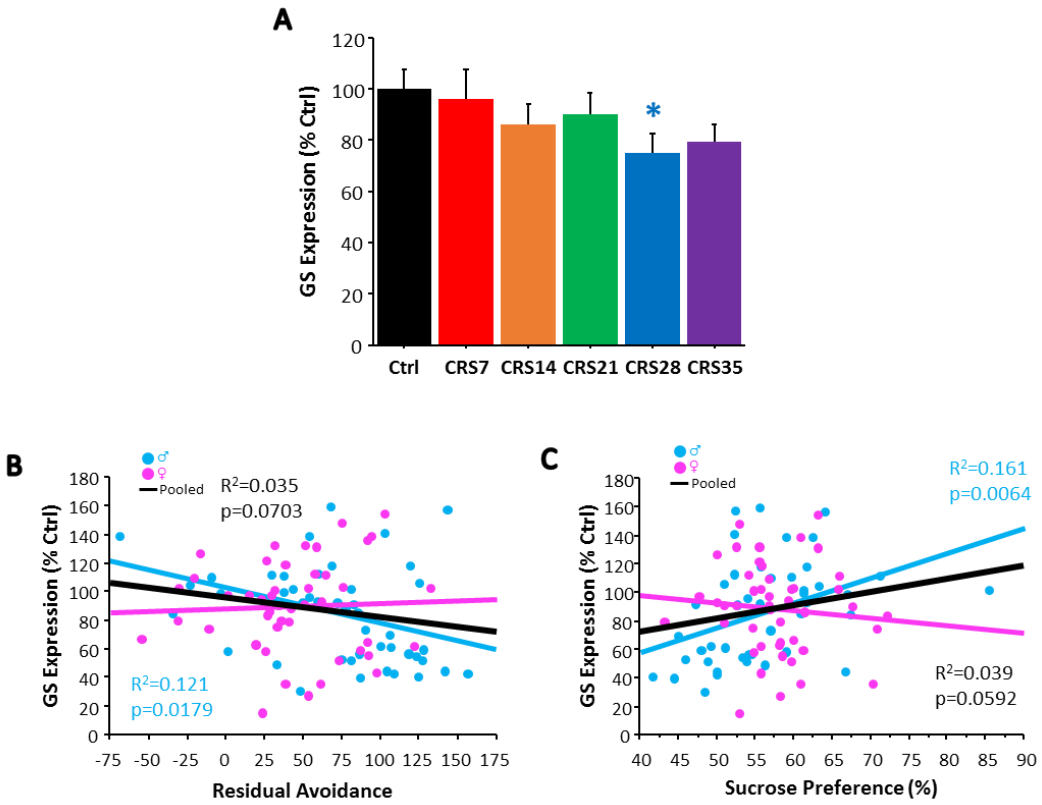

Figure 8. ***CRS results in decreased GS protein expression levels, which correlated with residual avoidance and sucrose preference.***

(**A**) Chronic restraint stress (CRS) reduces glutamine synthetase (GS) protein expression levels at 28 days of stress and a trend towards a decrease at 35 days of CRS, compared to controls. Groups (n=16/group): Ctrl (control; black), CRS7 (red), CRS14 (orange), CRS21 (green), CRS28 (blue), and CRS35 (purple). (**B**) GS protein expression levels negatively correlated with residual avoidance overall (black), and in males (light blue) but not in female (pink). (**C**) GS protein expression levels positively correlated with sucrose preference overall, in males (light blue) but not in females (pink). *p<0.05. Error bars ± SEM.

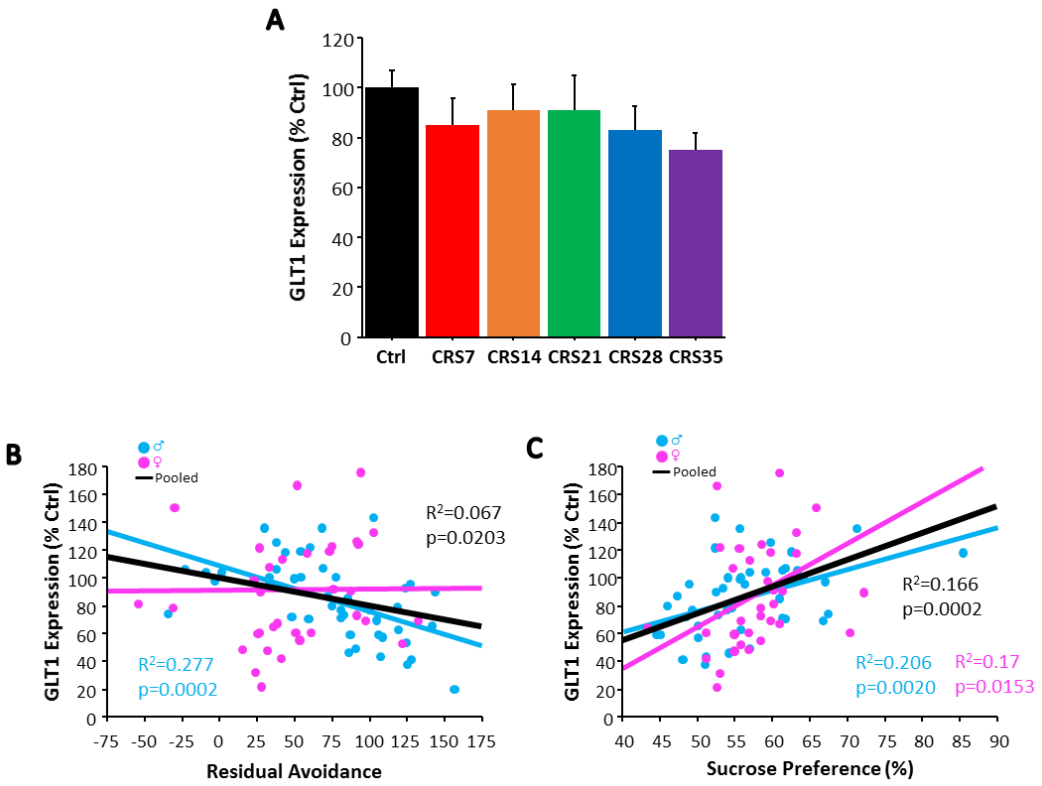

Figure 9. ***CRS induces a trend towards reduced GLT1 protein expression levels, which correlated with residual avoidance and sucrose preference.***

(**A**) Chronic restraint stress (CRS) animals displayed a trend towards reduced glutamate transporter 1 (GLT1) protein expression levels at 35 days of CRS, compared to controls. Groups (n=16/group): Ctrl (control; black), CRS7 (red), CRS14 (orange), CRS21 (green), CRS28 (blue), and CRS35 (purple). (**B**) GLT1 protein expression levels negatively correlated with residual avoidance overall (black), in males (light blue) but not in females (pink). (**C**) GLT1 protein expression levels positively correlated with sucrose preference overall, and in both sexes. Error bars ± SEM.

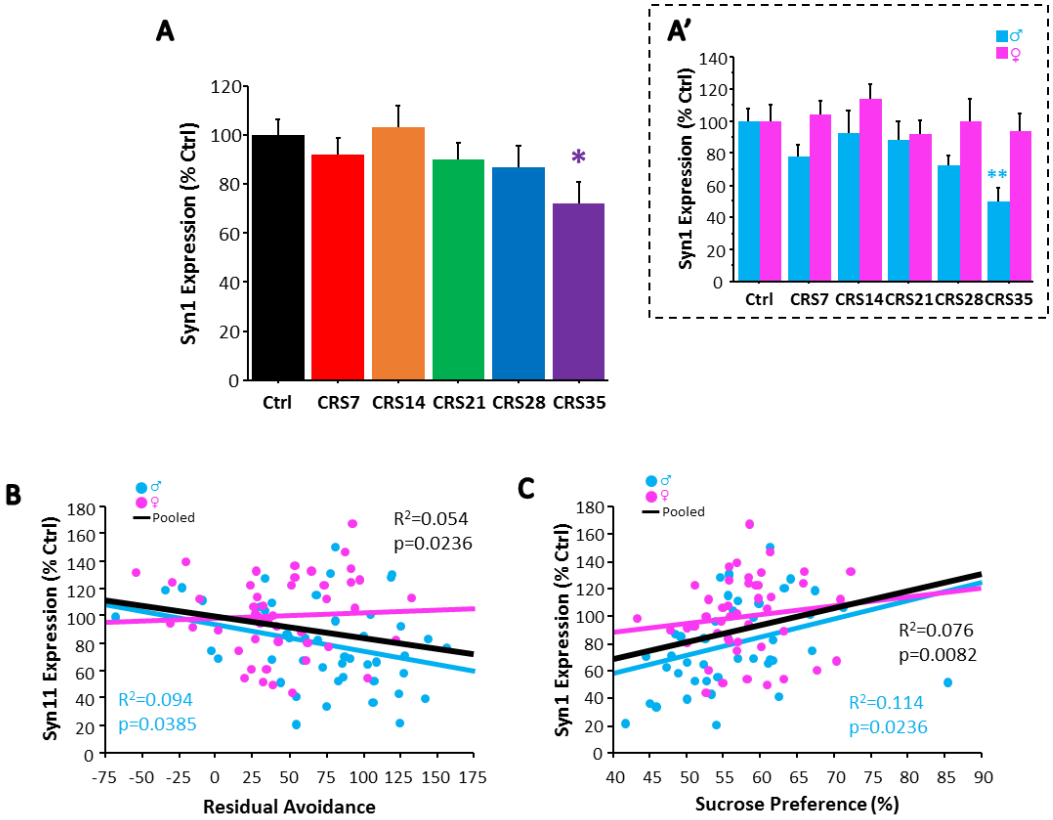

Figure 10. ***CRS results in decreased Syn1 protein expression levels, which correlated with residual avoidance and sucrose preference.***

(**A**) Chronic restraint stress (CRS) reduces synapsin 1 (Syn1) protein expression levels after 35 days of CRS, compared to controls. Groups (n=16/group): Ctrl (control; black), CRS7 (red), CRS14 (orange), CRS21 (green), CRS28 (blue), and CRS35 (purple). (**A'**) Sex differences in Syn1 protein levels. Males (light blue) overall showed greater reduction in Syn1 expression levels than females (pink) on CRS28 and CRS35. (**B**) Syn1 protein expression levels negatively correlated with residual avoidance overall (black), and in males (light blue) but not in females (pink). (**C**) Syn1 protein expression levels positively correlated with sucrose preference overall, and in males (light blue) and not in females (pink). **p*<0.05, ***p*<0.01. Error bars ± SEM.

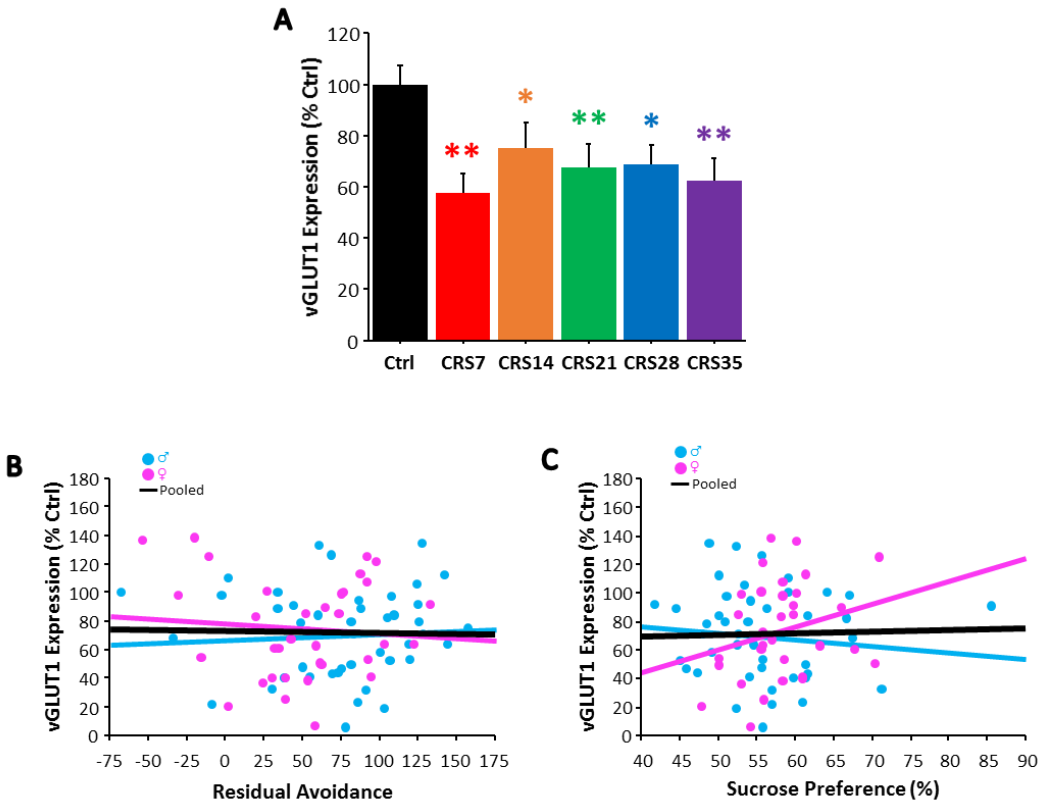

Figure 11. ***CRS results in decreased vGLUT1 protein expression levels.***

(**A**) Chronic restraint stress (CRS) reduces vesicular glutamate transporter (vGLUT1) protein expression levels from 7 days of CRS onwards, compared to controls. Groups (n=16/group): Ctrl (control; black), CRS7 (red), CRS14 (orange), CRS21 (green), CRS28 (blue), and CRS35 (purple). (**B**) vGLUT1 protein expression did not correlate with residual avoidance overall (black) or in either sexes (light blue and pink). (**C**) vGLUT1 protein expression did not correlate with sucrose preference overall (black) or in either sexes (light blue and pink). *p<0.05, **p<0.01. Error bars ± SEM.

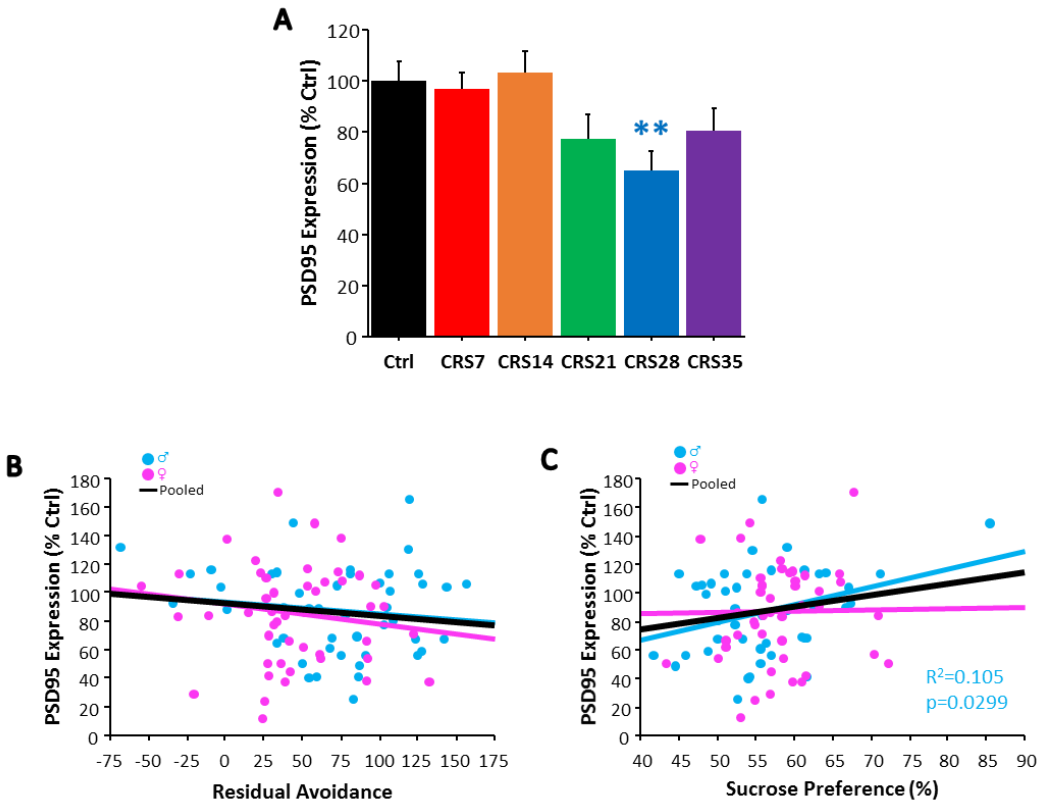

Figure 12. ***CRS results in decreased PSD95 protein expression levels.***

(**A**) Chronic restraint stress (CRS) reduces post-synaptic density 95 (PSD95) protein expression levels from 21 days of CRS onwards, compared to controls. Groups (n=16/group): Ctrl (control; black), CRS7 (red), CRS14 (orange), CRS21 (green), CRS28 (blue), and CRS35 (purple). (**B**) PSD95 protein expression did not correlate with residual avoidance. (**C**) PSD95 protein expression levels positively correlated with sucrose preference only in the males (light blue). ***p*<0.01. Error bars ± SEM.

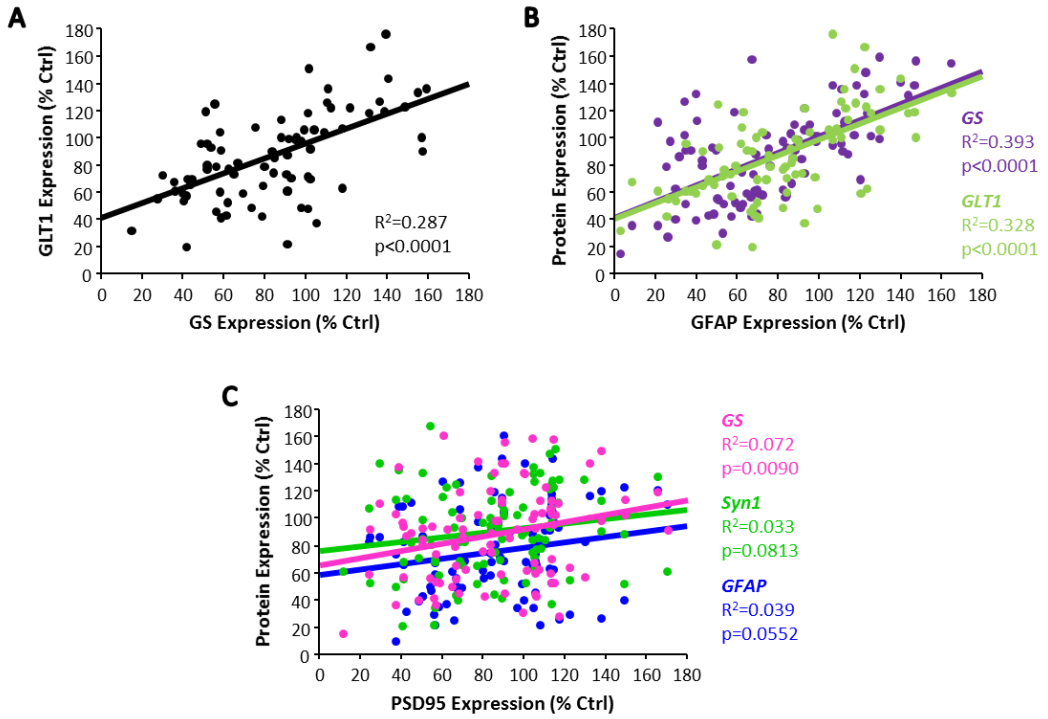

Figure 13. ***Marker vs. marker correlations of synaptic and astroglial proteins*****.**

(**A**-**B**) The three astrocytic markers (glutamate transporter 1 [GLT1], glutamine synthetase [GS], and glial fibrillary acidic protein [GFAP]) strongly correlated with each other. (**C**) The only synaptic protein that correlated with two astrocytic markers (GS and GFAP) and synapsin 1 (Syn1) was post-synaptic density 95 (PSD95). %Ctrl = percent control.

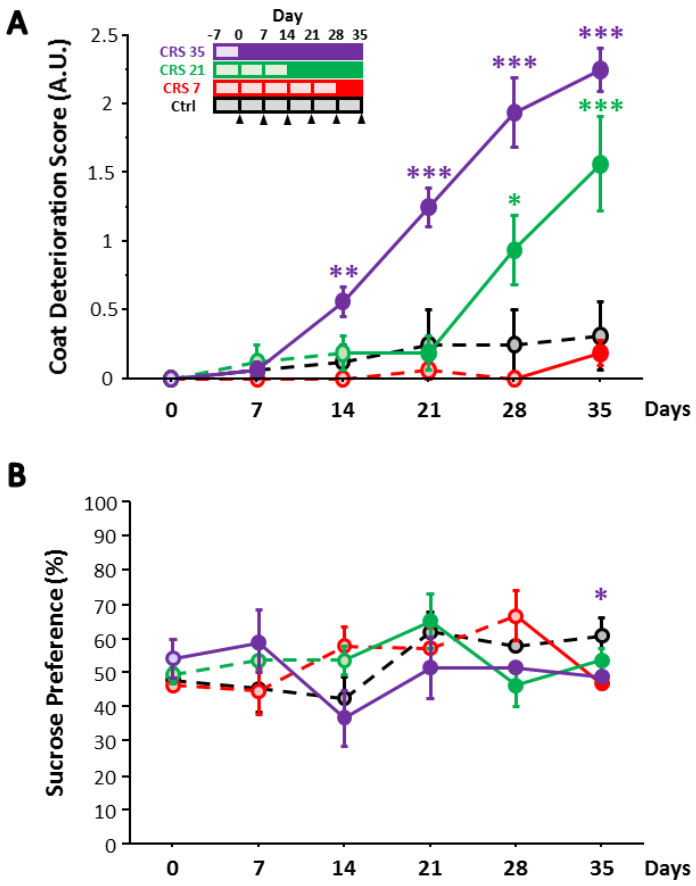

Figure 14. ***Effects of CRS on coat state quality and sucrose preference in GFAP-GFP mice (Experiment 2).***

Filled circles indicate the mice went through chronic restraint stress (CRS) before that testing time point, empty circles indicate mice did not go through CRS before that testing time point. Solid lines indicate CRS occurring for those 7 days, dotted lines indicate no CRS occurring. (**A**) A schematic of the experimental paradigm over 35 days. Empty squares indicate no CRS, filled squares indicate animal went through CRS that week, with behaviour assessed every week (black arrows). Groups (n=8/group): Ctrl (control; black), CRS7 (red), CRS21 (green), and CRS35 (purple). CRS-exposure exhibited greater coat state deterioration after 2 weeks of CRS (CRS35 from day 14, CRS21 from day 28). Coat state deterioration was greater as the length of CRS exposure increased. (**B**) Sucrose preference was only decreased for the CRS35 group after 35 days of CRS. *p<0.05, **p<0.01, ***p<0.001. Error bars ± SEM.

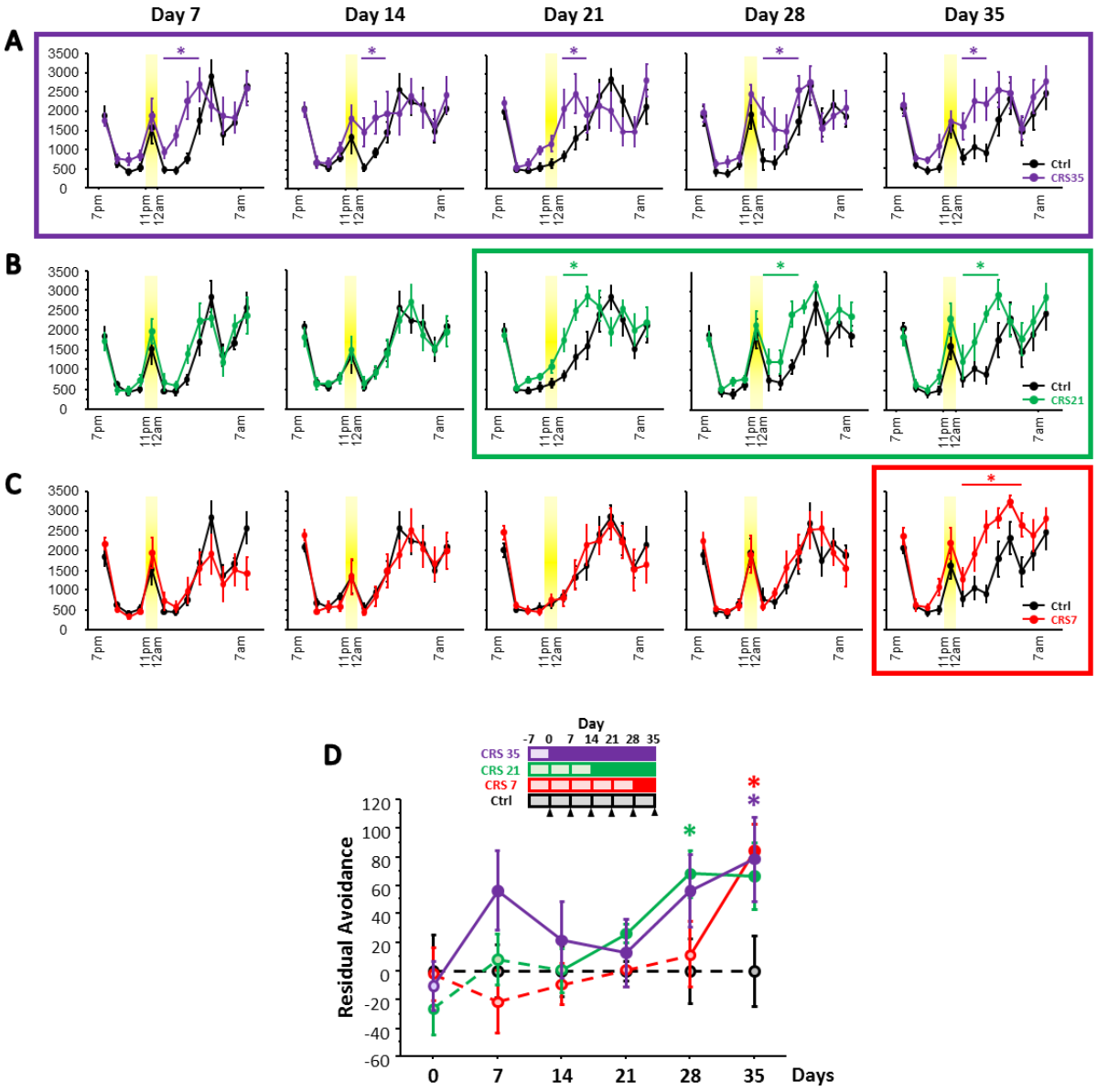
Day 7
Day 14
Day 21
Day 28
Day 35
A
B
C
D
Ctrl
CRS35
CRS21
CRS7
7pm
11pm
12am
7am
Day
-7 0 7 14 21 28 35
CRS 35
CRS 21
CRS 7
Ctrl
Residual Avoidance
Days

Figure 15. ***CRS induces greater residual avoidance in GFAP-GFP mice (Experiment 2)*****.**

(**A**) Chronic restraint stress (CRS) resulted in increased time spent in the shelter zone for 3-4 hours following the light challenge (indicated by yellow strip), as compared to controls, from Day 7 to Day 35. (**B**) CRS resulted in increased time spent in the shelter zone for 3-4 hours following the light challenge (indicated by yellow strip), as compared to controls, from Day 21 to Day 35. No difference between controls and CRS21 group when no CRS was applied (Day 7 and 14). (**C**) CRS resulted in increased time spent in the shelter zone for 6 hours following the light challenge (indicated by yellow strip), as compared to controls, on Day 35. No difference between controls and CRS7 group when no CRS was applied (Day 7 to 25). (**D**) Filled circles indicate the mice went through chronic restraint stress (CRS) before that testing time point, empty circles indicate mice did not go through CRS before that testing time point. Solid lines indicate CRS occurring for those 7 days, dotted lines indicate no CRS occurring. CRS-exposure exhibited greater residual avoidance overall. CRS35 mice showed increased residual avoidance after 7, 28, and 35 days of CRS. CRS21 mice displayed increased residual avoidance after 14 and 21 days of CRS. CRS7 mice displayed increased residual avoidance after 7 days of CRS*$p<0.05$. Error bars ± SEM.

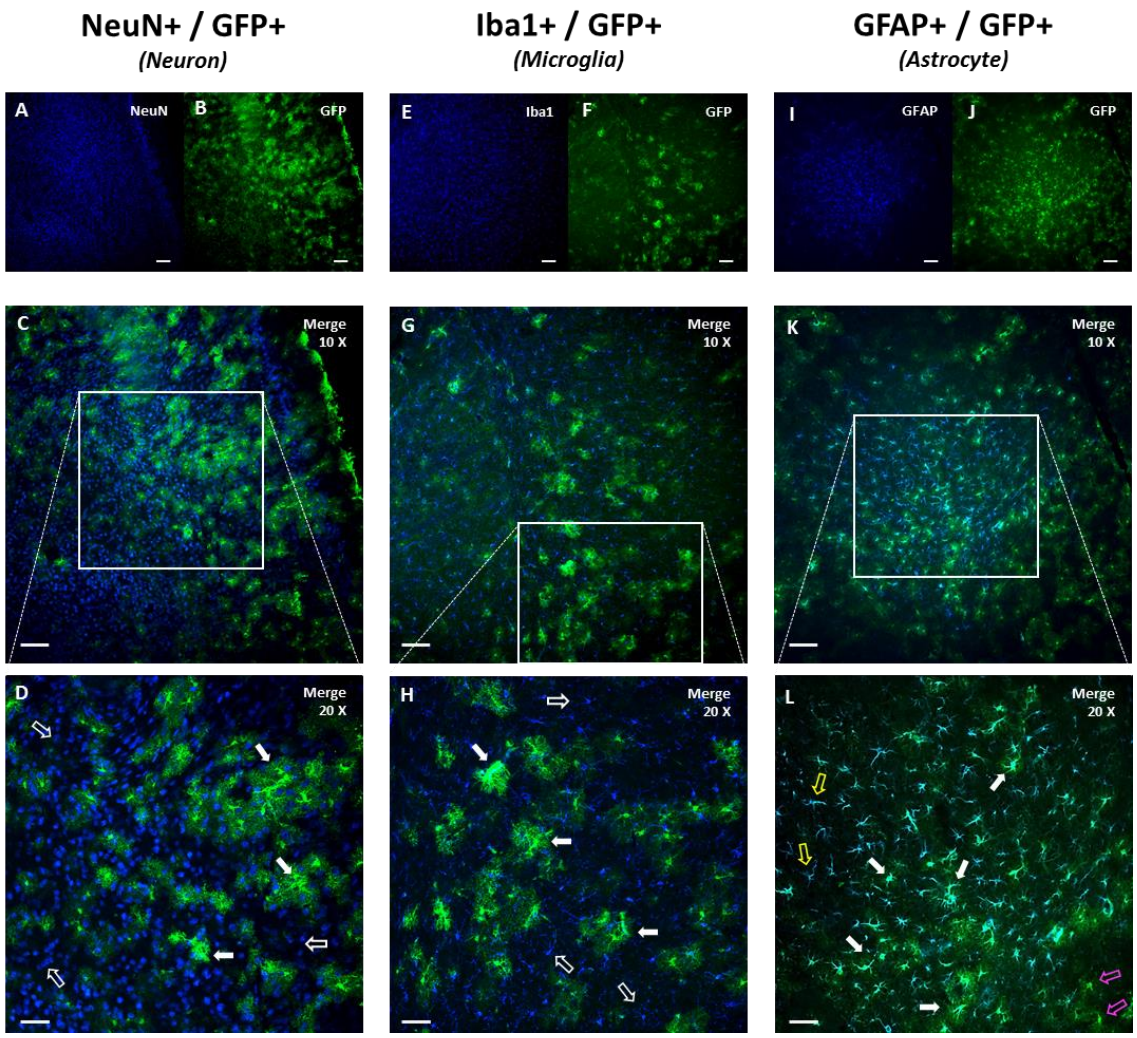

Figure 16. ***GFAP-GFP mice displayed GFP+ immunofluorescence overlap with GFAP+ cells*****.**

Images of wild type mouse prefrontal cortex (PFC) immunolabelled for either neuronal nuclei (NeuN) and green fluorescent protein (GFP) (**A-D**), ionized calcium binding adaptor molecule 1 (Iba1) and GFP (**E-H**), or glial fibrillary acidic protein (GFAP) and GFP (**I-L**). There were no GFP+ cells overlapping with NeuN+ (**C-D**) or Iba1+ cells (**G-H**). However, half of GFAP+ cells overlapped with GFP+ cells, and half of GFP+ cells overlapped with GFAP+ cells (**K-L**). Arrows: (**D**) Filled arrows pointing at GFP+ cells, empty arrows indicating NeuN+ cells; (**H**) Filled arrows pointing at GFP+ cells, empty arrows indicating Iba1+ cells; (**L**) Filled white arrows indicating GFAP+/GFP+ overlapping cells, empty yellow arrows indicating only GFAP+ cells (GFAP+/GFP-), empty pink arrows indicating only GFP+ cells (GFAP-/GFP+). (**A-C, E-G, I-K**) Scale bar = 100µm. (**D, H, L**) Scale bar = 50µm.

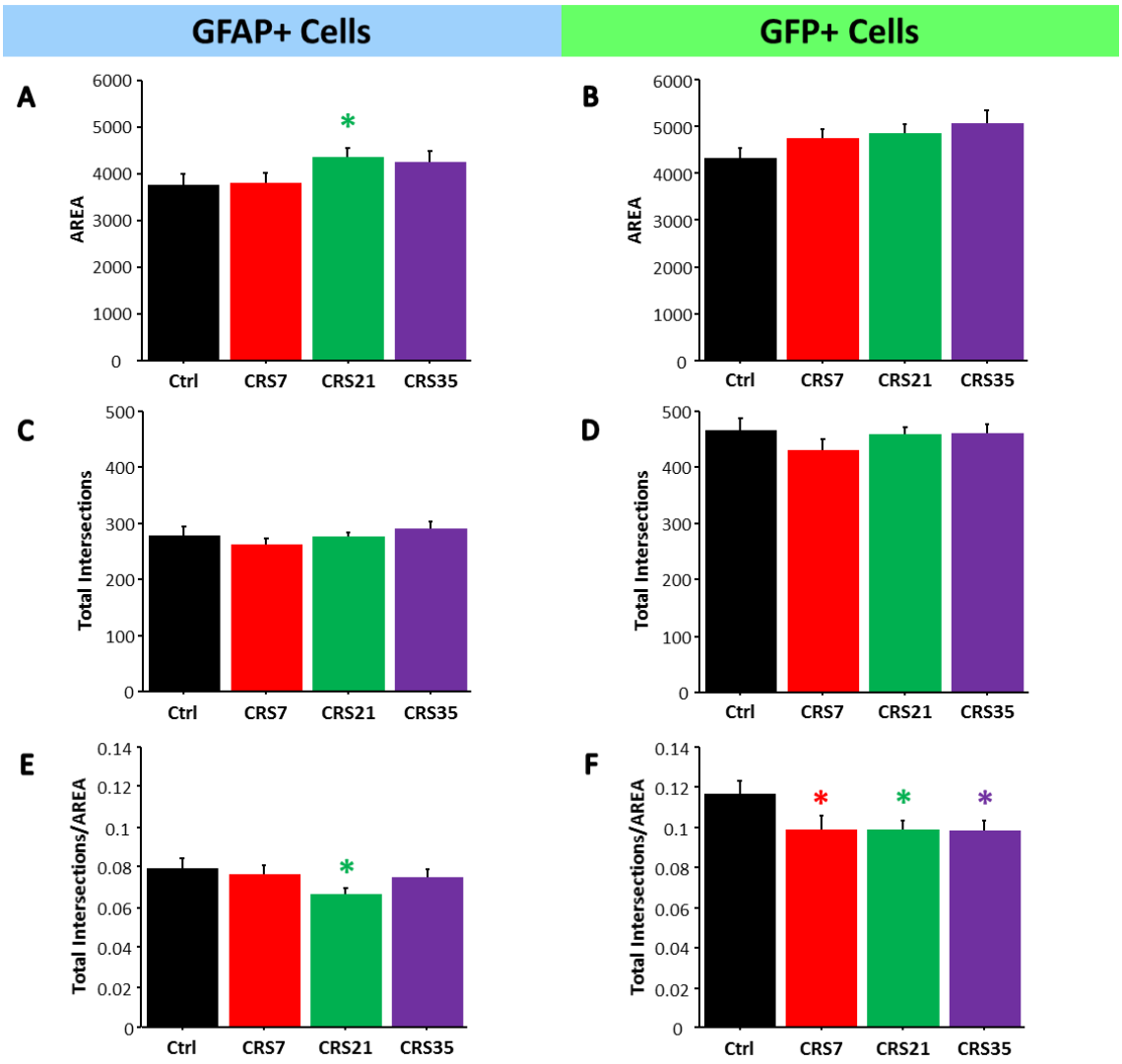

Figure 17. ***CRS results in reduced GFP+ cells Total Intersections/AREA.***

Groups: Ctrl (control; black), CRS7 (red), CRS21 (green), and CRS35 (purple). CRS = chronic restraint stress. ***AREA:*** Increased AREA seen in glial fibrillary acidic protein (GFAP+) cells of CRS21 group compared to controls (**A**), while no difference was seen between groups in green fluorescent protein (GFP+) cells (**B**). ***Total Intersections:*** No differences seen between controls and CRS groups in either GFAP+ cells (**C**) or GFP+ cells (**D**). ***Total Intersections/AREA:*** CRS exposure decreased GFAP+ total intersections per AREA in the CRS21 group (**E**), while all 3 groups exposed to CRS showed decreased total intersections per AREA of GFP+ cells (**F**), compared to controls. In general, GFAP+ cells had less AREA and total intersections (**A, C, E**) compared to GFP+ cells (**B, D, F**). *p<0.05. Error bars ± SEM.

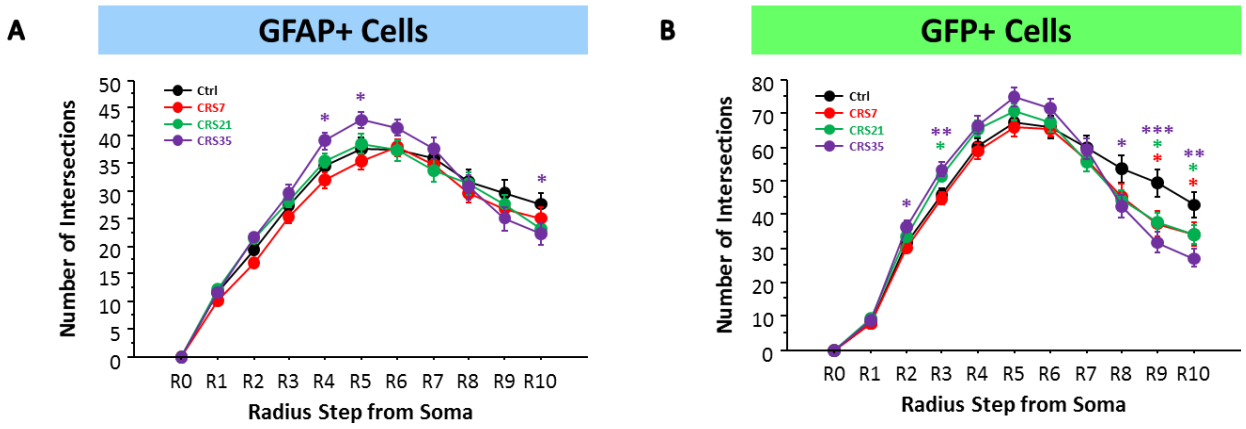

Figure 18. ***Sholl analysis reveals CRS-induced decreased in distal number of intersections per radius step while increasing proximal number of intersections, both more pronounced in GFP+ cells.***

Groups: Ctrl (control; black), CRS7 (red), CRS21 (green), and CRS35 (purple). CRS = chronic restraint stress. R = radius step from soma. CRS induces decreases in distal intersections (R8-R10) while increasing proximal intersections (R2-R5), compared to controls, in both glial fibrillary acidic protein (GFAP+) cells (**A**) and green fluorescent protein (GFP+) cells (**B**).

(**A**) Compared to GFAP+ cells in controls: CRS7 animals showed increased intersections at R2; CRS21 showed decreased intersections at R10; CRS35 showed increased intersections proximally (R2, R4-5) and decreased distal intersections (R9-10). (**B**) Compared to GFP+ cells in controls: CRS7 showed decreased distal intersections (R8-10); CRS21 showed decreased distal intersections (R8-10) and increased intersections at R3; CRS35 showed increased proximal intersections (R2-5) and decreased distal intersections (R8-10). *p<0.05, **p<0.01, ***p<0.001. Error bars ± SEM.

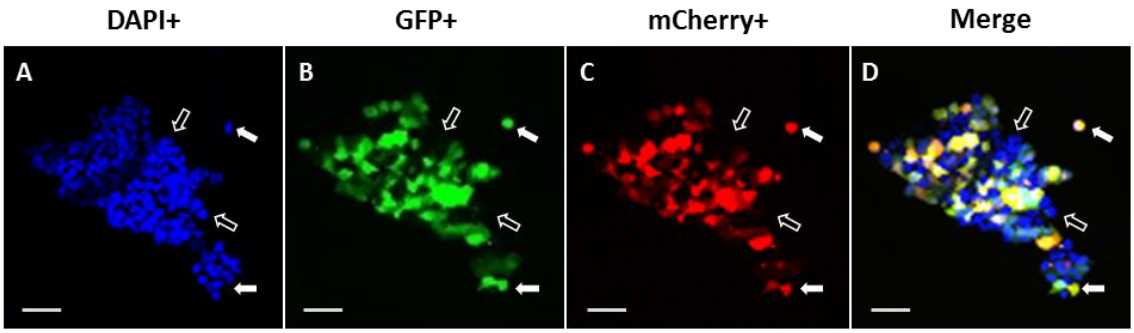

Figure 19. ***Co-transfection efficiency in HEK293 cells*****.**

Images of HEK293 cell culture co-transfected with AAV-GFP (green) and AAV-mCherry (red) plasmids. Cells stained with 4′,6-diamidino-2-phenylindole (DAPI, blue) (**A**), green fluorescent protein (GFP) (**B**), and mCherry (**C**). (**D**) DAPI+, GFP+, and mCherry+ images merged. Solid arrows indicate HEK293 cells expressing both GFP+ and mCherry+ immunofluorescence (DAPI+/GFP+/mCherry+) (**A**-**D**). Empty arrows indicate HEK293 cells stained with DAPI+ but did not express GFP or mCherry (DAPI+/GFP-/mCherry-) (**A**-**D**). Scale bar = 50µm.

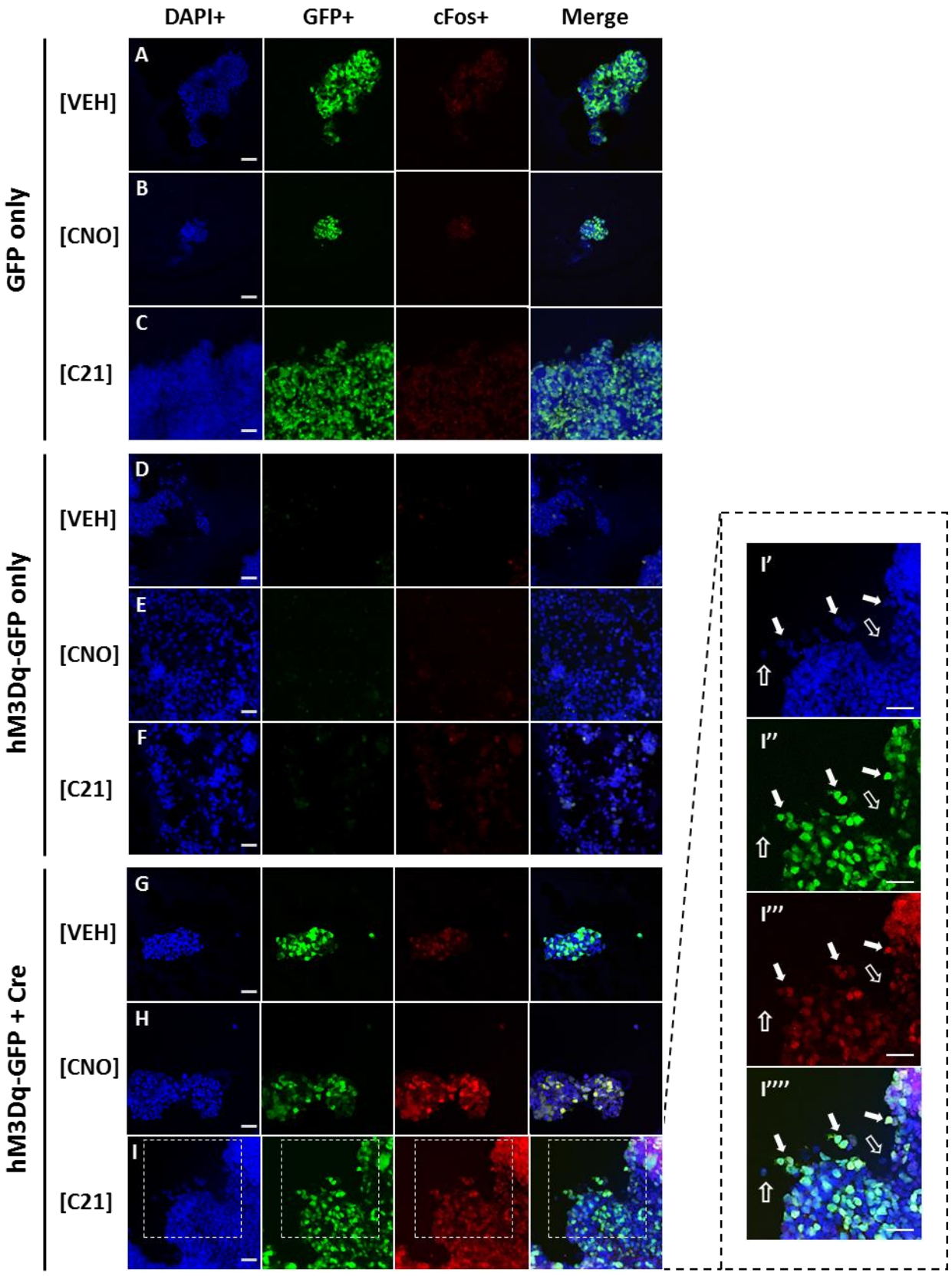
DAPI+
GFP+
cFos+
Merge
GFP only
[VEH]
[CNO]
[C21]
hM3Dq-GFP only
[VEH]
[CNO]
[C21]
hM3Dq-GFP + Cre
[VEH]
[CNO]
[C21]
A
B
C
D
E
F
G
H
I
I'
I''
I'''
I''''

Figure 20. ***HEK293 cells co-transfected with hM3Dq-GFP and Cre plasmids showed elevated levels of cFos when CNO or C21 is applied*****.**

Images of HEK293 cell culture co-transfected with AAV-GFP, hM3Dq-GFP, or hM3Dq-GFP and Cre plasmids. Cells stained with 4′,6-diamidino-2-phenylindole (DAPI) (blue, **column 1**), green fluorescent protein (GFP, green) (**column 2**), and cFos (**column 3, red**). **Column 4:** DAPI+, GFP+, and cFos+ images merged. Cells transfected with only the AAV-GFP plasmid expressed GFP but showed no increase in cFos+ labelling, regardless of ligand applied (**A-C**). Cells transfected with only the hM3Dq-GFP plasmid did not express GFP and showed elevation in cFos+ labelling, regardless of ligand applied (**D-F**). Cells transfected with both hM3Dq-GFP and AAV-Cre plasmid expressed GFP and showed elevated cFos+ labelling when CNO or C21 is applied (**H-I**), but not with vehicle exposure (**G**). (**I'-I'''**) Magnified area of boxed area (dotted square) in I. Solid arrows indicate HEK293 (DAPI+) cells expressing GFP also showing elevated levels of cFos labelling. Empty arrows indicate HEK293 (DAPI+) cells not expressing GFP showing low level of cFos labelling. Ligands: vehicle (VEH), clozapine-N-oxide (CNO), or DREADDs agonist 21 (C21). Scale bar = 50μm.

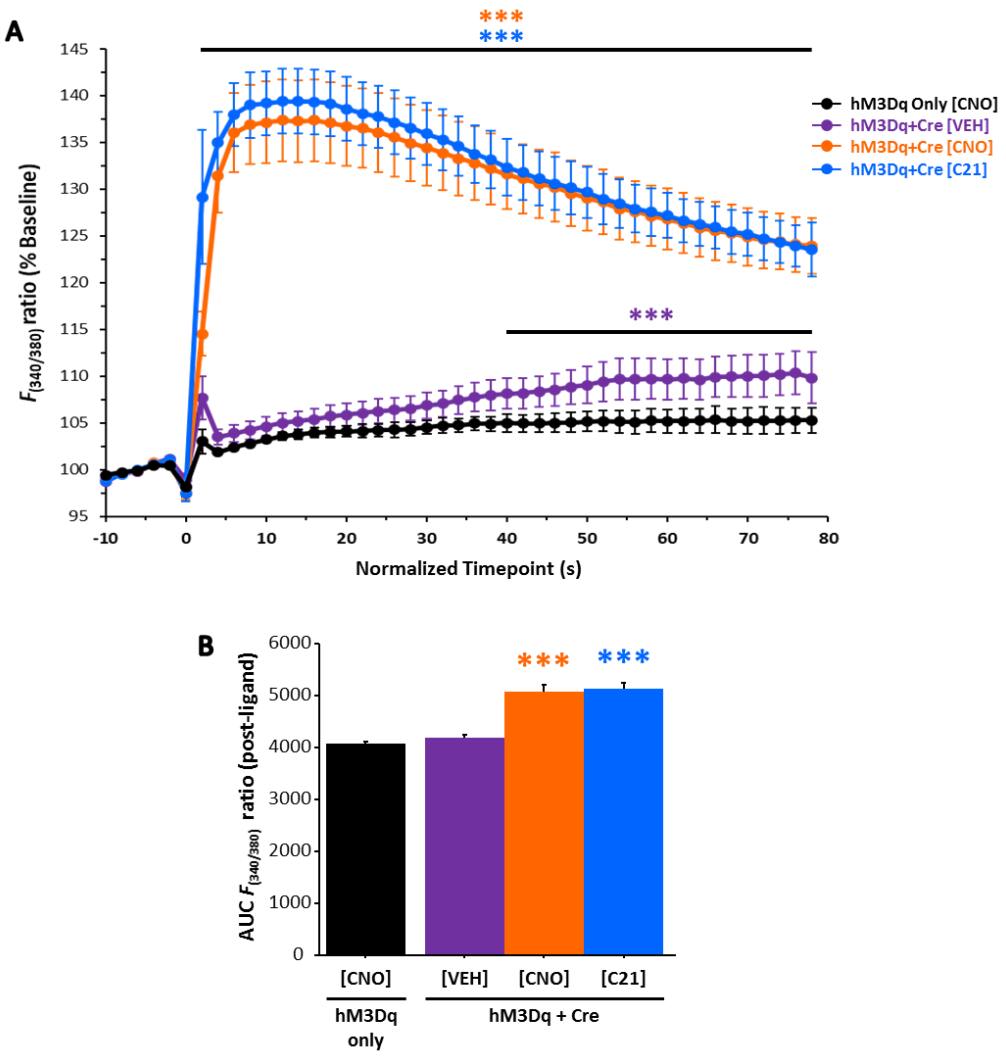

Figure 21. ***HEK293 cells co-transfected with hM3Dq and Cre plasmids display elevated levels of calcium mobilization after CNO or C21 exposure.***

(**A**) Averaged traces of calcium mobilization assay. Cells co-transfected with hM3Dq and Cre plasmids show greater calcium mobilization immediately after CNO or C21 exposure (Time 0), compared to hM3Dq+Cre [VEH] or hM3Dq only [CNO]. hM3Dq+Cre plasmids and exposed to VEH show slight elevated levels of calcium mobilization 40 seconds after exposure, compared to hM3Dq only [CNO]. (**B**) Area under the curve (AUC) calculation post-ligand exposure. Cells co-transfected with hM3Dq and Cre plasmids showed greater AUC after exposure to CNO or C21, compared to cells co-transfected with hM3Dq and Cre but exposed to VEH or cells transfected with only the hM3Dq plasmid and exposed to CNO. Ligands: vehicle (VEH), clozapine-N-oxide (CNO), or DREADDs agonist 21 (C21). ***p<0.001. Error bars ± SEM.

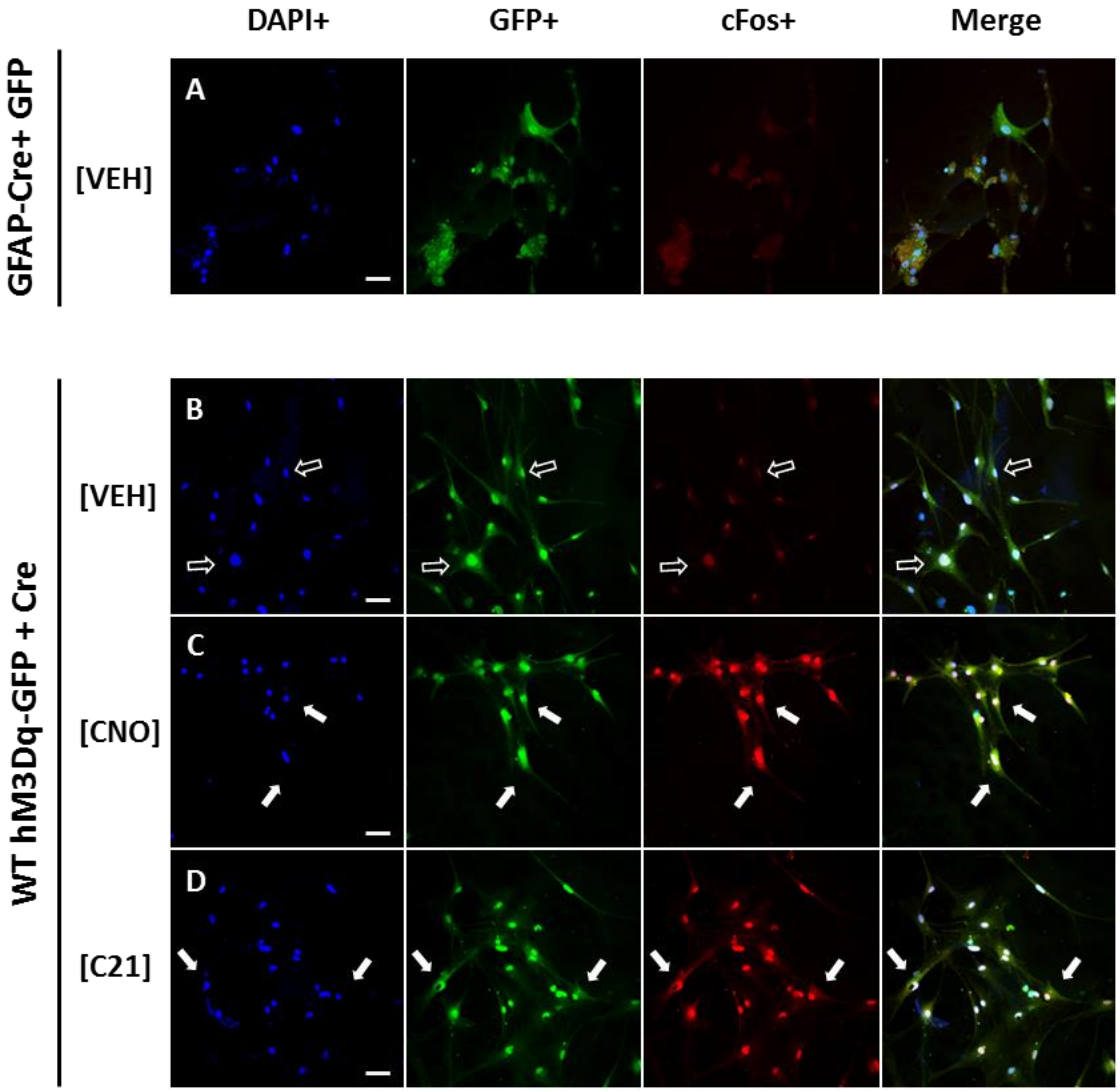
DAPI+
GFP+
cFos+
Merge
GFAP-Cre+ GFP
[VEH]
A
WT hM3Dq-GFP + Cre
[VEH]
B
[CNO]
C
[C21]
D

Figure 22. ***Primary astrocyte cultures from wild-type mice co-transfected with hM3Dq-GFP and Cre plasmids showed elevated levels of cFos when CNO or C21 is applied*****.**

Images of primary astrocyte cultures (PAC) from glial fibrillary acidic protein (GFAP)-Cre+ mice (transfected with AAV-GFP plasmid only) or wild-type littermates (co-transfected with hM3Dq-GFP+Cre plasmids) stained with 4′,6-diamidino-2-phenylindole (DAPI, blue) (**column 1**), green fluorescent protein (GFP, green) (**column 2**), and cFos (**column 3, red**). **Column 4:** DAPI+, GFP+, and cFos+ images merged. PAC from GFAP-Cre+ mice transfected with only the AAV-GFP plasmid expressed GFP but show no elevation cFos labelling (**A**). PAC from wild-type littermates co-transfected with hM3Dq-GFP and AAV-Cre plasmid expressed GFP and showed elevation cFos labelling when CNO or C21 is applied (**C**-**D**), but not with vehicle exposure (**B**). Solid arrows indicate PAC (DAPI+) cells expressing GFP and showing elevated cFos (**C**-**D**). Empty arrows indicate PAC (DAPI+) cells not expressing GFP showing low levels of cFos labelling (**B**). Ligands: vehicle (VEH), clozapine-N-oxide (CNO), or DREADDs agonist 21 (C21). Scale bar = 50μm.

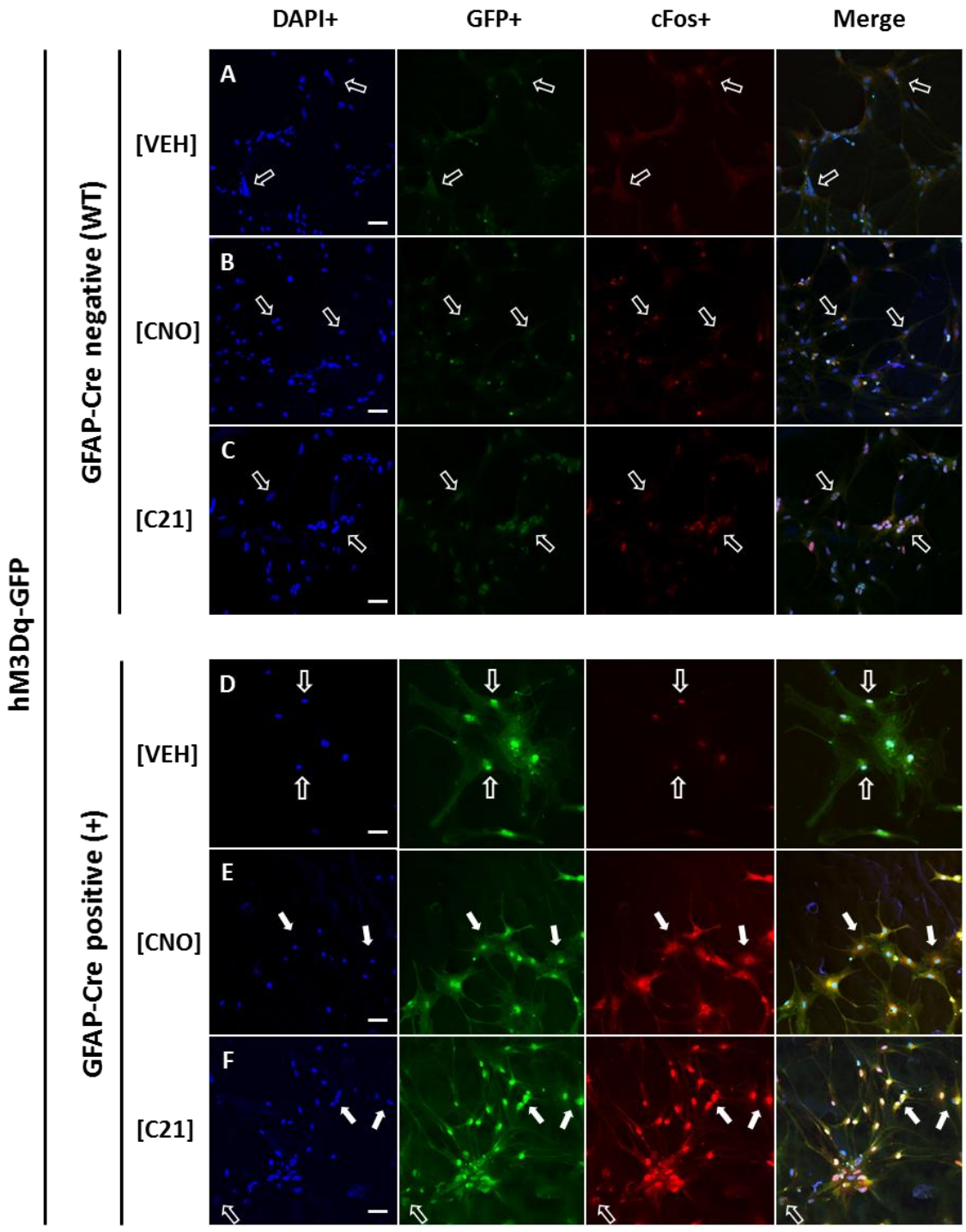
DAPI+
GFP+
cFos+
Merge
hM3Dq-GFP
GFAP-Cre negative (WT)
GFAP-Cre positive (+)
[VEH]
[CNO]
[C21]
A
B
C
D
E
F

Figure 23. ***Primary astrocyte cultures from GFAP-Cre mice, not wild type littermates, transfected with the hM3Dq-GFP plasmid showed elevated levels of cFos when CNO or C21 is applied.***

Images of primary astrocyte cultures (PAC) from glial fibrillary acidic protein (GFAP)-Cre+ mice or wild-type littermates, transfected with hM3Dq-GFP plasmids, stained with 4′,6-diamidino-2-phenylindole (DAPI, blue) (**column 1**), green fluorescent protein (GFP, green) (**column 2**), and cFos (red) (**column 3**). **Column 4:** DAPI+, GFP+, and cFos+ images merged. PAC from wild type mice transfected with hM3Dq-GFP did not express GFP and showed no elevation of cFos labelling, regardless of ligand applied (**A-C**). PAC from GFAP-Cre+ mice transfected with hM3Dq-GFP expressed GFP and showed elevated cFos labelling when CNO or C21 is applied (**E-F**), but not with vehicle exposure (**D**). Solid arrows indicate PAC (DAPI+) cells expressing GFP and elevated levels of cFos (**E-F**). Empty arrows indicate PAC (DAPI+) cells not expressing GFP showing low level of cFos labelling (**A-D, F**). Ligands: vehicle (VEH), clozapine-N-oxide (CNO), or DREADDs agonist 21 (C21). Scale bar = 50μm.

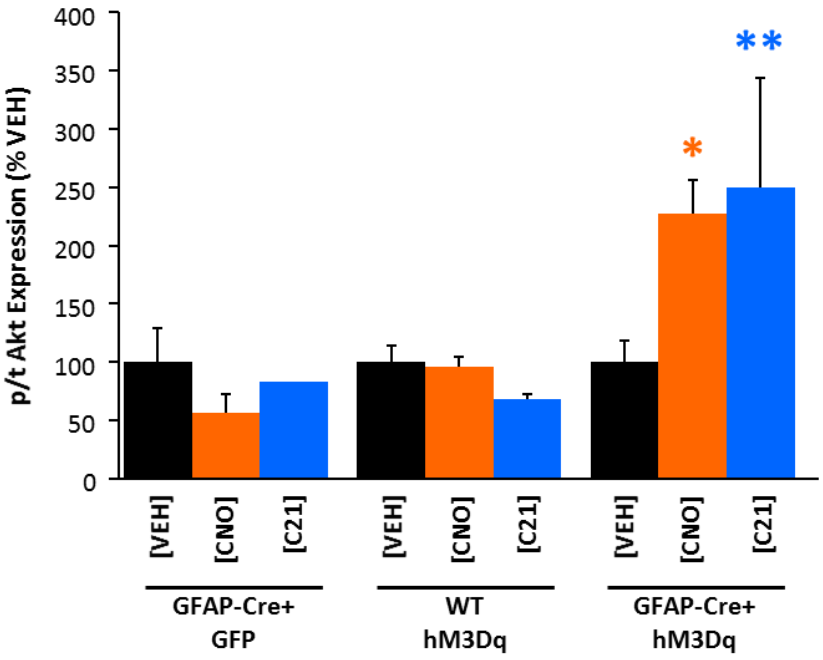

Figure 24. ***Primary astrocyte cultures from GFAP-Cre+ mice transfected with the hM3Dq plasmid display elevated levels of phosphorylated Akt after CNO or C21 exposure*.**

Primary astrocyte cultures (PAC) from glial fibrillary acidic protein (GFAP)-Cre+ mice transfected with the hM3Dq plasmid and exposed to CNO or C21 show increased levels of phosphorylated/total (p/t) Akt compared to GFAP-Cre+ cells transfected with hM3Dq plasmid exposed to vehicle. No difference was observed in p/t Akt levels between PAC from GFAP-Cre+ mice transfected with the AAV-GFP (green fluorescent protein) plasmid exposed to either VEH, CNO, or C21. Similarly, there were no differences in p/t Akt levels between PAC from wild type (WT) littermates transfected with the hM3Dq plasmid exposed to either VEH, CNO, or C21. Ligands: vehicle (VEH), clozapine-N-oxide (CNO), or DREADDs agonist 21 (C21). *p<0.05, **p<0.01. Error bars ± SEM.

References

Abdallah, C.G., Adams, T.G., Kelmendi, B., Esterlis, I., Sanacora, G., Krystal, J.H., 2016. Ketamine's Mechanism of Action: A Path to Rapid-Acting Antidepressants. Depression and anxiety 33, 689-697.

Acaz-Fonseca, E., Avila-Rodriguez, M., Garcia-Segura, L.M., Barreto, G.E., 2016. Regulation of astroglia by gonadal steroid hormones under physiological and pathological conditions. Progress in neurobiology 144, 5-26.

Adamsky, A., Kol, A., Kreisel, T., Doron, A., Ozeri-Engelhard, N., Melcer, T., Refaeli, R., Horn, H., Regev, L., Groysman, M., London, M., Goshen, I., 2018. Astrocytic Activation Generates De Novo Neuronal Potentiation and Memory Enhancement. Cell 174, 59-71 e14.

Al-Harbi, K.S., 2012. Treatment-resistant depression: therapeutic trends, challenges, and future directions. Patient preference and adherence 6, 369-388.

Albert, P.R., 2015. Why is depression more prevalent in women? Journal of psychiatry & neuroscience : JPN 40, 219-221.

Alexander, B.H., Barnes, H.M., Trimmer, E., Davidson, A.M., Ogola, B.O., Lindsey, S.H., Mostany, R., 2018. Stable Density and Dynamics of Dendritic Spines of Cortical Neurons Across the Estrous Cycle While Expressing Differential Levels of Sensory-Evoked Plasticity. Frontiers in molecular neuroscience 11, 83.

Alexopoulos, G.S., 2005. Depression in the elderly. Lancet 365, 1961-1970.

Allen, N.J., Eroglu, C., 2017. Cell Biology of Astrocyte-Synapse Interactions. Neuron 96, 697-708.

Ampuero, E., Luarte, A., Santibanez, M., Varas-Godoy, M., Toledo, J., Diaz-Veliz, G., Cavada, G., Rubio, F.J., Wyneken, U., 2015. Two Chronic Stress Models Based on Movement Restriction in Rats Respond Selectively to Antidepressant Drugs: Aldolase C As a Potential Biomarker. The international journal of neuropsychopharmacology 18, pyv038.

An, X.L., Zou, J.X., Wu, R.Y., Yang, Y., Tai, F.D., Zeng, S.Y., Jia, R., Zhang, X., Liu, E.Q., Broders, H., 2011. Strain and sex differences in anxiety-like and social behaviors in C57BL/6J and BALB/cJ mice. Experimental animals 60, 111-123.

Anacker, C., 2018. New Insight Into the Mechanisms of Fast-Acting Antidepressants: What We Learn From Scopolamine. Biological psychiatry 83, e5-e7.

Ancelin, M.L., Isabelle, C., Sylvaine, A., Jerome, M., Chantal, M., Karen, R., Joanne, R., Isabelle, C., 2018. Lifetime major depression and grey-matter volume. Journal of psychiatry & neuroscience : JPN 43.

Andrade, C., 2017. Ketamine for Depression, 1: Clinical Summary of Issues Related to Efficacy, Adverse Effects, and Mechanism of Action. The Journal of clinical psychiatry 78, e415-e419.

Arnone, D., 2019. Functional MRI findings, pharmacological treatment in major depression and clinical response. Progress in neuro-psychopharmacology & biological psychiatry 91, 28-37.

Arnone, D., McIntosh, A.M., Ebmeier, K.P., Munafo, M.R., Anderson, I.M., 2012. Magnetic resonance imaging studies in unipolar depression: systematic review and meta-regression analyses. European neuropsychopharmacology : the journal of the European College of Neuropsychopharmacology 22, 1-16.

Baek, J.H., Vignesh, A., Son, H., Lee, D.H., Roh, G.S., Kang, S.S., Cho, G.J., Choi, W.S., Kim, H.J., 2019. Glutamine Supplementation Ameliorates Chronic Stress-induced Reductions in Glutamate and Glutamine Transporters in the Mouse Prefrontal Cortex. Experimental neurobiology 28, 270-278.

Baghai, T.C., Varallo-Bedarida, G., Born, C., Hafner, S., Schule, C., Eser, D., Zill, P., Manook, A., Weigl, J., Jooyandeh, S., Nothdurfter, C., von Schacky, C., Bondy, B., Rupprecht, R., 2018. Classical Risk Factors and Inflammatory Biomarkers: One of the Missing Biological Links between Cardiovascular Disease and Major Depressive Disorder. International journal of molecular sciences 19.

Bai, X., Saab, A.S., Huang, W., Hoberg, I.K., Kirchhoff, F., Scheller, A., 2013. Genetic background affects human glial fibrillary acidic protein promoter activity. PloS one 8, e66873.

Bai, Y., Song, L., Dai, G., Xu, M., Zhu, L., Zhang, W., Jing, W., Ju, W., 2018. Antidepressant effects of magnolol in a mouse model of depression induced by chronic corticosterone injection. Steroids 135, 73-78.

Bair, M.J., Robinson, R.L., Katon, W., Kroenke, K., 2003. Depression and pain comorbidity: a literature review. Archives of internal medicine 163, 2433-2445.

Bambico, F.R., Li, Z., Oliveira, C., McNeill, S., Diwan, M., Raymond, R., Nobrega, J.N., 2019. Rostrocaudal subregions of the ventral tegmental area are differentially impacted by chronic stress. Psychopharmacology 236, 1917-1929.

Banasr, M., Chowdhury, G.M., Terwilliger, R., Newton, S.S., Duman, R.S., Behar, K.L., Sanacora, G., 2010. Glial pathology in an animal model of depression: reversal of stress-induced cellular, metabolic and behavioral deficits by the glutamate-modulating drug riluzole. Molecular psychiatry 15, 501-511.

Banasr, M., Duman, R.S., 2007. Regulation of neurogenesis and gliogenesis by stress and antidepressant treatment. CNS & neurological disorders drug targets 6, 311-320.

Banasr, M., Duman, R.S., 2008. Glial loss in the prefrontal cortex is sufficient to induce depressive-like behaviors. Biological psychiatry 64, 863-870.

Banasr, M., Dwyer, J.M., Duman, R.S., 2011. Cell atrophy and loss in depression: reversal by antidepressant treatment. Current opinion in cell biology 23, 730-737.

Banasr, M., Lepack, A., Fee, C., Duric, V., Maldonado-Aviles, J., DiLeone, R., Sibille, E., Duman, R.S., Sanacora, G., 2017. Characterization of GABAergic marker expression in the chronic unpredictable stress model of depression. Chronic stress 1.

Banasr, M., Valentine, G.W., Li, X.Y., Gourley, S.L., Taylor, J.R., Duman, R.S., 2007. Chronic unpredictable stress decreases cell proliferation in the cerebral cortex of the adult rat. Biological psychiatry 62, 496-504.

Banasr, M., Xu, M., Lepack, A., Kiselycznyk, C., Zhang, J., Wilber, S., Sanacora, G., Pittenger, C., Duman, R., 2014. Cortical GFAP astrocyte-specific ablation induces depressive-like and anxiety-like behaviors similar to chronic stressCortical GFAP astrocyte-specific ablation induces depressive-like and anxiety-like behaviors similar to chronic stress, Society for Neuroscience Annual Meeting, Washington, DC.

Belzung, C., Lemoine, M., 2011. Criteria of validity for animal models of psychiatric disorders: focus on anxiety disorders and depression. Biology of mood & anxiety disorders 1, 9.

Bernard, R., Kerman, I.A., Thompson, R.C., Jones, E.G., Bunney, W.E., Barchas, J.D., Schatzberg, A.F., Myers, R.M., Akil, H., Watson, S.J., 2011. Altered expression of glutamate signaling, growth factor, and glia genes in the locus coeruleus of patients with major depression. Molecular psychiatry 16, 634-646.

Bernstein, H.G., Meyer-Lotz, G., Dobrowolny, H., Bannier, J., Steiner, J., Walter, M., Bogerts, B., 2015. Reduced density of glutamine synthetase immunoreactive astrocytes in different cortical areas in major depression but not in bipolar I disorder. Frontiers in cellular neuroscience 9, 273.

Bhatia, T.N., Pant, D.B., Eckhoff, E.A., Gongaware, R.N., Do, T., Hutchison, D.F., Gleixner, A.M., Leak, R.K., 2019. Astrocytes do not forfeit their neuroprotective roles after surviving intense oxidative stress. Frontiers in molecular neuroscience 12, 87.

Blaukat, A., Barac, A., Cross, M.J., Offermanns, S., Dikic, I., 2000. G protein-coupled receptor-mediated mitogen-activated protein kinase activation through cooperation of Galpha(q) and Galpha(i) signals. Molecular and cellular biology 20, 6837-6848.

Boden, J.M., Fergusson, D.M., 2011. Alcohol and depression. Addiction 106, 906-914.

Boku, S., Nakagawa, S., Toda, H., Hishimoto, A., 2018. Neural basis of major depressive disorder: Beyond monoamine hypothesis. Psychiatry and clinical neurosciences 72, 3-12.

Bollinger, J.L., Salinas, I., Fender, E., Sengelaub, D.R., Wellman, C.L., 2019. Gonadal hormones differentially regulate sex-specific stress effects on glia in the medial prefrontal cortex. Journal of neuroendocrinology, e12762.

Bolton, M.M., Eroglu, C., 2009. Look who is weaving the neural web: glial control of synapse formation. Current opinion in neurobiology 19, 491-497.

Bosker, F.J., Hartman, C.A., Nolte, I.M., Prins, B.P., Terpstra, P., Posthuma, D., van Veen, T., Willemsen, G., DeRijk, R.H., de Geus, E.J., Hoogendijk, W.J., Sullivan, P.F., Penninx, B.W.,

Boomsma, D.I., Snieder, H., Nolen, W.A., 2011. Poor replication of candidate genes for major depressive disorder using genome-wide association data. Molecular psychiatry 16, 516-532.

Bradl, M., Lassmann, H., 2010. Oligodendrocytes: biology and pathology. Acta neuropathologica 119, 37-53.

Bremner, J.D., Narayan, M., Anderson, E.R., Staib, L.H., Miller, H.L., Charney, D.S., 2000. Hippocampal volume reduction in major depression. The American journal of psychiatry 157, 115-118.

Camp, N.J., Lowry, M.R., Richards, R.L., Plenk, A.M., Carter, C., Hensel, C.H., Abkevich, V., Skolnick, M.H., Shattuck, D., Rowe, K.G., Hughes, D.C., Cannon-Albright, L.A., 2005. Genome-wide linkage analyses of extended Utah pedigrees identifies loci that influence recurrent, early-onset major depression and anxiety disorders. American journal of medical genetics. Part B, Neuropsychiatric genetics : the official publication of the International Society of Psychiatric Genetics 135B, 85-93.

Caspi, A., Sugden, K., Moffitt, T.E., Taylor, A., Craig, I.W., Harrington, H., McClay, J., Mill, J., Martin, J., Braithwaite, A., Poulton, R., 2003. Influence of life stress on depression: moderation by a polymorphism in the 5-HTT gene. Science 301, 386-389.

Castanheira, L., Ferreira, M.F., Sebastiao, A.M., Telles-Correia, D., 2018. Anxiety Assessment in Pre-clinical Tests and in Clinical Trials: A Critical Review. Current topics in medicinal chemistry 18, 1656-1676.

Cavalleri, L., Merlo Pich, E., Millan, M.J., Chiamulera, C., Kunath, T., Spano, P.F., Collo, G., 2018. Ketamine enhances structural plasticity in mouse mesencephalic and human iPSC-derived dopaminergic neurons via AMPAR-driven BDNF and mTOR signaling. Molecular psychiatry 23, 812-823.

Chang, L.C., Jamain, S., Lin, C.W., Rujescu, D., Tseng, G.C., Sibille, E., 2014. A conserved BDNF, glutamate- and GABA-enriched gene module related to human depression identified by coexpression meta-analysis and DNA variant genome-wide association studies. PloS one 9, e90980.

Chen, C.H., Ridler, K., Suckling, J., Williams, S., Fu, C.H., Merlo-Pich, E., Bullmore, E., 2007. Brain imaging correlates of depressive symptom severity and predictors of symptom improvement after antidepressant treatment. Biological psychiatry 62, 407-414.

Chen, J.R., Yan, Y.T., Wang, T.J., Chen, L.J., Wang, Y.J., Tseng, G.F., 2009. Gonadal hormones modulate the dendritic spine densities of primary cortical pyramidal neurons in adult female rat. Cereb Cortex 19, 2719-2727.

Chen, X., Nelson, C.D., Li, X., Winters, C.A., Azzam, R., Sousa, A.A., Leapman, R.D., Gainer, H., Sheng, M., Reese, T.S., 2011. PSD-95 is required to sustain the molecular organization of the postsynaptic density. The Journal of neuroscience : the official journal of the Society for Neuroscience 31, 6329-6338.

Choi, M., Lee, S.H., Park, M.H., Kim, Y.S., Son, H., 2017. Ketamine induces brain-derived neurotrophic factor expression via phosphorylation of histone deacetylase 5 in rats. Biochemical and biophysical research communications 489, 420-425.

Choudary, P.V., Molnar, M., Evans, S.J., Tomita, H., Li, J.Z., Vawter, M.P., Myers, R.M., Bunney, W.E., Jr., Akil, H., Watson, S.J., Jones, E.G., 2005. Altered cortical glutamatergic and GABAergic signal transmission with glial involvement in depression. Proc Natl Acad Sci U S A 102, 15653-15658.

Chowen, J.A., Argente-Arizon, P., Freire-Regatillo, A., Argente, J., 2018. Sex differences in the neuroendocrine control of metabolism and the implication of astrocytes. Frontiers in neuroendocrinology 48, 3-12.

CMHA, 2013. Depression.

Cobb, J.A., O'Neill, K., Milner, J., Mahajan, G.J., Lawrence, T.J., May, W.L., Miguel-Hidalgo, J., Rajkowska, G., Stockmeier, C.A., 2016. Density of GFAP-immunoreactive astrocytes is decreased in left hippocampi in major depressive disorder. Neuroscience 316, 209-220.

Cobb, J.A., Simpson, J., Mahajan, G.J., Overholser, J.C., Jurjus, G.J., Dieter, L., Herbst, N., May, W., Rajkowska, G., Stockmeier, C.A., 2013. Hippocampal volume and total cell numbers in major depressive disorder. Journal of psychiatric research 47, 299-306.

Cohen, L.S., Soares, C.N., Vitonis, A.F., Otto, M.W., Harlow, B.L., 2006. Risk for new onset of depression during the menopausal transition: the Harvard study of moods and cycles. Archives of general psychiatry 63, 385-390.

Collins, D.P., Anastasiades, P.G., Marlin, J.J., Carter, A.G., 2018. Reciprocal Circuits Linking the Prefrontal Cortex with Dorsal and Ventral Thalamic Nuclei. Neuron 98, 366-379 e364.

Cook, S.C., Wellman, C.L., 2004. Chronic stress alters dendritic morphology in rat medial prefrontal cortex. Journal of neurobiology 60, 236-248.

Cotter, D., Mackay, D., Chana, G., Beasley, C., Landau, S., Everall, I.P., 2002. Reduced neuronal size and glial cell density in area 9 of the dorsolateral prefrontal cortex in subjects with major depressive disorder. Cereb Cortex 12, 386-394.

Cotter, D.R., Pariante, C.M., Everall, I.P., 2001. Glial cell abnormalities in major psychiatric disorders: the evidence and implications. Brain research bulletin 55, 585-595.

Cryan, J.F., Mombereau, C., 2004. In search of a depressed mouse: utility of models for studying depression-related behavior in genetically modified mice. Molecular psychiatry 9, 326-357.

Cryan, J.F., Sweeney, F.F., 2011. The age of anxiety: role of animal models of anxiolytic action in drug discovery. British journal of pharmacology 164, 1129-1161.

Cui, W., Mizukami, H., Yanagisawa, M., Aida, T., Nomura, M., Isomura, Y., Takayanagi, R., Ozawa, K., Tanaka, K., Aizawa, H., 2014. Glial dysfunction in the mouse habenula causes

depressive-like behaviors and sleep disturbance. The Journal of neuroscience : the official journal of the Society for Neuroscience 34, 16273-16285.

Cullinan, W.E., Herman, J.P., Battaglia, D.F., Akil, H., Watson, S.J., 1995. Pattern and time course of immediate early gene expression in rat brain following acute stress. Neuroscience 64, 477-505.

Currie, S.R., Patten, S.B., Williams, J.V., Wang, J., Beck, C.A., El-Guebaly, N., Maxwell, C., 2005. Comorbidity of major depression with substance use disorders. Canadian journal of psychiatry. Revue canadienne de psychiatrie 50, 660-666.

Czeh, B., Simon, M., Schmelting, B., Hiemke, C., Fuchs, E., 2006. Astroglial plasticity in the hippocampus is affected by chronic psychosocial stress and concomitant fluoxetine treatment. Neuropsychopharmacology 31, 1616-1626.

Deschenes, S.S., Burns, R.J., Schmitz, N., 2015. Associations between diabetes, major depressive disorder and generalized anxiety disorder comorbidity, and disability: findings from the 2012 Canadian Community Health Survey--Mental Health (CCHS-MH). J Psychosom Res. 78, 137-142.

Deussing, J.M., 2006. Animal models of depression. Drug Discovery Today: Disease Models 3, 375-383.

Disabato, B.M., Morris, C., Hranilovich, J., D'Angelo, G.M., Zhou, G., Wu, N., Doraiswamy, P.M., Sheline, Y.I., 2014. Comparison of brain structural variables, neuropsychological factors, and treatment outcome in early-onset versus late-onset late-life depression. The American journal of geriatric psychiatry : official journal of the American Association for Geriatric Psychiatry 22, 1039-1046.

Domingues, H.S., Portugal, C.C., Socodato, R., Relvas, J.B., 2016. Oligodendrocyte, Astrocyte, and Microglia Crosstalk in Myelin Development, Damage, and Repair. Frontiers in cell and developmental biology 4, 71.

Donohue, H.S., Gabbott, P.L., Davies, H.A., Rodriguez, J.J., Cordero, M.I., Sandi, C., Medvedev, N.I., Popov, V.I., Colyer, F.M., Peddie, C.J., Stewart, M.G., 2006. Chronic restraint stress induces changes in synapse morphology in stratum lacunosum-moleculare CA1 rat hippocampus: a stereological and three-dimensional ultrastructural study. Neuroscience 140, 597-606.

Doucet, M.V., Harkin, A., Dev, K.K., 2012. The PSD-95/nNOS complex: new drugs for depression? Pharmacology & therapeutics 133, 218-229.

Drevets, W.C., Price, J.L., Furey, M.L., 2008. Brain structural and functional abnormalities in mood disorders: implications for neurocircuitry models of depression. Brain structure & function 213, 93-118.

Drevets, W.C., Zarate, C.A., Jr., Furey, M.L., 2013. Antidepressant effects of the muscarinic cholinergic receptor antagonist scopolamine: a review. Biological psychiatry 73, 1156-1163.

DSM-V, 2013. Diagnostic and statistical manual of mental disorders : DSM-5. American Psychiatric Association, Arlington, VA.

Duman, C.H., Duman, R.S., 2015. Spine synapse remodeling in the pathophysiology and treatment of depression. Neuroscience letters 601, 20-29.

Duman, R.S., Aghajanian, G.K., Sanacora, G., Krystal, J.H., 2016. Synaptic plasticity and depression: new insights from stress and rapid-acting antidepressants. Nature medicine 22, 238-249.

Duman, R.S., Sanacora, G., Krystal, J.H., 2019. Altered Connectivity in Depression: GABA and Glutamate Neurotransmitter Deficits and Reversal by Novel Treatments. Neuron 102, 75-90.

Dunkley, D.M., Lewkowski, M., Lee, I.A., Preacher, K.J., Zuroff, D.C., Berg, J.L., Foley, J.E., Myhr, G., Westreich, R., 2017. Daily Stress, Coping, and Negative and Positive Affect in Depression: Complex Trigger and Maintenance Patterns. Behavior therapy 48, 349-365.

Duric, V., Banasr, M., Stockmeier, C.A., Simen, A.A., Newton, S.S., Overholser, J.C., Jurjus, G.J., Dieter, L., Duman, R.S., 2013. Altered expression of synapse and glutamate related genes in post-mortem hippocampus of depressed subjects. The international journal of neuropsychopharmacology 16, 69-82.

Durkee, C.A., Covelo, A., Lines, J., Kofuji, P., Aguilar, J., Araque, A., 2019. Gi/o protein-coupled receptors inhibit neurons but activate astrocytes and stimulate gliotransmission. Glia 67, 1076-1093.

Dusi, N., Barlati, S., Vita, A., Brambilla, P., 2015. Brain Structural Effects of Antidepressant Treatment in Major Depression. Current neuropharmacology 13, 458-465.

Edgar, N., Sibille, E., 2012. A putative functional role for oligodendrocytes in mood regulation. Translational psychiatry 2, e109.

Eishingdrelo, H., Kongsamut, S., 2013. Minireview: Targeting GPCR Activated ERK Pathways for Drug Discovery. Current chemical genomics and translational medicine 7, 9-15.

Elsayed, M., Magistretti, P.J., 2015. A New Outlook on Mental Illnesses: Glial Involvement Beyond the Glue. Frontiers in cellular neuroscience 9, 468.

Ernst, C., Nagy, C., Kim, S., Yang, J.P., Deng, X., Hellstrom, I.C., Choi, K.H., Gershenfeld, H., Meaney, M.J., Turecki, G., 2011. Dysfunction of astrocyte connexins 30 and 43 in dorsal lateral prefrontal cortex of suicide completers. Biological psychiatry 70, 312-319.

Eroglu, C., Barres, B.A., 2010. Regulation of synaptic connectivity by glia. Nature 468, 223-231.

Fatima, M., Srivastav, S., Mondal, A.C., 2017. Prenatal stress and depression associated neuronal development in neonates. International journal of developmental neuroscience : the official journal of the International Society for Developmental Neuroscience 60, 1-7.

Fava, M., 2003. Diagnosis and definition of treatment-resistant depression. Biological psychiatry 53, 649-659.

Ferreira, M.F., Castanheira, L., Sebastiao, A.M., Telles-Correia, D., 2018. Depression Assessment in Clinical Trials and Pre-clinical Tests: A Critical Review. Current topics in medicinal chemistry 18, 1677-1703.

Feyissa, A.M., Chandran, A., Stockmeier, C.A., Karolewicz, B., 2009. Reduced levels of NR2A and NR2B subunits of NMDA receptor and PSD-95 in the prefrontal cortex in major depression. Progress in neuro-psychopharmacology & biological psychiatry 33, 70-75.

Fiske, A., Wetherell, J.L., Gatz, M., 2009. Depression in older adults. Annual review of clinical psychology 5, 363-389.

Franceschelli, A., Herchick, S., Thelen, C., Papadopoulou-Daifoti, Z., Pitychoutis, P.M., 2014. Sex differences in the chronic mild stress model of depression. Behavioural pharmacology 25, 372-383.

Frank, E., Carpenter, L.L., Kupfer, D.J., 1988. Sex differences in recurrent depression: are there any that are significant? The American journal of psychiatry 145, 41-45.

Fried, E.I., Epskamp, S., Nesse, R.M., Tuerlinckx, F., Borsboom, D., 2016. What are 'good' depression symptoms? Comparing the centrality of DSM and non-DSM symptoms of depression in a network analysis. Journal of affective disorders 189, 314-320.

Frodl, T., Jager, M., Smajstrlova, I., Born, C., Bottlender, R., Palladino, T., Reiser, M., Moller, H.J., Meisenzahl, E.M., 2008. Effect of hippocampal and amygdala volumes on clinical outcomes in major depression: a 3-year prospective magnetic resonance imaging study. Journal of psychiatry & neuroscience : JPN 33, 423-430.

Fugger, G., Dold, M., Bartova, L., Kautzky, A., Souery, D., Mendlewicz, J., Serretti, A., Zohar, J., Montgomery, S., Frey, R., Kasper, S., 2019. Major Depression and Comorbid Diabetes - Findings from the European Group for the Study of Resistant Depression. Progress in neuro-psychopharmacology & biological psychiatry 94, 109638.

Fullana, M.N., Ruiz-Bronchal, E., Ferres-Coy, A., Juarez-Escoto, E., Artigas, F., Bortolozzi, A., 2019. Regionally selective knockdown of astroglial glutamate transporters in infralimbic cortex induces a depressive phenotype in mice. Glia 67, 1122-1137.

Gameiro, G.H., Gameiro, P.H., Andrade Ada, S., Pereira, L.F., Arthuri, M.T., Marcondes, F.K., Veiga, M.C., 2006. Nociception- and anxiety-like behavior in rats submitted to different periods of restraint stress. Physiology & behavior 87, 643-649.

Gao, J., Pan, Z., Jiao, Z., Li, F., Zhao, G., Wei, Q., Pan, F., Evangelou, E., 2012. TPH2 gene polymorphisms and major depression--a meta-analysis. PloS one 7, e36721.

Garcia-Garcia, A.L., Elizalde, N., Matrov, D., Harro, J., Wojcik, S.M., Venzala, E., Ramirez, M.J., Del Rio, J., Tordera, R.M., 2009. Increased vulnerability to depressive-like behavior of mice with decreased expression of VGLUT1. Biological psychiatry 66, 275-282.

Gasull-Camos, J., Tarres-Gatius, M., Artigas, F., Castane, A., 2017. Glial GLT-1 blockade in infralimbic cortex as a new strategy to evoke rapid antidepressant-like effects in rats. Translational psychiatry 7, e1038.

Ghosal, S., Bang, E., Yue, W., Hare, B.D., Lepack, A.E., Girgenti, M.J., Duman, R.S., 2018. Activity-Dependent Brain-Derived Neurotrophic Factor Release Is Required for the Rapid Antidepressant Actions of Scopolamine. Biological psychiatry 83, 29-37.

Goldstein, B.I., Carnethon, M.R., Matthews, K.A., McIntyre, R.S., Miller, G.E., Raghuveer, G., Stoney, C.M., Wasiak, H., McCrindle, B.W., American Heart Association, A., Hypertension, Obesity in Youth Committee of the Council on Cardiovascular Disease in the, Y., 2015. Major Depressive Disorder and Bipolar Disorder Predispose Youth to Accelerated Atherosclerosis and Early Cardiovascular Disease: A Scientific Statement From the American Heart Association. Circulation 132, 965-986.

Gomez, J.L., Bonaventura, J., Lesniak, W., Mathews, W.B., Sysa-Shah, P., Rodriguez, L.A., Ellis, R.J., Richie, C.T., Harvey, B.K., Dannals, R.F., Pomper, M.G., Bonci, A., Michaelides, M., 2017. Chemogenetics revealed: DREADD occupancy and activation via converted clozapine. Science 357, 503-507.

Gosselin, R.D., Gibney, S., O'Malley, D., Dinan, T.G., Cryan, J.F., 2009. Region specific decrease in glial fibrillary acidic protein immunoreactivity in the brain of a rat model of depression. Neuroscience 159, 915-925.

Gourley, S.L., Espitia, J.W., Sanacora, G., Taylor, J.R., 2012. Antidepressant-like properties of oral riluzole and utility of incentive disengagement models of depression in mice. Psychopharmacology 219, 805-814.

Groves, A., Kihara, Y., Jonnalagadda, D., Rivera, R., Kennedy, G., Mayford, M., Chun, J., 2018. A Functionally Defined In Vivo Astrocyte Population Identified by c-Fos Activation in a Mouse Model of Multiple Sclerosis Modulated by S1P Signaling: Immediate-Early Astrocytes (ieAstrocytes). eNeuro 5.

Guarnieri, D.J., Brayton, C.E., Richards, S.M., Maldonado-Aviles, J., Trinko, J.R., Nelson, J., Taylor, J.R., Gourley, S.L., DiLeone, R.J., 2012. Gene profiling reveals a role for stress hormones in the molecular and behavioral response to food restriction. Biological psychiatry 71, 358-365.

Guilloux, J.P., Douillard-Guilloux, G., Kota, R., Wang, X., Gardier, A.M., Martinowich, K., Tseng, G.C., Lewis, D.A., Sibille, E., 2012. Molecular evidence for BDNF- and GABA-related dysfunctions in the amygdala of female subjects with major depression. Mol Psychiatry 17, 1130-1142.

Haas, J., Erdo, S.L., 1991. Quisqualate-induced excitotoxic death of glial cells: transient vulnerability of cultured astrocytes. Glia 4, 111-114.

Hamani, C., Machado, D.C., Hipolide, D.C., Dubiela, F.P., Suchecki, D., Macedo, C.E., Tescarollo, F., Martins, U., Covolan, L., Nobrega, J.N., 2012. Deep brain stimulation reverses

anhedonic-like behavior in a chronic model of depression: role of serotonin and brain derived neurotrophic factor. Biological psychiatry 71, 30-35.

Hamilton, J.P., Gotlib, I.H., 2008. Neural substrates of increased memory sensitivity for negative stimuli in major depression. Biological psychiatry 63, 1155-1162.

Hammarstrom, A., Lehti, A., Danielsson, U., Bengs, C., Johansson, E.E., 2009. Gender-related explanatory models of depression: a critical evaluation of medical articles. Public health 123, 689-693.

Hariri, A.R., Holmes, A., 2015. Finding translation in stress research. Nature neuroscience 18, 1347-1352.

Hastings, R.S., Parsey, R.V., Oquendo, M.A., Arango, V., Mann, J.J., 2004. Volumetric analysis of the prefrontal cortex, amygdala, and hippocampus in major depression. Neuropsychopharmacology 29, 952-959.

Haydon, P.G., 2001. GLIA: listening and talking to the synapse. Nat Rev Neurosci 2, 185-193.

Hertz, L., Dringen, R., Schousboe, A., Robinson, S.R., 1999. Astrocytes: glutamate producers for neurons. Journal of neuroscience research 57, 417-428.

Hillhouse, T.M., Porter, J.H., 2015. A brief history of the development of antidepressant drugs: from monoamines to glutamate. Experimental and clinical psychopharmacology 23, 1-21.

Hirschfeld, R.M., 2001. The Comorbidity of Major Depression and Anxiety Disorders: Recognition and Management in Primary Care. Primary care companion to the Journal of clinical psychiatry 3, 244-254.

Holtzheimer, P.E., Mayberg, H.S., 2011. Deep brain stimulation for psychiatric disorders. Annual review of neuroscience 34, 289-307.

Homberg, J.R., Molteni, R., Calabrese, F., Riva, M.A., 2014. The serotonin-BDNF duo: developmental implications for the vulnerability to psychopathology. Neuroscience and biobehavioral reviews 43, 35-47.

Hosang, G.M., Shiles, C., Tansey, K.E., McGuffin, P., Uher, R., 2014. Interaction between stress and the BDNF Val66Met polymorphism in depression: a systematic review and meta-analysis. BMC medicine 12, 7.

Imbe, H., Kimura, A., Donishi, T., Kaneoke, Y., 2012. Chronic restraint stress decreases glial fibrillary acidic protein and glutamate transporter in the periaqueductal gray matter. Neuroscience 223, 209-218.

Jendryka, M., Palchaudhuri, M., Ursu, D., van der Veen, B., Liss, B., Katzel, D., Nissen, W., Pekcec, A., 2019. Pharmacokinetic and pharmacodynamic actions of clozapine-N-oxide, clozapine, and compound 21 in DREADD-based chemogenetics in mice. Scientific reports 9, 4522.

Jha, M.K., Jo, M., Kim, J.H., Suk, K., 2019. Microglia-Astrocyte Crosstalk: An Intimate Molecular Conversation. The Neuroscientist : a review journal bringing neurobiology, neurology and psychiatry 25, 227-240.

John, C.S., Smith, K.L., Van't Veer, A., Gompf, H.S., Carlezon, W.A., Jr., Cohen, B.M., Ongur, D., Bechtholt-Gompf, A.J., 2012. Blockade of astrocytic glutamate uptake in the prefrontal cortex induces anhedonia. Neuropsychopharmacology 37, 2467-2475.

John, C.S., Sypek, E.I., Carlezon, W.A., Cohen, B.M., Ongur, D., Bechtholt, A.J., 2015. Blockade of the GLT-1 Transporter in the Central Nucleus of the Amygdala Induces both Anxiety and Depressive-Like Symptoms. Neuropsychopharmacology 40, 1700-1708.

Kang, H.J., Voleti, B., Hajszan, T., Rajkowska, G., Stockmeier, C.A., Licznerski, P., Lepack, A., Majik, M.S., Jeong, L.S., Banasr, M., Son, H., Duman, R.S., 2012. Decreased expression of synapse-related genes and loss of synapses in major depressive disorder. Nature medicine 18, 1413-1417.

Karolewicz, B., Szebeni, K., Gilmore, T., Maciag, D., Stockmeier, C.A., Ordway, G.A., 2009. Elevated levels of NR2A and PSD-95 in the lateral amygdala in depression. The international journal of neuropsychopharmacology 12, 143-153.

Kazi, J.A., Mori, S., Kuchiiwa, S., Nakagawa, S., 2004. Prolonged expression of c-Fos protein in the lateral habenular nucleus of the Japanese monkey (Macaca fuscata) after eye enucleation. Neuro-Signals 13, 130-133.

Kendler, K.S., 2016. The Phenomenology of Major Depression and the Representativeness and Nature of DSM Criteria. The American journal of psychiatry 173, 771-780.

Kendler, K.S., Gatz, M., Gardner, C.O., Pedersen, N.L., 2006. A Swedish national twin study of lifetime major depression. The American journal of psychiatry 163, 109-114.

Kessler, R.C., 2003. Epidemiology of women and depression. Journal of affective disorders 74, 5-13.

Kessler, R.C., Chiu, W.T., Demler, O., Merikangas, K.R., Walters, E.E., 2005. Prevalence, severity, and comorbidity of 12-month DSM-IV disorders in the National Comorbidity Survey Replication. Arch Gen Psychiatry 62, 617-627.

Kessler, R.C., McGonagle, K.A., Swartz, M., Blazer, D.G., Nelson, C.B., 1993. Sex and depression in the National Comorbidity Survey. I: Lifetime prevalence, chronicity and recurrence. Journal of affective disorders 29, 85-96.

Kiray, H., Lindsay, S.L., Hosseinzadeh, S., Barnett, S.C., 2016. The multifaceted role of astrocytes in regulating myelination. Experimental neurology 283, 541-549.

Koenig, H.G., Blazer, D.G., 1992. Epidemiology of geriatric affective disorders. Clinics in geriatric medicine 8, 235-251.

Kohler, S., Cierpinsky, K., Kronenberg, G., Adli, M., 2016. The serotonergic system in the neurobiology of depression: Relevance for novel antidepressants. Journal of psychopharmacology 30, 13-22.

Konarski, J.Z., McIntyre, R.S., Kennedy, S.H., Rafi-Tari, S., Soczynska, J.K., Ketter, T.A., 2008. Volumetric neuroimaging investigations in mood disorders: bipolar disorder versus major depressive disorder. Bipolar disorders 10, 1-37.

Kucukdereli, H., Allen, N.J., Lee, A.T., Feng, A., Ozlu, M.I., Conatser, L.M., Chakraborty, C., Workman, G., Weaver, M., Sage, E.H., Barres, B.A., Eroglu, C., 2011. Control of excitatory CNS synaptogenesis by astrocyte-secreted proteins Hevin and SPARC. Proceedings of the National Academy of Sciences of the United States of America 108, E440-449.

Labaka, A., Goni-Balentziaga, O., Lebena, A., Perez-Tejada, J., 2018. Biological Sex Differences in Depression: A Systematic Review. Biological research for nursing 20, 383-392.

Lambert, O., Bourin, M., 2002. SNRIs: mechanism of action and clinical features. Expert review of neurotherapeutics 2, 849-858.

Law, N.C., White, M.F., Hunzicker-Dunn, M.E., 2016. G protein-coupled receptors (GPCRs) That Signal via Protein Kinase A (PKA) Cross-talk at Insulin Receptor Substrate 1 (IRS1) to Activate the phosphatidylinositol 3-kinase (PI3K)/AKT Pathway. The Journal of biological chemistry 291, 27160-27169.

Lee, B.H., Kim, Y.K., 2010. The roles of BDNF in the pathophysiology of major depression and in antidepressant treatment. Psychiatry investigation 7, 231-235.

Lee, Y., Son, H., Kim, G., Kim, S., Lee, D.H., Roh, G.S., Kang, S.S., Cho, G.J., Choi, W.S., Kim, H.J., 2013. Glutamine deficiency in the prefrontal cortex increases depressive-like behaviours in male mice. Journal of psychiatry & neuroscience : JPN 38, 183-191.

Li, N., Lee, B., Liu, R.J., Banasr, M., Dwyer, J.M., Iwata, M., Li, X.Y., Aghajanian, G., Duman, R.S., 2010. mTOR-dependent synapse formation underlies the rapid antidepressant effects of NMDA antagonists. Science 329, 959-964.

Li, N., Liu, R.J., Dwyer, J.M., Banasr, M., Lee, B., Son, H., Li, X.Y., Aghajanian, G., Duman, R.S., 2011. Glutamate N-methyl-D-aspartate receptor antagonists rapidly reverse behavioral and synaptic deficits caused by chronic stress exposure. Biological psychiatry 69, 754-761.

Lin, L.C., Sibille, E., 2013. Reduced brain somatostatin in mood disorders: a common pathophysiological substrate and drug target? Frontiers in pharmacology 4, 110.

Lin, L.C., Sibille, E., 2015. Somatostatin, neuronal vulnerability and behavioral emotionality. Mol Psychiatry 20, 377-387.

Liu, J., Dietz, K., Hodes, G.E., Russo, S.J., Casaccia, P., 2018. Widespread transcriptional alternations in oligodendrocytes in the adult mouse brain following chronic stress. Developmental neurobiology 78, 152-162.

Lopez de Lara, C., Brezo, J., Rouleau, G., Lesage, A., Dumont, M., Alda, M., Benkelfat, C., Turecki, G., 2007. Effect of tryptophan hydroxylase-2 gene variants on suicide risk in major depression. Biological psychiatry 62, 72-80.

Lowery-Gionta, E.G., Crowley, N.A., Bukalo, O., Silverstein, S., Holmes, A., Kash, T.L., 2018. Chronic stress dysregulates amygdalar output to the prefrontal cortex. Neuropharmacology 139, 68-75.

Luscher, B., Shen, Q., Sahir, N., 2011. The GABAergic deficit hypothesis of major depressive disorder. Molecular psychiatry 16, 383-406.

Ma, L., Shen, Q., Yang, S., Xie, X., Xiao, Q., Yu, C., Cao, L., Fu, Z., 2018. Effect of chronic corticosterone-induced depression on circadian rhythms and age-related phenotypes in mice. Acta biochimica et biophysica Sinica 50, 1236-1246.

Machado, M., Einarson, T.R., 2010. Comparison of SSRIs and SNRIs in major depressive disorder: a meta-analysis of head-to-head randomized clinical trials. Journal of clinical pharmacy and therapeutics 35, 177-188.

MacLaren, D.A., Browne, R.W., Shaw, J.K., Krishnan Radhakrishnan, S., Khare, P., Espana, R.A., Clark, S.D., 2016. Clozapine N-Oxide Administration Produces Behavioral Effects in Long-Evans Rats: Implications for Designing DREADD Experiments. eNeuro 3.

MacQueen, G.M., Campbell, S., McEwen, B.S., Macdonald, K., Amano, S., Joffe, R.T., Nahmias, C., Young, L.T., 2003. Course of illness, hippocampal function, and hippocampal volume in major depression. Proceedings of the National Academy of Sciences of the United States of America 100, 1387-1392.

Mahar, I., Bambico, F.R., Mechawar, N., Nobrega, J.N., 2014. Stress, serotonin, and hippocampal neurogenesis in relation to depression and antidepressant effects. Neuroscience and biobehavioral reviews 38, 173-192.

Major Depressive Disorder Working Group of the Psychiatric GWAS Consortium, Ripke, S., Wray, N.R., Lewis, C.M., Hamilton, S.P., Weissman, M.M., Breen, G., Byrne, E.M., Blackwood, D.H., Boomsma, D.I., Cichon, S., Heath, A.C., Holsboer, F., Lucae, S., Madden, P.A., Martin, N.G., McGuffin, P., Muglia, P., Noethen, M.M., Penninx, B.P., Pergadia, M.L., Potash, J.B., Rietschel, M., Lin, D., Muller-Myhsok, B., Shi, J., Steinberg, S., Grabe, H.J., Lichtenstein, P., Magnusson, P., Perlis, R.H., Preisig, M., Smoller, J.W., Stefansson, K., Uher, R., Kutalik, Z., Tansey, K.E., Teumer, A., Viktorin, A., Barnes, M.R., Bettecken, T., Binder, E.B., Breuer, R., Castro, V.M., Churchill, S.E., Coryell, W.H., Craddock, N., Craig, I.W., Czamara, D., De Geus, E.J., Degenhardt, F., Farmer, A.E., Fava, M., Frank, J., Gainer, V.S., Gallagher, P.J., Gordon, S.D., Goryachev, S., Gross, M., Guipponi, M., Henders, A.K., Herms, S., Hickie, I.B., Hoefels, S., Hoogendijk, W., Hottenga, J.J., Iosifescu, D.V., Ising, M., Jones, I., Jones, L., Jung-Ying, T., Knowles, J.A., Kohane, I.S., Kohli, M.A., Korszun, A., Landen, M., Lawson, W.B., Lewis, G., Macintyre, D., Maier, W., Mattheisen, M., McGrath, P.J., McIntosh, A., McLean, A., Middeldorp, C.M., Middleton, L., Montgomery, G.M., Murphy, S.N., Nauck, M., Nolen, W.A., Nyholt, D.R., O'Donovan, M., Oskarsson, H., Pedersen, N., Scheftner, W.A., Schulz, A., Schulze, T.G., Shyn, S.I., Sigurdsson, E., Slager, S.L., Smit, J.H., Stefansson, H., Steffens, M., Thorgeirsson, T., Tozzi, F., Treutlein, J., Uhr, M., van den Oord, E.J., Van

Grootheest, G., Volzke, H., Weilburg, J.B., Willemsen, G., Zitman, F.G., Neale, B., Daly, M., Levinson, D.F., Sullivan, P.F., 2013. A mega-analysis of genome-wide association studies for major depressive disorder. Molecular psychiatry 18, 497-511.

Maller, J.J., Broadhouse, K., Rush, A.J., Gordon, E., Koslow, S., Grieve, S.M., 2018. Increased hippocampal tail volume predicts depression status and remission to anti-depressant medications in major depression. Molecular psychiatry 23, 1737-1744.

Maluach, A.M., Misquitta, K.A., Prevot, T.D., Fee, C., Sibille, E., Banasr, M., Andreazza, A.C., 2017. Increased Neuronal DNA/RNA Oxidation in the Frontal Cortex of Mice Subjected to Unpredictable Chronic Mild Stress. Chronic stress 1.

Manchanda, R.K., Jaggi, A.S., Singh, N., 2011. Ameliorative potential of sodium cromoglycate and diethyldithiocarbamic acid in restraint stress-induced behavioral alterations in rats. Pharmacological reports : PR 63, 54-63.

Mann, J.J., 2003. Neurobiology of suicidal behaviour. Nature reviews 4, 819-828.

Manvich, D.F., Webster, K.A., Foster, S.L., Farrell, M.S., Ritchie, J.C., Porter, J.H., Weinshenker, D., 2018. The DREADD agonist clozapine N-oxide (CNO) is reverse-metabolized to clozapine and produces clozapine-like interoceptive stimulus effects in rats and mice. Scientific reports 8, 3840.

Martin-Fernandez, M., Jamison, S., Robin, L.M., Zhao, Z., Martin, E.D., Aguilar, J., Benneyworth, M.A., Marsicano, G., Araque, A., 2017. Synapse-specific astrocyte gating of amygdala-related behavior. Nature neuroscience 20, 1540-1548.

Martin, D.L., Rimvall, K., 1993. Regulation of gamma-aminobutyric acid synthesis in the brain. J Neurochem 60, 395-407.

Matute, C., Alberdi, E., Domercq, M., Sánchez-Gómez, M.V., Pérez-Samartín, A., Rodríguez-Antigüedad, A., Pérez-Cerdá, F., 2007. Excitotoxic damage to white matter. Journal of Anatomy 210, 693-702.

McCarthy, M.M., Todd, B.J., Amateau, S.K., 2003. Estradiol modulation of astrocytes and the establishment of sex differences in the brain. Annals of the New York Academy of Sciences 1007, 283-297.

McEwen, B.S., Conrad, C.D., Kuroda, Y., Frankfurt, M., Magarinos, A.M., McKittrick, C., 1997. Prevention of stress-induced morphological and cognitive consequences. European neuropsychopharmacology : the journal of the European College of Neuropsychopharmacology 7 Suppl 3, S323-328.

McGarry, L.M., Carter, A.G., 2017. Prefrontal Cortex Drives Distinct Projection Neurons in the Basolateral Amygdala. Cell reports 21, 1426-1433.

McMahon, F.J., Akula, N., Schulze, T.G., Muglia, P., Tozzi, F., Detera-Wadleigh, S.D., Steele, C.J., Breuer, R., Strohmaier, J., Wendland, J.R., Mattheisen, M., Muhleisen, T.W., Maier, W., Nothen, M.M., Cichon, S., Farmer, A., Vincent, J.B., Holsboer, F., Preisig, M., Rietschel, M.,

Bipolar Disorder Genome Study, C., 2010. Meta-analysis of genome-wide association data identifies a risk locus for major mood disorders on 3p21.1. Nature genetics 42, 128-131.

Mechawar, N., Savitz, J., 2016. Neuropathology of mood disorders: do we see the stigmata of inflammation? Translational psychiatry 6, e946.

Melartin, T.K., Rytsala, H.J., Leskela, U.S., Lestela-Mielonen, P.S., Sokero, T.P., Isometsa, E.T., 2002. Current comorbidity of psychiatric disorders among DSM-IV major depressive disorder patients in psychiatric care in the Vantaa Depression Study. The Journal of clinical psychiatry 63, 126-134.

Meyer, J.H., 2017. Neuroprogression and Immune Activation in Major Depressive Disorder. Modern trends in pharmacopsychiatry 31, 27-36.

Meyer, J.H., Ginovart, N., Boovariwala, A., Sagrati, S., Hussey, D., Garcia, A., Young, T., Praschak-Rieder, N., Wilson, A.A., Houle, S., 2006. Elevated monoamine oxidase a levels in the brain: an explanation for the monoamine imbalance of major depression. Archives of general psychiatry 63, 1209-1216.

Middeldorp, C.M., Sullivan, P.F., Wray, N.R., Hottenga, J.J., de Geus, E.J., van den Berg, M., Montgomery, G.W., Coventry, W.L., Statham, D.J., Andrews, G., Slagboom, P.E., Boomsma, D.I., Martin, N.G., 2009. Suggestive linkage on chromosome 2, 8, and 17 for lifetime major depression. American journal of medical genetics. Part B, Neuropsychiatric genetics : the official publication of the International Society of Psychiatric Genetics 150B, 352-358.

Miguel-Hidalgo, J.J., Baucom, C., Dilley, G., Overholser, J.C., Meltzer, H.Y., Stockmeier, C.A., Rajkowska, G., 2000. Glial fibrillary acidic protein immunoreactivity in the prefrontal cortex distinguishes younger from older adults in major depressive disorder. Biological psychiatry 48, 861-873.

Miguel-Hidalgo, J.J., Hall, K.O., Bonner, H., Roller, A.M., Syed, M., Park, C.J., Ball, J.P., Rothenberg, M.E., Stockmeier, C.A., Romero, D.G., 2017. MicroRNA-21: Expression in oligodendrocytes and correlation with low myelin mRNAs in depression and alcoholism. Progress in neuro-psychopharmacology & biological psychiatry 79, 503-514.

Miguel-Hidalgo, J.J., Moulana, M., Deloach, P.H., Rajkowska, G., 2018. Chronic Unpredictable Stress Reduces Immunostaining for Connexins 43 and 30 and Myelin Basic Protein in the Rat Prelimbic and Orbitofrontal Cortices. Chronic stress 2.

Miguel-Hidalgo, J.J., Waltzer, R., Whittom, A.A., Austin, M.C., Rajkowska, G., Stockmeier, C.A., Glial and glutamatergic markers in depression, alcoholism, and their comorbidity. Journal of affective disorders.

Miguel-Hidalgo, J.J., Waltzer, R., Whittom, A.A., Austin, M.C., Rajkowska, G., Stockmeier, C.A., 2010. Glial and glutamatergic markers in depression, alcoholism, and their comorbidity. Journal of affective disorders 127, 230-240.

Miguel-Hidalgo, J.J., Wei, J., Andrew, M., Overholser, J.C., Jurjus, G., Stockmeier, C.A., Rajkowska, G., 2002. Glia pathology in the prefrontal cortex in alcohol dependence with and without depressive symptoms. Biological psychiatry 52, 1121-1133.

Mitchell, A.J., Subramaniam, H., 2005. Prognosis of depression in old age compared to middle age: a systematic review of comparative studies. The American journal of psychiatry 162, 1588-1601.

Mitra, S., Sameer Kumar, G.S., Jyothi Lakshmi, B., Thakur, S., Kumar, S., 2018. Absence of Wdr13 Gene Predisposes Mice to Mild Social Isolation - Chronic Stress, Leading to Depression-Like Phenotype Associated With Differential Expression of Synaptic Proteins. Frontiers in molecular neuroscience 11, 133.

Miyata, S., Hattori, T., Shimizu, S., Ito, A., Tohyama, M., 2015. Disturbance of oligodendrocyte function plays a key role in the pathogenesis of schizophrenia and major depressive disorder. BioMed research international 2015, 492367.

Miyata, S., Taniguchi, M., Koyama, Y., Shimizu, S., Tanaka, T., Yasuno, F., Yamamoto, A., Iida, H., Kudo, T., Katayama, T., Tohyama, M., 2016. Association between chronic stress-induced structural abnormalities in Ranvier nodes and reduced oligodendrocyte activity in major depression. Scientific reports 6, 23084.

Moon, Y., Kim, H.J., Kim, J.Y., Kim, H., Kim, W.R., Sun, W., 2011. Different expression of human GFAP promoter-derived GFP in different subsets of astrocytes in the mouse brain. Animal Cells and Systems 15, 268-273.

Morales-Medina, J.C., Iannitti, T., Freeman, A., Caldwell, H.K., 2017. The olfactory bulbectomized rat as a model of depression: The hippocampal pathway. Behavioural brain research 317, 562-575.

Mulinari, S., 2012. Monoamine theories of depression: historical impact on biomedical research. Journal of the history of the neurosciences 21, 366-392.

Munoz-Cobo, I., Belloch, F.B., Diaz-Perdigon, T., Puerta, E., Tordera, R.M., 2017. SIRT2 inhibition reverses anhedonia in the VGLUT1+/- depression model. Behavioural brain research 335, 128-131.

Murga, C., Laguinge, L., Wetzker, R., Cuadrado, A., Gutkind, J.S., 1998. Activation of Akt/protein kinase B by G protein-coupled receptors. A role for alpha and beta gamma subunits of heterotrimeric G proteins acting through phosphatidylinositol-3-OH kinasegamma. The Journal of biological chemistry 273, 19080-19085.

Nagayama, H., Sasaki, M., Ichii, S., Hanada, K., Okawa, M., Ohta, T., Asano, Y., Sugita, Y., Yamazaki, J., Kohsaka, M., et al., 1991. Atypical depressive symptoms possibly predict responsiveness to phototherapy in seasonal affective disorder. Journal of affective disorders 23, 185-189.

Nagy, C., Suderman, M., Yang, J., Szyf, M., Mechawar, N., Ernst, C., Turecki, G., 2015. Astrocytic abnormalities and global DNA methylation patterns in depression and suicide. Molecular psychiatry 20, 320-328.

Nakano, M., Matsuo, K., Nakashima, M., Matsubara, T., Harada, K., Egashira, K., Masaki, H., Takahashi, K., Watanabe, Y., 2014. Gray matter volume and rapid decision-making in major depressive disorder. Progress in neuro-psychopharmacology & biological psychiatry 48, 51-56.

Nakano, N., Matsuda, S., Ichimura, M., Minami, A., Ogino, M., Murai, T., Kitagishi, Y., 2017. PI3K/AKT signaling mediated by G proteincoupled receptors is involved in neurodegenerative Parkinson's disease (Review). International journal of molecular medicine 39, 253-260.

Narasimhan, S., Lohoff, F.W., 2012. Pharmacogenetics of antidepressant drugs: current clinical practice and future directions. Pharmacogenomics 13, 441-464.

Nelson, L.H., Lenz, K.M., 2017. The immune system as a novel regulator of sex differences in brain and behavioral development. Journal of neuroscience research 95, 447-461.

Nikolova, Y.S., Misquitta, K.A., Rocco, B.R., Prevot, T.D., Knodt, A.R., Ellegood, J., Voineskos, A.N., Lerch, J.P., Hariri, A.R., Sibille, E., Banasr, M., 2018. Shifting priorities: highly conserved behavioral and brain network adaptations to chronic stress across species. Translational psychiatry 8, 26.

Nollet, M., Le Guisquet, A.M., Belzung, C., 2013. Models of depression: unpredictable chronic mild stress in mice. Current protocols in pharmacology Chapter 5, Unit 5 65.

Nolte, C., Matyash, M., Pivneva, T., Schipke, C.G., Ohlemeyer, C., Hanisch, U.K., Kirchhoff, F., Kettenmann, H., 2001. GFAP promoter-controlled EGFP-expressing transgenic mice: a tool to visualize astrocytes and astrogliosis in living brain tissue. Glia 33, 72-86.

Northoff, G., Sibille, E., 2014. Cortical GABA neurons and self-focus in depression: a model linking cellular, biochemical and neural network findings. Mol Psychiatry 19, 959.

Nutt, D.J., Forshall, S., Bell, C., Rich, A., Sandford, J., Nash, J., Argyropoulos, S., 1999. Mechanisms of action of selective serotonin reuptake inhibitors in the treatment of psychiatric disorders. European neuropsychopharmacology : the journal of the European College of Neuropsychopharmacology 9 Suppl 3, S81-86.

Olivier, J.D., Akerud, H., Kaihola, H., Pawluski, J.L., Skalkidou, A., Hogberg, U., Sundstrom-Poromaa, I., 2013. The effects of maternal depression and maternal selective serotonin reuptake inhibitor exposure on offspring. Frontiers in cellular neuroscience 7, 73.

Ongur, D., Drevets, W.C., Price, J.L., 1998. Glial reduction in the subgenual prefrontal cortex in mood disorders. Proc Natl Acad Sci USA 95, 13290-13295.

Palmer, A.L., Ousman, S.S., 2018. Astrocytes and aging. Front Aging Neurosci 10, 337.

Pantazatos, S.P., Huang, Y.Y., Rosoklija, G.B., Dwork, A.J., Arango, V., Mann, J.J., 2017. Whole-transcriptome brain expression and exon-usage profiling in major depression and suicide: evidence for altered glial, endothelial and ATPase activity. Molecular psychiatry 22, 760-773.

Papp, M., Gruca, P., Lason-Tyburkiewicz, M., Willner, P., 2017. Antidepressant, anxiolytic and procognitive effects of subacute and chronic ketamine in the chronic mild stress model of depression. Behavioural pharmacology 28, 1-8.

Payne, J.L., Palmer, J.T., Joffe, H., 2009. A reproductive subtype of depression: conceptualizing models and moving toward etiology. Harvard review of psychiatry 17, 72-86.

Peng, S., Li, W., Lv, L., Zhang, Z., Zhan, X., 2018. BDNF as a biomarker in diagnosis and evaluation of treatment for schizophrenia and depression. Discovery medicine 26, 127-136.

Pepper, R.E., Pitman, K.A., Cullen, C.L., Young, K.M., 2018. How Do Cells of the Oligodendrocyte Lineage Affect Neuronal Circuits to Influence Motor Function, Memory and Mood? Frontiers in cellular neuroscience 12, 399.

Perona, M.T., Waters, S., Hall, F.S., Sora, I., Lesch, K.P., Murphy, D.L., Caron, M., Uhl, G.R., 2008. Animal models of depression in dopamine, serotonin, and norepinephrine transporter knockout mice: prominent effects of dopamine transporter deletions. Behavioural pharmacology 19, 566-574.

Pham, T.H., Gardier, A.M., 2019. Fast-acting antidepressant activity of ketamine: highlights on brain serotonin, glutamate, and GABA neurotransmission in preclinical studies. Pharmacology & therapeutics 199, 58-90.

Piccinelli, M., Wilkinson, G., 2000. Gender differences in depression. Critical review. The British journal of psychiatry : the journal of mental science 177, 486-492.

Ping, L., Xu, J., Zhou, C., Lu, J., Lu, Y., Shen, Z., Jiang, L., Dai, N., Xu, X., Cheng, Y., 2019. Tryptophan hydroxylase-2 polymorphism is associated with white matter integrity in first-episode, medication-naive major depressive disorder patients. Psychiatry research. Neuroimaging 286, 4-10.

Popoli, M., Yan, Z., McEwen, B.S., Sanacora, G., 2011. The stressed synapse: the impact of stress and glucocorticoids on glutamate transmission. Nature reviews 13, 22-37.

Prevot, T.D., Li, G., Vidojevic, A., Misquitta, K.A., Fee, C., Santrac, A., Knutson, D.E., Stephen, M.R., Kodali, R., Zahn, N.M., Arnold, L.A., Scholze, P., Fisher, J.L., Markovic, B.D., Banasr, M., Cook, J.M., Savic, M., Sibille, E., 2019a. Novel Benzodiazepine-Like Ligands with Various Anxiolytic, Antidepressant, or Pro-Cognitive Profiles. Molecular neuropsychiatry 5, 84-97.

Prevot, T.D., Misquitta, K.A., Fee, C., Newton, D.F., Chatterjee, D., Nikolova, Y.S., Sibille, E., Banasr, M., 2019b. Residual avoidance: A new, consistent and repeatable readout of chronic stress-induced conflict anxiety reversible by antidepressant treatment. Neuropharmacology 153, 98-110.

Qiao, H., Li, M.X., Xu, C., Chen, H.B., An, S.C., Ma, X.M., 2016. Dendritic Spines in Depression: What We Learned from Animal Models. Neural Plast 2016, 8056370.

Radley, J.J., Rocher, A.B., Miller, M., Janssen, W.G., Liston, C., Hof, P.R., McEwen, B.S., Morrison, J.H., 2006. Repeated stress induces dendritic spine loss in the rat medial prefrontal cortex. Cereb Cortex 16, 313-320.

Radley, J.J., Sisti, H.M., Hao, J., Rocher, A.B., McCall, T., Hof, P.R., McEwen, B.S., Morrison, J.H., 2004. Chronic behavioral stress induces apical dendritic reorganization in pyramidal neurons of the medial prefrontal cortex. Neuroscience 125, 1-6.

Rai, D., Zitko, P., Jones, K., Lynch, J., Araya, R., 2013. Country- and individual-level socioeconomic determinants of depression: multilevel cross-national comparison. The British journal of psychiatry : the journal of mental science 202, 195-203.

Rajkowska, G., 2000. Postmortem studies in mood disorders indicate altered numbers of neurons and glial cells. Biol Psychiatry 48, 766-777.

Rajkowska, G., Hughes, J., Stockmeier, C.A., Javier Miguel-Hidalgo, J., Maciag, D., 2013. Coverage of blood vessels by astrocytic endfeet is reduced in major depressive disorder. Biological psychiatry 73, 613-621.

Rajkowska, G., Legutko, B., Moulana, M., Syed, M., Romero, D.G., Stockmeier, C.A., Miguel-Hidalgo, J.J., 2018. Astrocyte pathology in the ventral prefrontal white matter in depression. Journal of psychiatric research 102, 150-158.

Rajkowska, G., Mahajan, G., Maciag, D., Sathyanesan, M., Iyo, A.H., Moulana, M., Kyle, P.B., Woolverton, W.L., Miguel-Hidalgo, J.J., Stockmeier, C.A., Newton, S.S., 2015. Oligodendrocyte morphometry and expression of myelin - Related mRNA in ventral prefrontal white matter in major depressive disorder. Journal of psychiatric research 65, 53-62.

Rajkowska, G., Miguel-Hidalgo, J.J., 2007. Gliogenesis and glial pathology in depression. CNS & neurological disorders drug targets 6, 219-233.

Rajkowska, G., O'Dwyer, G., Teleki, Z., Stockmeier, C.A., Miguel-Hidalgo, J.J., 2007. GABAergic neurons immunoreactive for calcium binding proteins are reduced in the prefrontal cortex in major depression. Neuropsychopharmacology 32, 471-482.

Rajkowska, G., Selemon, L.D., Goldman-Rakic, P.S., 1998. Neuronal and glial somal size in the prefrontal cortex: a postmortem morphometric study of schizophrenia and Huntington disease. Archives of general psychiatry 55, 215-224.

Rajkowska, G., Stockmeier, C.A., 2013. Astrocyte pathology in major depressive disorder: insights from human postmortem brain tissue. Current drug targets 14, 1225-1236.

Rajkumar, R., Dawe, G.S., 2018. OBscure but not OBsolete: Perturbations of the frontal cortex in common between rodent olfactory bulbectomy model and major depression. Journal of chemical neuroanatomy 91, 63-100.

Rantala, M.J., Luoto, S., Krams, I., Karlsson, H., 2018. Depression subtyping based on evolutionary psychiatry: Proximate mechanisms and ultimate functions. Brain, behavior, and immunity 69, 603-617.

Rao, C., Shi, H., Zhou, C., Zhu, D., Zhao, M., Wang, Z., Yang, Y., Chen, J., Liao, L., Tang, J., Wu, Y., Zhou, J., Cheng, K., Xie, P., 2016. Hypothalamic Proteomic Analysis Reveals Dysregulation of Glutamate Balance and Energy Metabolism in a Mouse Model of Chronic Mild Stress-Induced Depression. Neurochemical research 41, 2443-2456.

Raper, J., Morrison, R.D., Daniels, J.S., Howell, L., Bachevalier, J., Wichmann, T., Galvan, A., 2017. Metabolism and Distribution of Clozapine-N-oxide: Implications for Nonhuman Primate Chemogenetics. ACS chemical neuroscience 8, 1570-1576.

Rappeneau, V., Blaker, A., Petro, J.R., Yamamoto, B.K., Shimamoto, A., 2016. Disruption of the Glutamate-Glutamine Cycle Involving Astrocytes in an Animal Model of Depression for Males and Females. Frontiers in behavioral neuroscience 10, 231.

Read, J.R., Sharpe, L., Modini, M., Dear, B.F., 2017. Multimorbidity and depression: A systematic review and meta-analysis. Journal of affective disorders 221, 36-46.

Reus, G.Z., de Moura, A.B., Silva, R.H., Resende, W.R., Quevedo, J., 2018. Resilience Dysregulation in Major Depressive Disorder: Focus on Glutamatergic Imbalance and Microglial Activation. Current neuropharmacology 16, 297-307.

Reus, G.Z., Fries, G.R., Stertz, L., Badawy, M., Passos, I.C., Barichello, T., Kapczinski, F., Quevedo, J., 2015. The role of inflammation and microglial activation in the pathophysiology of psychiatric disorders. Neuroscience 300, 141-154.

Rial, D., Lemos, C., Pinheiro, H., Duarte, J.M., Goncalves, F.Q., Real, J.I., Prediger, R.D., Goncalves, N., Gomes, C.A., Canas, P.M., Agostinho, P., Cunha, R.A., 2015. Depression as a Glial-Based Synaptic Dysfunction. Frontiers in cellular neuroscience 9, 521.

Risher, W.C., Patel, S., Kim, I.H., Uezu, A., Bhagat, S., Wilton, D.K., Pilaz, L.J., Singh Alvarado, J., Calhan, O.Y., Silver, D.L., Stevens, B., Calakos, N., Soderling, S.H., Eroglu, C., 2014. Astrocytes refine cortical connectivity at dendritic spines. eLife 3.

Rosedale, M., Strauss, S.M., Knight, C., Malaspina, D., 2015. Awareness of Prediabetes and Diabetes among Persons with Clinical Depression. International journal of endocrinology 2015, 839152.

Rush, A.J., Trivedi, M.H., Wisniewski, S.R., Nierenberg, A.A., Stewart, J.W., Warden, D., Niederehe, G., Thase, M.E., Lavori, P.W., Lebowitz, B.D., McGrath, P.J., Rosenbaum, J.F., Sackeim, H.A., Kupfer, D.J., Luther, J., Fava, M., 2006. Acute and longer-term outcomes in depressed outpatients requiring one or several treatment steps: a STAR*D report. The American journal of psychiatry 163, 1905-1917.

Sacchet, M.D., Gotlib, I.H., 2017. Myelination of the brain in Major Depressive Disorder: An in vivo quantitative magnetic resonance imaging study. Scientific reports 7, 2200.

Sanacora, G., 2010. Cortical inhibition, gamma-aminobutyric acid, and major depression: there is plenty of smoke but is there fire? Biol Psychiatry 67, 397-398.

Sanacora, G., Banasr, M., 2013. From pathophysiology to novel antidepressant drugs: glial contributions to the pathology and treatment of mood disorders. Biological psychiatry 73, 1172-1179.

Sanacora, G., Treccani, G., Popoli, M., 2012. Towards a glutamate hypothesis of depression: an emerging frontier of neuropsychopharmacology for mood disorders. Neuropharmacology 62, 63-77.

Savas, M., Vinkers, C., Rosmalen, J., Hartman, C., Wester, V.L., van den Akker, E.L.T., Iyer, A., McEwen, B.S., van Rossum, E.F.C., 2019. Systemic and local corticosteroid use is associated with reduced executive cognition, and mood and anxiety disorders. Neuroendocrinology.

Schaakxs, R., Comijs, H.C., Lamers, F., Kok, R.M., Beekman, A.T.F., Penninx, B., 2018. Associations between age and the course of major depressive disorder: a 2-year longitudinal cohort study. The lancet. Psychiatry 5, 581-590.

Scheinost, D., Holmes, S.E., DellaGioia, N., Schleifer, C., Matuskey, D., Abdallah, C.G., Hampson, M., Krystal, J.H., Anticevic, A., Esterlis, I., 2018. Multimodal Investigation of Network Level Effects Using Intrinsic Functional Connectivity, Anatomical Covariance, and Structure-to-Function Correlations in Unmedicated Major Depressive Disorder. Neuropsychopharmacology 43, 1119-1127.

Schindelin, J., Arganda-Carreras, I., Frise, E., Kaynig, V., Longair, M., Pietzsch, T., Preibisch, S., Rueden, C., Saalfeld, S., Schmid, B., Tinevez, J.Y., White, D.J., Hartenstein, V., Eliceiri, K., Tomancak, P., Cardona, A., 2012. Fiji: an open-source platform for biological-image analysis. Nature methods 9, 676-682.

Schousboe, A., Waagepetersen, H.S., 2006. Glial modulation of GABAergic and glutamat ergic neurotransmission. Curr Top Med Chem 6, 929-934.

Sen, S., Duman, R., Sanacora, G., 2008. Serum brain-derived neurotrophic factor, depression, and antidepressant medications: meta-analyses and implications. Biol Psychiatry 64, 527-532.

Seney, M.L., Sibille, E., 2014. Sex differences in mood disorders: perspectives from humans and rodent models. Biology of sex differences 5, 17.

Seney, M.L., Tripp, A., McCune, S., Lewis, D.A., Sibille, E., 2015. Laminar and cellular analyses of reduced somatostatin gene expression in the subgenual anterior cingulate cortex in major depression. Neurobiology of disease 73, 213-219.

Serrano, A., Haddjeri, N., Lacaille, J.C., Robitaille, R., 2006. GABAergic network activation of glial cells underlies hippocampal heterosynaptic depression. J Neurosci 26, 5370-5382.

Serretti, A., Mandelli, L., Lorenzi, C., Pirovano, A., Olgiati, P., Colombo, C., Smeraldi, E., 2007. Serotonin transporter gene influences the time course of improvement of "core" depressive and

somatic anxiety symptoms during treatment with SSRIs for recurrent mood disorders. Psychiatry research 149, 185-193.

Sheline, Y.I., Gado, M.H., Kraemer, H.C., 2003. Untreated depression and hippocampal volume loss. The American journal of psychiatry 160, 1516-1518.

Sheline, Y.I., Liston, C., McEwen, B.S., 2019. Parsing the Hippocampus in Depression: Chronic Stress, Hippocampal Volume, and Major Depressive Disorder. Biological psychiatry 85, 436-438.

Si, X., Miguel-Hidalgo, J.J., O'Dwyer, G., Stockmeier, C.A., Rajkowska, G., 2004. Age-dependent reductions in the level of glial fibrillary acidic protein in the prefrontal cortex in major depression. Neuropsychopharmacology 29, 2088-2096.

Sickmann, H.M., Skoven, C., Bastlund, J.F., Dyrby, T.B., Plath, N., Kohlmeier, K.A., Kristensen, M.P., 2018. Sleep patterning changes in a prenatal stress model of depression. Journal of developmental origins of health and disease 9, 102-111.

Silverstein, B., 2002. Gender differences in the prevalence of somatic versus pure depression: a replication. The American journal of psychiatry 159, 1051-1052.

Simard, S., Coppola, G., Rudyk, C.A., Hayley, S., McQuaid, R.J., Salmaso, N., 2018. Profiling changes in cortical astroglial cells following chronic stress. Neuropsychopharmacology 43, 1961-1971.

Singh, A., Abraham, W.C., 2017. Astrocytes and synaptic plasticity in health and disease. Experimental brain research 235, 1645-1655.

Singhal, G., Baune, B.T., 2017. Microglia: An Interface between the Loss of Neuroplasticity and Depression. Frontiers in cellular neuroscience 11, 270.

Smith, D.J., Kyle, S., Forty, L., Cooper, C., Walters, J., Russell, E., Caesar, S., Farmer, A., McGuffin, P., Jones, I., Jones, L., Craddock, N., 2008. Differences in depressive symptom profile between males and females. Journal of affective disorders 108, 279-284.

Soderlund, J., Lindskog, M., 2018. Relevance of Rodent Models of Depression in Clinical Practice: Can We Overcome the Obstacles in Translational Neuropsychiatry? The international journal of neuropsychopharmacology 21, 668-676.

Son, H., Banasr, M., Choi, M., Chae, S.Y., Licznerski, P., Lee, B., Voleti, B., Li, N., Lepack, A., Fournier, N.M., Lee, K.R., Lee, I.Y., Kim, J., Kim, J.H., Kim, Y.H., Jung, S.J., Duman, R.S., 2012. Neuritin produces antidepressant actions and blocks the neuronal and behavioral deficits caused by chronic stress. Proceedings of the National Academy of Sciences of the United States of America 109, 11378-11383.

Song, C., Leonard, B.E., 2005. The olfactory bulbectomised rat as a model of depression. Neuroscience and biobehavioral reviews 29, 627-647.

Soumier, A., Sibille, E., 2014. Opposing effects of acute versus chronic blockade of frontal cortex somatostatin-positive inhibitory neurons on behavioral emotionality in mice. Neuropsychopharmacology 39, 2252-2262.

Stahl, S.M., 1998. Mechanism of action of serotonin selective reuptake inhibitors. Serotonin receptors and pathways mediate therapeutic effects and side effects. Journal of affective disorders 51, 215-235.

Statistics Canada, 2013. Depression.

Steffens, D.C., Potter, G.G., 2008. Geriatric depression and cognitive impairment. Psychological medicine 38, 163-175.

Steiner, J., Walter, M., Gos, T., Guillemin, G.J., Bernstein, H.G., Sarnyai, Z., Mawrin, C., Brisch, R., Bielau, H., Meyer zu Schwabedissen, L., Bogerts, B., Myint, A.M., 2011. Severe depression is associated with increased microglial quinolinic acid in subregions of the anterior cingulate gyrus: evidence for an immune-modulated glutamatergic neurotransmission? Journal of neuroinflammation 8, 94.

Strasburger, S.E., Bhimani, P.M., Kaabe, J.H., Krysiak, J.T., Nanchanatt, D.L., Nguyen, T.N., Pough, K.A., Prince, T.A., Ramsey, N.S., Savsani, K.H., Scandlen, L., Cavaretta, M.J., Raffa, R.B., 2017. What is the mechanism of Ketamine's rapid-onset antidepressant effect? A concise overview of the surprisingly large number of possibilities. Journal of clinical pharmacy and therapeutics 42, 147-154.

Strekalova, T., Spanagel, R., Bartsch, D., Henn, F.A., Gass, P., 2004. Stress-induced anhedonia in mice is associated with deficits in forced swimming and exploration. Neuropsychopharmacology 29, 2007-2017.

Strekalova, T., Steinbusch, H.W., 2010. Measuring behavior in mice with chronic stress depression paradigm. Progress in neuro-psychopharmacology & biological psychiatry 34, 348-361.

Suarez, I., Bodega, G., Fernandez, B., 2002. Glutamine synthetase in brain: effect of ammonia. Neurochemistry international 41, 123-142.

Sullivan, P.F., Neale, M.C., Kendler, K.S., 2000. Genetic epidemiology of major depression: review and meta-analysis. The American journal of psychiatry 157, 1552-1562.

Sun, J.D., Liu, Y., Yuan, Y.H., Li, J., Chen, N.H., 2012. Gap junction dysfunction in the prefrontal cortex induces depressive-like behaviors in rats. Neuropsychopharmacology 37, 1305-1320.

Sun, Q., Turrigiano, G.G., 2011. PSD-95 and PSD-93 play critical but distinct roles in synaptic scaling up and down. The Journal of neuroscience : the official journal of the Society for Neuroscience 31, 6800-6808.

Swardfager, W., Herrmann, N., Marzolini, S., Saleem, M., Farber, S.B., Kiss, A., Oh, P.I., Lanctot, K.L., 2011. Major depressive disorder predicts completion, adherence, and outcomes in

cardiac rehabilitation: a prospective cohort study of 195 patients with coronary artery disease. The Journal of clinical psychiatry 72, 1181-1188.

Takahashi, A., Chung, J.R., Zhang, S., Zhang, H., Grossman, Y., Aleyasin, H., Flanigan, M.E., Pfau, M.L., Menard, C., Dumitriu, D., Hodes, G.E., McEwen, B.S., Nestler, E.J., Han, M.H., Russo, S.J., 2017. Establishment of a repeated social defeat stress model in female mice. Scientific reports 7, 12838.

Takahashi, K., Foster, J.B., Lin, C.L., 2015. Glutamate transporter EAAT2: regulation, function, and potential as a therapeutic target for neurological and psychiatric disease. Cellular and molecular life sciences : CMLS 72, 3489-3506.

Ten Have, M., Lamers, F., Wardenaar, K., Beekman, A., de Jonge, P., van Dorsselaer, S., Tuithof, M., Kleinjan, M., de Graaf, R., 2016. The identification of symptom-based subtypes of depression: A nationally representative cohort study. Journal of affective disorders 190, 395-406.

Testen, A., Ali, M., Sexton, H.G., Hodges, S., Dubester, K., Reissner, K.J., Swartzwelder, H.S., Risher, M.L., 2019. Region-Specific Differences in Morphometric Features and Synaptic Colocalization of Astrocytes During Development. Neuroscience 400, 98-109.

Thaipisuttikul, P., Ittasakul, P., Waleeprakhon, P., Wisajun, P., Jullagate, S., 2014. Psychiatric comorbidities in patients with major depressive disorder. Neuropsychiatric disease and treatment 10, 2097-2103.

Thase, M.E., 2008. Are SNRIs more effective than SSRIs? A review of the current state of the controversy. Psychopharmacology bulletin 41, 58-85.

Thompson, K.J., Khajehali, E., Bradley, S.J., Navarrete, J.S., Huang, X.P., Slocum, S., Jin, J., Liu, J., Xiong, Y., Olsen, R.H.J., Diberto, J.F., Boyt, K.M., Pina, M.M., Pati, D., Molloy, C., Bundgaard, C., Sexton, P.M., Kash, T.L., Krashes, M.J., Christopoulos, A., Roth, B.L., Tobin, A.B., 2018. DREADD Agonist 21 Is an Effective Agonist for Muscarinic-Based DREADDs in Vitro and in Vivo. ACS pharmacology & translational science 1, 61-72.

Torres-Platas, S.G., Nagy, C., Wakid, M., Turecki, G., Mechawar, N., 2016. Glial fibrillary acidic protein is differentially expressed across cortical and subcortical regions in healthy brains and downregulated in the thalamus and caudate nucleus of depressed suicides. Molecular psychiatry 21, 509-515.

Uemura, T., Green, M., Warsh, J.J., 2016. Chronic LiCl pretreatment suppresses thrombin-stimulated intracellular calcium mobilization through TRPC3 in astroglioma cells. Bipolar disorders 18, 549-562.

Uezato, A., Meador-Woodruff, J.H., McCullumsmith, R.E., 2009. Vesicular glutamate transporter mRNA expression in the medial temporal lobe in major depressive disorder, bipolar disorder, and schizophrenia. Bipolar disorders 11, 711-725.

Urban, D.J., Roth, B.L., 2015. DREADDs (designer receptors exclusively activated by designer drugs): chemogenetic tools with therapeutic utility. Annual Review of Pharmacology and Toxicology 55, 399-417.

Valentine, G., Dow, A., Banasr, M., Pittman, B., Duman, R., 2008. Differential effects of chronic antidepressant treatment on shuttle box escape deficits induced by uncontrollable stress. Psychopharmacology 200, 585-596.

Vasile, F., Dossi, E., Rouach, N., 2017. Human astrocytes: structure and functions in the healthy brain. Brain structure & function 222, 2017-2029.

Verkhratsky, A., Zorec, R., Parpura, V., 2017. Stratification of astrocytes in healthy and diseased brain. Brain pathology 27, 629-644.

Vetulani, J., 2013. Early maternal separation: a rodent model of depression and a prevailing human condition. Pharmacological reports : PR 65, 1451-1461.

Voleti, B., Navarria, A., Liu, R.J., Banasr, M., Li, N., Terwilliger, R., Sanacora, G., Eid, T., Aghajanian, G., Duman, R.S., 2013. Scopolamine rapidly increases mammalian target of rapamycin complex 1 signaling, synaptogenesis, and antidepressant behavioral responses. Biological psychiatry 74, 742-749.

Wang, Y.L., Han, Q.Q., Gong, W.Q., Pan, D.H., Wang, L.Z., Hu, W., Yang, M., Li, B., Yu, J., Liu, Q., 2018. Microglial activation mediates chronic mild stress-induced depressive- and anxiety-like behavior in adult rats. Journal of neuroinflammation 15, 21.

Ward, M.P., Irazoqui, P.P., 2010. Evolving refractory major depressive disorder diagnostic and treatment paradigms: toward closed-loop therapeutics. Frontiers in neuroengineering 3, 7.

Weissman, M.M., Leaf, P.J., Tischler, G.L., Blazer, D.G., Karno, M., Bruce, M.L., Florio, L.P., 1988. Affective disorders in five United States communities. Psychological medicine 18, 141-153.

Whiteford, H.A., Degenhardt, L., Rehm, J., Baxter, A.J., Ferrari, A.J., Erskine, H.E., Charlson, F.J., Norman, R.E., Flaxman, A.D., Johns, N., Burstein, R., Murray, C.J., Vos, T., 2013. Global burden of disease attributable to mental and substance use disorders: findings from the Global Burden of Disease Study 2010. Lancet 382, 1575-1586.

WHO, 2017. Depression.

WHO, 2018. Depression.

Wiese, S., Karus, M., Faissner, A., 2012. Astrocytes as a source for extracellular matrix molecules and cytokines. Frontiers in pharmacology 3, 120.

Willner, P., 2005. Chronic mild stress (CMS) revisited: consistency and behavioural-neurobiological concordance in the effects of CMS. Neuropsychobiology 52, 90-110.

Willner, P., 2017a. The chronic mild stress (CMS) model of depression: History, evaluation and usage. Neurobiology of stress 6, 78-93.

Willner, P., 2017b. Reliability of the chronic mild stress model of depression: A user survey. Neurobiology of stress 6, 68-77.

Willner, P., Belzung, C., 2015. Treatment-resistant depression: are animal models of depression fit for purpose? Psychopharmacology 232, 3473-3495.

Wilson, S., Hicks, B.M., Foster, K.T., McGue, M., Iacono, W.G., 2015. Age of onset and course of major depressive disorder: associations with psychosocial functioning outcomes in adulthood. Psychological medicine 45, 505-514.

Witt, S.H., Streit, F., Jungkunz, M., Frank, J., Awasthi, S., Reinbold, C.S., Treutlein, J., Degenhardt, F., Forstner, A.J., Heilmann-Heimbach, S., Dietl, L., Schwarze, C.E., Schendel, D., Strohmaier, J., Abdellaoui, A., Adolfsson, R., Air, T.M., Akil, H., Alda, M., Alliey-Rodriguez, N., Andreassen, O.A., Babadjanova, G., Bass, N.J., Bauer, M., Baune, B.T., Bellivier, F., Bergen, S., Bethell, A., Biernacka, J.M., Blackwood, D.H.R., Boks, M.P., Boomsma, D.I., Borglum, A.D., Borrmann-Hassenbach, M., Brennan, P., Budde, M., Buttenschon, H.N., Byrne, E.M., Cervantes, P., Clarke, T.K., Craddock, N., Cruceanu, C., Curtis, D., Czerski, P.M., Dannlowski, U., Davis, T., de Geus, E.J.C., Di Florio, A., Djurovic, S., Domenici, E., Edenberg, H.J., Etain, B., Fischer, S.B., Forty, L., Fraser, C., Frye, M.A., Fullerton, J.M., Gade, K., Gershon, E.S., Giegling, I., Gordon, S.D., Gordon-Smith, K., Grabe, H.J., Green, E.K., Greenwood, T.A., Grigoroiu-Serbanescu, M., Guzman-Parra, J., Hall, L.S., Hamshere, M., Hauser, J., Hautzinger, M., Heilbronner, U., Herms, S., Hitturlingappa, S., Hoffmann, P., Holmans, P., Hottenga, J.J., Jamain, S., Jones, I., Jones, L.A., Jureus, A., Kahn, R.S., Kammerer-Ciernioch, J., Kirov, G., Kittel-Schneider, S., Kloiber, S., Knott, S.V., Kogevinas, M., Landen, M., Leber, M., Leboyer, M., Li, Q.S., Lissowska, J., Lucae, S., Martin, N.G., Mayoral-Cleries, F., McElroy, S.L., McIntosh, A.M., McKay, J.D., McQuillin, A., Medland, S.E., Middeldorp, C.M., Milaneschi, Y., Mitchell, P.B., Montgomery, G.W., Morken, G., Mors, O., Muhleisen, T.W., Muller-Myhsok, B., Myers, R.M., Nievergelt, C.M., Nurnberger, J.I., O'Donovan, M.C., Loohuis, L.M.O., Ophoff, R., Oruc, L., Owen, M.J., Paciga, S.A., Penninx, B., Perry, A., Pfennig, A., Potash, J.B., Preisig, M., Reif, A., Rivas, F., Rouleau, G.A., Schofield, P.R., Schulze, T.G., Schwarz, M., Scott, L., Sinnamon, G.C.B., Stahl, E.A., Strauss, J., Turecki, G., Van der Auwera, S., Vedder, H., Vincent, J.B., Willemsen, G., Witt, C.C., Wray, N.R., Xi, H.S., Bipolar Disorders Working Group of the Psychiatric Genomics, C., Major Depressive Disorder Working Group of the Psychiatric Genomics, C., Schizophrenia Working Group of the Psychiatric Genomics, C., Tadic, A., Dahmen, N., Schott, B.H., Cichon, S., Nothen, M.M., Ripke, S., Mobascher, A., Rujescu, D., Lieb, K., Roepke, S., Schmahl, C., Bohus, M., Rietschel, M., 2017. Genome-wide association study of borderline personality disorder reveals genetic overlap with bipolar disorder, major depression and schizophrenia. Translational psychiatry 7, e1155.

Wohleb, E.S., Franklin, T., Iwata, M., Duman, R.S., 2016. Integrating neuroimmune systems in the neurobiology of depression. Nature reviews 17, 497-511.

Wohleb, E.S., Gerhard, D., Thomas, A., Duman, R.S., 2017. Molecular and Cellular Mechanisms of Rapid-Acting Antidepressants Ketamine and Scopolamine. Current neuropharmacology 15, 11-20.

Wolf, S.A., Boddeke, H.W., Kettenmann, H., 2017. Microglia in Physiology and Disease. Annual review of physiology 79, 619-643.

Wood, G.E., Norris, E.H., Waters, E., Stoldt, J.T., McEwen, B.S., 2008. Chronic immobilization stress alters aspects of emotionality and associative learning in the rat. Behavioral neuroscience 122, 282-292.

Wray, N.R., Pergadia, M.L., Blackwood, D.H., Penninx, B.W., Gordon, S.D., Nyholt, D.R., Ripke, S., MacIntyre, D.J., McGhee, K.A., Maclean, A.W., Smit, J.H., Hottenga, J.J., Willemsen, G., Middeldorp, C.M., de Geus, E.J., Lewis, C.M., McGuffin, P., Hickie, I.B., van den Oord, E.J., Liu, J.Z., Macgregor, S., McEvoy, B.P., Byrne, E.M., Medland, S.E., Statham, D.J., Henders, A.K., Heath, A.C., Montgomery, G.W., Martin, N.G., Boomsma, D.I., Madden, P.A., Sullivan, P.F., 2012. Genome-wide association study of major depressive disorder: new results, meta-analysis, and lessons learned. Molecular psychiatry 17, 36-48.

Yalcin, I., Aksu, F., Belzung, C., 2005. Effects of desipramine and tramadol in a chronic mild stress model in mice are altered by yohimbine but not by pindolol. European journal of pharmacology 514, 165-174.

Yirmiya, R., Rimmerman, N., Reshef, R., 2015. Depression as a microglial disease. Trends in neurosciences 38, 637-658.

Yoon, B.E., Woo, J., Lee, C.J., 2012. Astrocytes as GABA-ergic and GABA-ceptive cells. Neurochem Res 37, 2474-2479.

Young, M.A., Fogg, L.F., Scheftner, W.A., Keller, M.B., Fawcett, J.A., 1990. Sex differences in the lifetime prevalence of depression: does varying the diagnostic criteria reduce the female/male ratio? Journal of affective disorders 18, 187-192.

Yu, H., Li, M., Zhou, D., Lv, D., Liao, Q., Lou, Z., Shen, M., Wang, Z., Li, M., Xiao, X., Zhang, Y., Wang, C., 2018. Vesicular glutamate transporter 1 (VGLUT1)-mediated glutamate release and membrane GluA1 activation is involved in the rapid antidepressant-like effects of scopolamine in mice. Neuropharmacology 131, 209-222.

Zarate, C.A., Manji, H.K., 2008. Riluzole in psychiatry: a systematic review of the literature. Expert opinion on drug metabolism & toxicology 4, 1223-1234.

Zhang, H., Zhao, Y., Wang, Z., 2015. Chronic corticosterone exposure reduces hippocampal astrocyte structural plasticity and induces hippocampal atrophy in mice. Neurosci Lett 592, 76-81.

Zhang, J.Y., Liu, T.H., He, Y., Pan, H.Q., Zhang, W.H., Yin, X.P., Tian, X.L., Li, B.M., Wang, X.D., Holmes, A., Yuan, T.F., Pan, B.X., 2019. Chronic Stress Remodels Synapses in an Amygdala Circuit-Specific Manner. Biological psychiatry 85, 189-201.

Zhao, J., Verwer, R.W., van Wamelen, D.J., Qi, X.R., Gao, S.F., Lucassen, P.J., Swaab, D.F., 2016. Prefrontal changes in the glutamate-glutamine cycle and neuronal/glial glutamate transporters in depression with and without suicide. Journal of psychiatric research 82, 8-15.

Zhao, Y., Lin, Z., Chen, L., Ouyang, L., Gu, L., Chen, F., Zhang, Q., 2018. ippocampal astrocyte atrophy in a mouse depression model induced by corticosterone is reversed by fluoxetine instead

of benzodiazepine diazepam. Progress in Neuro-Psychopharmacology & Biological Psychiatry 83, 99-109.

Zimmerman, M., Balling, C., Chelminski, I., Dalrymple, K., 2018. Understanding the severity of depression: Which symptoms of depression are the best indicators of depression severity? Comprehensive psychiatry 87, 84-88.

Zink, M., Vollmayr, B., Gebicke-Haerter, P.J., Henn, F.A., 2010. Reduced expression of glutamate transporters vGluT1, EAAT2 and EAAT4 in learned helpless rats, an animal model of depression. Neuropharmacology 58, 465-473.

Appendices

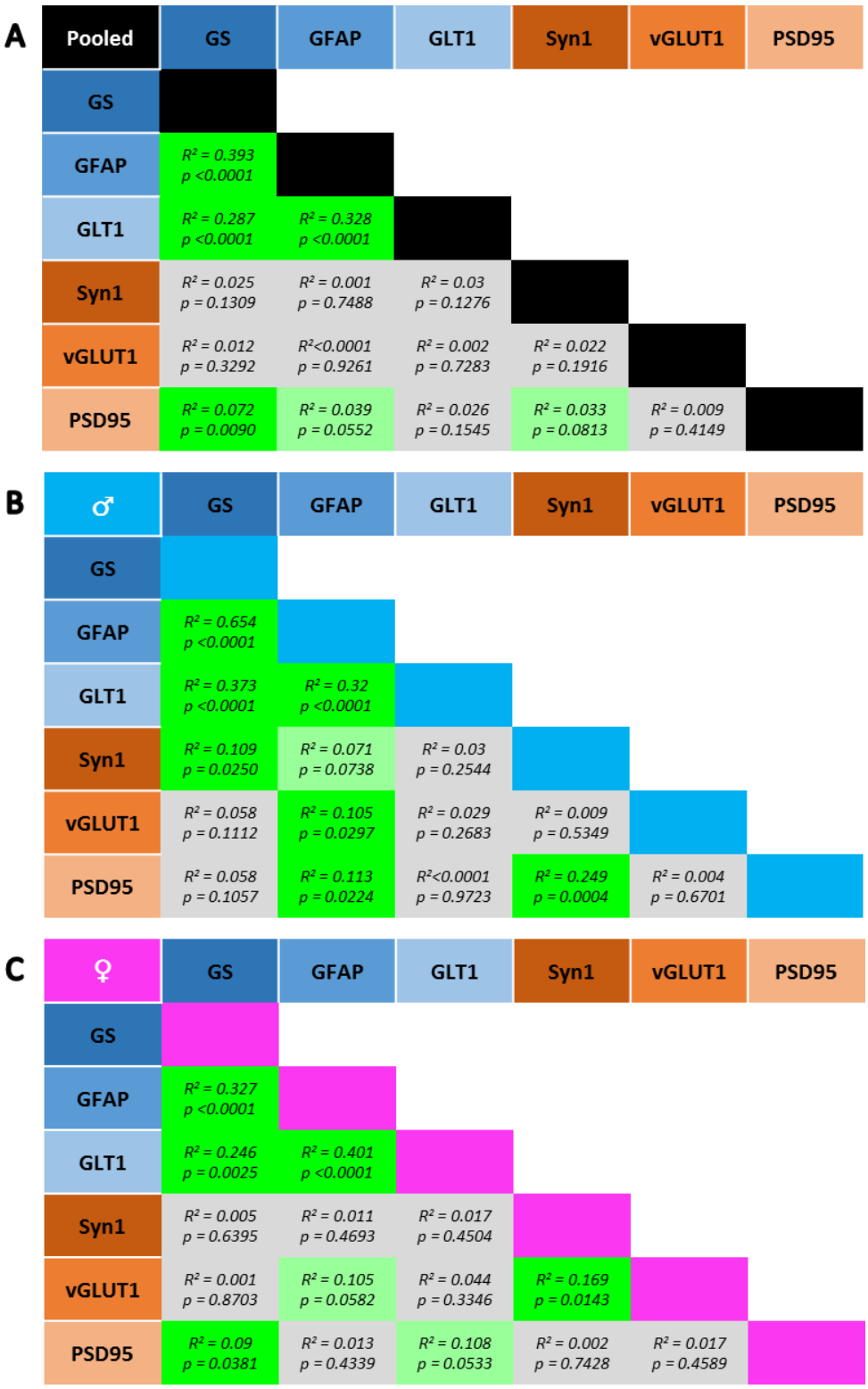
A
Pooled
GS
GFAP
GLT1
Syn1
vGLUT1
PSD95
GS
GFAP
R² = 0.393
p <0.0001
GLT1
R² = 0.287
p <0.0001
R² = 0.328
p <0.0001
Syn1
R² = 0.025
p = 0.1309
R² = 0.001
p = 0.7488
R² = 0.03
p = 0.1276
vGLUT1
R² = 0.012
p = 0.3292
R²<0.0001
p = 0.9261
R² = 0.002
p = 0.7283
R² = 0.022
p = 0.1916
PSD95
R² = 0.072
p = 0.0090
R² = 0.039
p = 0.0552
R² = 0.026
p = 0.1545
R² = 0.033
p = 0.0813
R² = 0.009
p = 0.4149
B
♂
GS
GFAP
GLT1
Syn1
vGLUT1
PSD95
GS
GFAP
R² = 0.654
p <0.0001
GLT1
R² = 0.373
p <0.0001
R² = 0.32
p <0.0001
Syn1
R² = 0.109
p = 0.0250
R² = 0.071
p = 0.0738
R² = 0.03
p = 0.2544
vGLUT1
R² = 0.058
p = 0.1112
R² = 0.105
p = 0.0297
R² = 0.029
p = 0.2683
R² = 0.009
p = 0.5349
PSD95
R² = 0.058
p = 0.1057
R² = 0.113
p = 0.0224
R²<0.0001
p = 0.9723
R² = 0.249
p = 0.0004
R² = 0.004
p = 0.6701
C
♀
GS
GFAP
GLT1
Syn1
vGLUT1
PSD95
GS
GFAP
R² = 0.327
p <0.0001
GLT1
R² = 0.246
p = 0.0025
R² = 0.401
p <0.0001
Syn1
R² = 0.005
p = 0.6395
R² = 0.011
p = 0.4693
R² = 0.017
p = 0.4504
vGLUT1
R² = 0.001
p = 0.8703
R² = 0.105
p = 0.0582
R² = 0.044
p = 0.3346
R² = 0.169
p = 0.0143
PSD95
R² = 0.09
p = 0.0381
R² = 0.013
p = 0.4339
R² = 0.108
p = 0.0533
R² = 0.002
p = 0.7428
R² = 0.017
p = 0.4589

Appendix 1. ***Marker x marker correlations between all six proteins, and correlations split by sex*****.**

Markers: glutamine synthetase (GS), glial fibrillary acidic protein (GFAP), glutamate transporter 1 (GLT1), synapsin 1 (Syn1), vesicular glutamate transporter (vGLUT1), postsynaptic density protein 95 (PSD95).

(**A**) Pooled results (both sexes) of marker x marker correlations. GS, GFAP, and GLT1 strongly correlated with each other. PSD95 correlated with GS, GFAP, and Syn1.
(**B**) Marker x marker correlations, split by sex (males only). GS, GFAP, and GLT1 strongly correlated with each other. GFAP also correlated with all 3 synaptic proteins (Syn1, vGLUT1, PSD95). Syn1 correlated with GS and PSD95.
(**C**) Marker x marker correlations, split by sex (females only). GS, GFAP, and GLT1 strongly correlated with each other. vGLUT1 correlated with GFAP and Syn1, while PSD95 correlated with GS and GLT1.

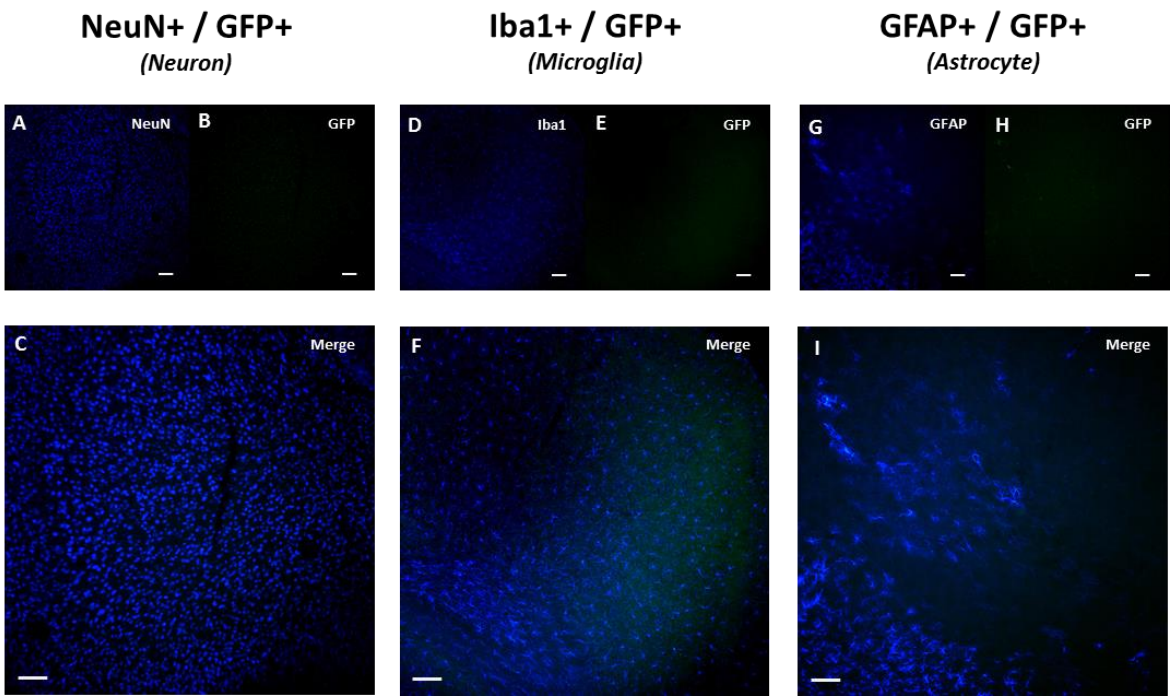

Appendix 2. ***GFAP-GFP wild type littermates displayed no GFP+ immunofluorescence*****.**

Images of wild type mouse prefrontal cortex (PFC) immunolabelled with either neuronal nuclei (NeuN, blue) and green fluorescent protein (GFP, green) (**A-C**), ionized calcium binding adaptor molecule 1 (Iba1, blue) and GFP (**D-F**), or glial fibrillary acidic protein (GFAP, blue) and GFP (**G-I**). There were no GFP+ cells (**B, E, H**) in wild type littermates of GFAP-GFP mice. Scale bar = 100µm.

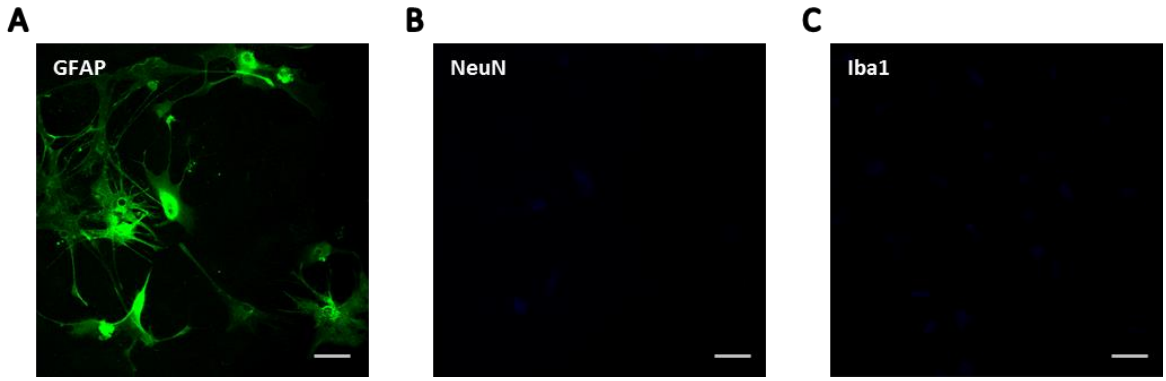

Appendix 3. ***Primary astrocyte culture purity verification*****.**

Example of images of primary astrocyte cultures from GFAP-Cre+ mice or wild type littermates, immunolabelled for glial fibrillary acidic protein (GFAP) (**A**), neuronal nuclei (NeuN) (**B**), or ionized calcium binding adaptor molecule 1 (Iba1) (**C**). Only GFAP+ staining showed immunofluorescence (**A**). No NeuN and Iba1+ cells were found (**B-C**). Scale bar = 50µm.